FATE AND BEHAVIOUR OF NANO TITANIUM DIOXIDE (NANO-TiO_2) IN A SIMULATED WASTEWATER TREATMENT PLANT WITH DYE EFFLUENT

Report to the

WATER RESEARCH COMMISSION

by

Lwazi Charles Mahlalela, Jane Catherine Ngila & Langelihle Nsikayezwe Dlamini

Department of Applied Chemistry

University of Johannesburg

WRC Report No 2503/1/18

ISBN 978-1-4312-0995-8

June 2018

WATER RESEARCH COMMISSION

Obtainable from:

Water Research Commission
Private Bag X03
Gezina, 0031
Republic of South Africa

orders@wrc.org.za or download from www.wrc.org.za

Printed in the Republic of South Africa

EXECUTIVE SUMMARY

BACKGROUND

A report released by the Royal Society and the Royal Academy of Engineering on nanoscience and nanotechnology drew the attention of environmental managers and policy makers to the possible toxicological and pathological risks to human health and to the environment that may be presented by engineered nanomaterials (ENMs) (Engineering, 2004; Moore, 2006). In order to accurately assess the risk involved in the use of nanoparticles and consider the eventual environmental liabilities associated with ENMs, a thorough understanding of the behaviour of nanoparticles in organisms and the ecosystem is needed (Belen, Fidalgo & Cortalezzi, 2013). Moreover, a correlation of the physiological properties of nanoparticles with their fate and behaviour relies on accurate characterisation of the nanoparticles before, during and after applications (Fang et al., 2009; Jiang et al., 2009; Koetsem et al., 2015).

Nanotechnology holds great potential for advancing water and wastewater treatment efficiencies (Qu, Alvarez & Li, 2013). Thus, an exponential increase in the production and application of ENMs is anticipated. Inadvertently, ecosystems will be exposed to significant levels of such materials. Once they are released into the environment, ENMs will to some extent agglomerate with suspended solids or sediments, potentially accumulate in organisms and finally entre the food chain or drinking water (Gottschalk & Nowack, 2011). ENMs generate reactive oxygen species such as free radicals (OH^-), singlet oxygen ($_1O^2$) and superoxides (O_2^-) which exert adverse effects on microorganisms including disruption of cell walls and damage to DNA/RNA (Eduok et al., 2013; Pelletier et al., 2010). Therefore, ENMs are among the increasing emerging contaminants in wastewater treatment plants (WWTPs) (Gottschalk & Nowack, 2011).

WWTPs have been utilised for the removal and/or degradation of contaminants from wastewater for generations, and they still play a pivotal role in sustainable wastewater recycling. The treated wastewater effluent is discharged into natural water reservoirs that include rivers and lakes. The sludge generated during wastewater treatment has several applications that include use as a fertiliser in agriculture. However, under certain circumstances, the sludge is disposed for incineration, where the residue ashes are landfilled or the sludge is landfilled without any further treatment (Chaúque, 2014). Once nanoparticles are in the soil, a number of processes can affect their fate and bioavailability. The key processes include dissolution, sorption/aggregation, plant bioaccumulation, invertebrate accumulation and toxicity, microbial toxicity and particle migration (Klaine et al., 2008).

RATIONALE

Nanoscience and nanotechnology are widely seen as having huge benefits in many areas and are attracting investment from governments and business in many parts of the world. Yet their application in different scientific fields including engineering and biotechnology, and biomedical, environmental and materials sciences, may raise new challenges in the safety, regulatory or ethics domain (Engineering, 2004; Sillanpää, Paunu & Sainio, 2011).

Exposure assessment is very important because the environmental impact of ENMs as they are released into the biosphere, whether inadvertently of intentionally, is poorly understood (Dwivedi et al., 2015). The interaction between nanoparticles and water components in the formation or breakage of aggregates is mainly determined by their surface properties which are controlled by the solution chemistry (Baalousha, 2009; Xiao-hong et al., 2015). Solution pH and surface charge are important factors governing the stability of nanoparticles in aqueous solution. Nanoparticles are mobile in most pH ranges except where the pH is close to the point of zero charge. Inorganic salts also have a direct effect on aggregation of nanoparticles and additives such as surfactants and natural organic matter significantly improve the dispersion of nanoparticles. The natural environment, groundwater aquifers and surface water have high concentrations of magnesium and calcium which favour high aggregation and deposition of nanoparticles (Fang et al., 2009; Finnegan, 2006; Snoswell et al., 2005). This makes wastewater an appropriate matrix for the investigation of the behaviour of nanoparticles, as properties greatly vary.

WWTPs receives significant amounts of nanomaterials from both domestic and industrial sources. Some are expected to precipitate into the sludge but may find their way back into the aquatic system via sludge used as fertiliser, and the remaining effluent will enter directly into both fresh water and marine environments (Jennings, Goodhead & Tyler, 2015). Thus, understanding the fate and behaviour of nanoparticles in different environmental matrices is crucial for predicting their potential ecotoxic effects in various environmental species (Engineering, 2004).

OBJECTIVES AND AIMS

The specific aims for this study were:

AIM 1

To monitor the fate and behaviour of titanium dioxide (TiO_2) nanoparticles in a simulated wastewater treatment plant (SWWTP) with respect to their physicochemical characteristics.

AIM 2

To investigate the chemical stability of TiO_2 nanoparticles in wastewater and how they are affected by changes in pH, ionic strength, mono- and divalent cations and natural organic matter content.

AIM 3

To establish possible mechanisms of TiO_2 accumulation and/or degradation in wastewater sludge during wastewater treatment.

METHODOLOGY

In this study, TiO_2 nanoparticles, synthesised via the sol-gel method, were used to prepare the suspensions. The different suspensions were prepared using deionized water (DI), monovalent cation electrolyte (NaCl) and divalent cation electrolytes ($CaCl_2$ and $MgCl_2$). Disperse dye-stuff was used as a representation of natural organic matter. Stock solutions of the different aqueous mixtures were prepared for experiments with and without dye-stuff. A concentration of 1 mg/L of dye-stuff was used for all the dye-stuff experiments.

In order to assess the change in behaviour of the nanoparticles in the treatment plant, secondary influent was collected from Pretoria (Daspoort wastewater treatment works) which mainly receives domestic wastewater. Sampling was done weekly to give the wastewater a life span of seven days at 4˚C as suggested by the OECD 303A guidelines. To formulate the influent for the SWWTP, the secondary influent was mixed with synthetic industrial dye-stuff effluent to reach acclimatisation until the system was run with only synthetic industrial dye-stuff effluent. Details about the plant operating conditions are discussed in **Chapter 3** of this report.

RESULTS AND DISCUSSION

Pristine TiO_2 nanoparticles were synthesised using the sol-gel method. Morphological and size distribution patterns of the photocatalyst were determined using transmission electron microscopy (TEM), scanning electron microscopy (SEM) and Brunauer-Emmett-Teller (BET) technique. Raman spectroscopy and powder X-ray diffraction were carried out to yield the structural composition of TiO_2.

Stability studies were conducted for different solutions (deionized water (DI), NaCl, $CaCl_2$, and $MgCl_2$) at different pH range. Agglomeration and zeta potential were influenced by ionic strength, type of electrolyte, and the presence of dye-stuff. The Derjaguin-Landau-Verwey-Overbeek (DLVO) theory was used to analyse the stability and/or agglomeration of the nanoparticles in the different solutions. Repulsive or attractive forces stipulated by the DLVO theory were used to quantitatively discuss the stability of NPs. An increase in ionic strength increased agglomeration which was linked to pH point-of-zero charge (pzc), as there were minimal electrostatic repulsions at the pzc, yet the attractive van der Waals forces were dominant. Addition of the dye-stuff significantly decreased agglomeration, as the dye stuff changed the overall zeta potential of the TiO_2 nanoparticles to negative across the entire pH range, which improved stability as there were increased particle–particle repulsions. In the presence of increased Ca^{2+}, the mean diameter of the nanoparticles increased as it effectively suppressed the electrical double layer (EDL) of the nanoparticles, thus enhancing agglomeration. The DLVO theory was successful at explaining, in terms of the interaction energies between nanoparticles, the phenomena that caused either agglomeration or stability of the as-synthesised TiO_2 nanoparticles in the different solutions.

The study also focused on assessing quantitatively the pathway and mass balance of TiO_2 in the influent and sludge. To achieve such measurements, activated sludge was successfully acclimatised to a synthetic industrial dye-stuff effluent. The effects of TiO_2 nanoparticles on the treatment process efficiency were then investigated. The data obtained from this project revealed that the addition – as high as 15 mg/L – of TiO_2 nanoparticles had no effect on chemical oxygen demand (COD) removal efficiency, which remained >80%. Measured total plate count (TPC) affirmed that the addition of TiO_2 nanoparticles had no effect on the treatment process. The TPC was measured to check the viability of aerobic bacteria in the activated sludge after the addition of TiO_2 nanoparticles. The availability of viable bacteria inferred that the nanoparticles had no adverse effect on the functionality of the treatment process.

Results from powdered X-ray diffraction (XRD) confirmed that the anatase phase of the added TiO_2 nanoparticles remained unchanged even after exposure to the treatment plant. Removal of the nanoparticles from the influent was facilitated by sorption of the nanoparticles on the activated sludge, as evinced by the presence of anatase phase TiO_2 in the sludge sample from the test unit of the SWWTP. Possible dissolution of titanium from TiO_2 nanoparticles was evidenced by an increase in conductivity. About 90% of TiO_2 was retained in the activated sludge while 10-12% accompanied the treated effluents. Scanning electron micrographs and energy dispersive X-ray spectroscopy (EDS) confirmed the presence of Ti in the sludge.

CONCLUSIONS

- TiO_2 nanoparticles were synthesised successfully, and characterisation with XRD and Raman confirmed anatase polymorph. The average particle size, from TEM, was 12 nm which was comparable to the 15 nm calculated from the XRD using the Debye-Scherrer equation. BET analysis indicated mesoporous material, as the TiO_2 nanoparticles had an isotherm characteristic to type VI, containing a type H1 hysteresis loop. This type of hysteresis loop was ascribed to porous materials that have agglomerates. The agglomerates were clearly observed on TEM and SEM imaging and were further confirmed by calculating average particle size using the S_{BET} and $\rho_{(TiO2)}$, which was 28 nm. This value was comparable to 25 nm which was the maximum particle size measured on TEM.

- Characteristics of solution matrices such as ionic strength, the nature of the electrolytes, solution pH and dye-stuff were paramount in explaining the stability of TiO_2 nanoparticles in solution, as they affect properties such as surface charge and electrical double layer. An increase in ionic strength was seen to increase agglomeration of TiO_2 nanoparticles, while the dye-stuff decreased the hydrodynamic sizes. The increase in the hydrodynamic sizes of TiO_2 nanoparticles for $CaCl_2$ experiment in an alkaline pH range was due to the Ca^{2+} to effectively reduce the electrical double layer. This was observed even in the presence of dye-stuff. Thus, factors such as steric forces were important in explaining the role of dye-stuff in the stability of nanoparticles. However, the presence of Ca^{2+} effectively neutralised negatively charged TiO_2 surfaces even in the presence of negatively charged dye-stuff molecules on the surfaces of nanoparticles. Divalent cations were seen to have a

neutralising effect on the surfaces of nanoparticles as Mg^{2+} behaved in a similar manner.

- Using the DLVO theory, the extent of stability and/or agglomeration of nanoparticles was explained. The TEM and SEM images also confirmed the agglomeration of TiO_2 nanoparticles to even larger hydrodynamic sizes in solution. Thus, variations in the behaviour of the TiO_2 nanoparticles in different suspensions provided evidence that nanoparticles will take several environmental pathways influenced by their size, surface charge and agglomeration state.

- Prior to exposing the SWTP to TiO_2 nanoparticles, acclimatisation of the activated sludge to synthetic industrial dye-stuff effluent was conducted and achieved successfully. Measurements of COD removal clearly affirmed the acclimatisation after a steady state with an average removal of >80% was observed at sludge retention time (SRT) 7–9. The addition of nanoparticles was conducted at SRT 10–12 and the removal of COD remained >80%. This signified that the nanoparticles had no effect on the treatment process.

- Parameters such as pH, conductivity and total suspended solids further confirmed the efficiency of the treatment, as these parameters met the limit values of both local and international standards. According to the XRD results, to check the behaviour, the TiO_2 that was present in the sludge did not change, as it maintained the anatase crystal structure of the TiO_2 nanoparticles before exposure to the SWWTP.

- Coming to the fate of the nanoparticles, the results showed that about 90% of the TiO_2 was retained in the activated sludge and 10-12% escaped with the treatment effluents. Thus the TiO_2 nanoparticles were removed effectively by the SWWTP from the influent. Sorption of the nanoparticles on the activated sludge facilitated the removal. SEM mapping showed the presence of Ti on the sludge to further confirm the sorption of the TiO_2 nanoparticles on the activated sludge.

RECOMMENDATIONS FOR FUTURE RESEARCH

- Work needs to be done on culturing activated sludge microorganisms, to know the genera and thus the structural properties of the cells. This is important in understanding the interactions of TiO_2 nanoparticles with the cell walls of the microorganisms, to reach proper conclusions on the sorption, be it chemisorption, physisorption or biosorption. This may further be used to understand the removal of the dye-stuff during treatment.
- The system needs to be extended to include a photocatalytic section that will use photocatalysts, either in suspension or embedded on a support, to provide a more realistic approach for the photocatalytic removal of organics. The positioning of the photocatalytic section would be determined by the type of wastewater to be degraded, based on parameters such as toxicity.
- Apart from the removal of organics, utilisation of the small fraction of nanoparticles that escapes with the effluent can be investigated. This may be used in conjunction with UV light to assist in the disinfection of the effluent for the removal of any microorganisms present in the effluent before release into the environment.

Modifications of the SWWTP to include anaerobic and anoxic stages can be considered in future studies. This would provide a more realistic approach in the study of the fate of nanomaterials in WWTPs. WWTPs in South Africa are not limited to aerobic treatment but include a combination of anaerobic, aerobic and anoxic treatment.

ACKNOWLEDGEMENTS

The authors would like to thank the Reference Group of the WRC Project for the assistance and the constructive discussions during the duration of the project:

Reference Group	Affiliation
Dr. Jo Burgess	Water Research Commission
Dr. Zikhona Tetana	University of Witwatersrand
Prof. Ndeke Musee	University of Pretoria
Prof. Corrine Greyling	Cape Peninsula University of Technology
Dr. Lucky Sikhwivlilu	Mintek
Prof. Victor Wepener	North West University
Dr. John Ngoni Zvimba	Water Research Commission
Others	
Dr. Bhekisisa Dlamini	University of Johannesburg
Dr. Malefetse Tshepo	Mintek

TABLE OF CONTENTS

LIST OF FIGURES

LIST OF TABLES

LIST OF ABBREVIATIONS

A549	Human lung epithelial cells
AOP	Advanced oxidation process
AS	Activated sludge
BEAS-2B	Human bronchial epithelial cell line
BET	Brunauer-Emmett-Teller
BOD_5	Five-day biological oxygen demand
BPA	Bisphenol A
CFU	Colony-forming unit
CNTs	Carbon nanotubes
COD	Chemical oxygen demand
DI	Deionised water
DLS	Dynamic light scattering
DLVO	Derjaguin-Landau-Verwey-Overbeek
DNA	Deoxyribonucleic acid
DO	Dissolved oxygen
EDC	Endocrine disrupting chemical
EDL	Electrical double layer
EDS	Energy dispersive X-ray spectroscopy
ELS	Electrophoretic light scattering
ENMs	Engineered nanomaterials
ENPs	Engineered nanoparticles
F/M	Food to microorganism ratio
HDF	Human dermal fibroblasts
HRT	Hydraulic retention time
ICDD	International centre for diffraction data
ICP-OES	Inductively coupled plasma – optical emission spectroscopy
ISO	International organisation for standardisation

MIPs	Molecular imprinted polymers
MLSS	Mixed liquor suspended solids
MLVSS	Mixed liquor volatile suspended solids
NOM	Natural organic matter
NP	Nanoparticle
OECD	Organization for Economic Co-Operation and Development
PAHs	Polyaromatic hydrocarbons
pzc	point of zero charge
RAS	Return activated sludge
SD	Standard deviation
SEM	Scanning Electron Microscopy
SRT	Sludge retention time
SWWTP	Simulated wastewater treatment plant
TEM	Transmission electron microscopy
TN	Total nitrogen
TOC	Total organic carbon
TPC	Total plate count
TSS	Total suspended solids
UV	Ultraviolet
V_A	Van der Waals attraction
vdW	Van der Waal
V_R	Double layer repulsion
V_T	Net total interaction
WWTP	Wastewater treatment plant
XRD	X-ray diffraction spectroscopy

1 INTRODUCTION AND OBJECTIVES

1.1 Introduction

Water is the most essential substance for all life on earth and a precious resource for human civilisation. Reliable access to clean and affordable water is considered one of the most basic humanitarian goals, yet it remains a major global challenge for the 21st century. Current water quality challenges prevent a large number of people from accessing safe drinking water (Qu et al., 2013).

Wastewater treatment plants (WWTPs) have been used for generations worldwide to remove or degrade contaminants from wastewater. The treated wastewater effluent is then discharged into the natural water resources that include rivers and lakes, with the sludge used for several applications including use an agricultural fertiliser. Today WWTPs still play a pivotal role in the treatment and purification of wastewater for domestic use (Chaüque, 2012).

Successes in the development of nanotechnology for novel application across many disciplines have increased the demand for mass production of engineered nanomaterials (ENMs). The advantages of nanotechnology are expected to provide potential solutions for health, water and energy problems. However, they also pose a potential hazard when released into the environment. ENMs enter environmental systems such as aquatic ecosystems, soil and air from direct and indirect sources. Indirect sources of ENMs include industrial and domestic effluents and solid waste streams (Chaüque, 2012; Gottschalk and Nowack, 2011). The direct release of ENMs may be through open windows in factories manufacturing ENMs, through the windows when powder form ENMs are used without caution, and through any kind of spills involving ENMs (Gottschalk & Nowack, 2011). The nanoecotoxicological data on ENMs shows they exhibit diverse and complex effects in different biological organisms (Chaüque, 2012).

Several studies have been carried out in pursuit of quantifying the releases of ENMs into the environment. However, these studies remain inadequate to support comprehensive risk assessment of chemicals with nanoscale dimensions in different environmental compartments (Musee, 2011). The exponential use of nanoproducts has led to the classification of ENMs among the increasing emerging contaminants (Sharif, Westerhoff & Herkes, 2013). In addition to the impact of these contaminants not being well understood, current wastewater treatment systems are not capable of removing them from wastewater. Furthermore, the fate and behaviour of ENMs from the influent point to the effluent discharge point of WWTPs is also not well understood (Chaüque, 2012).

Nanosized materials have attracted a lot of attention from the science community due to their unique physicochemical properties (Sillanpää et al., 2011). Nanoparticles have been present in as many as 800 consumer products since 2009, and it was estimated that they would be

incorporated in more than 15% of all products by 2014 (Chakraborty, 2009). These materials have been used in various scientific fields, including engineering, biotechnology, and biomedical, environmental and materials sciences (Chakraborty, 2009; Sillanpää et al., 2011). Due to new properties associated with conventional or surface-modified materials at nanoscale, some of the nanomaterials have exceptional environmental behaviour and effects (Sillanpää et al., 2011).

Probabilistic modelling was used to predict environmental emissions of engineered nanomaterials. Sun et al. (2016) have used dynamic probabilistic material flow modelling to predict the flows of four ENMs (titanium dioxide nanoparticles (nano-TiO_2), zinc oxide nanoparticles (nano-ZnO), silver nanoparticles (nano-Ag) and carbon nanotubes (CNTs) to the environment and quantify their amounts. Nano-TiO_2 was found to have the highest concentrations compared to the other ENMs. Concentrations ranging from 6.7 µg/kg (CNTs) to about 40 000 µg/kg (nano-TiO_2) were predicted from sediment modelling.

The release of ENMs in wastewater may negatively affect the performance of bacteria responsible for the proper functioning of the WWTP process. The ways in which the wastewater treatment may be affected include inhibition of microorganisms in the secondary treatment process or a decrease in the overall efficiency of treatment processes (Chakraborty, 2009). Thus, due to the substantial use of nanosized materials and their potential release into WWTPs, it is important to understand their potential impact in WWTP environments upon release of household and industrial effluents (Field, 2012).

1.2 Aim and objectives of this study

The aim of the study was to monitor the fate and behaviour of TiO_2 in a simulated WWTP with respect to its physicochemical properties, while studying the photocatalytic impact of pristine TiO_2.

The objectives of the study were:

i. To synthesise pristine and TiO_2 nanoparticles (NPs) and characterise the physicochemical properties of the synthesized pristine TiO_2 NPs before and after introducing them into a simulated WWTP. The characterisation was be carried out using scanning electron microscopy (SEM), transmission electron microscopy (TEM), Malvern zetasizer nanoZS, Brunauer-Emmett-Teller (BET), energy dispersive X-ray spectroscopy (EDS) and x-ray diffraction spectroscopy (XRD).

ii. To monitor the TiO_2 NPs present in the influent, sludge and effluent, using inductively coupled plasma – optical emission spectroscopy ICP-OES), and determine the mass balance.

iii. To determine the effect of TiO_2 NPs on the functionality of a WWTP by monitoring chemical oxygen demand (COD), five-day biological oxygen demand (BOD_5) and total nitrogen (TN) measurements.

2 LITERATURE REVIEW

2.1 Introduction

Engineered nanomaterials (ENMs) pose many ecological risks to the environment (Crosera et al., 2009; Kiser et al., 2009; Westerhoff et al., 2011). As industrial application of nanoparticles increases and nanoparticles are incorporated into more commercial products, the probability of ENMs making their way into municipal wastewater and WWTPs increases (Crosera et al., 2009; Kiser et al., 2009; Musee, 2011; Westerhoff et al., 2011). Furthermore, the preponderance of ENMs in environmental water systems is exacerbated by their extensive use in the removal of pollutants from wastewaters. ENMs have found use in wastewater treatment include nanosorbents, nanocatalysts, bioactive nanoparticles, biomimetic membranes and molecular imprinted polymers (MIPs) (Prachi et al., 2013). Therefore, an increased use of ENMs has led to studies that seek to understand their fate, behaviour and transport in environmental media (Keller et al., 2010). There is an urgent need to tackle the fate and behaviour of ENMs from WWTPs since such WWTPs are the major points of release of ENMs into receiving waters (streams, lakes, rivers) (Westerhoff et al., 2011). An understanding of the physicochemical properties of ENMs is thus crucial since these properties play a major role in the behaviour of ENMs in WWTPs and receiving waters, and understanding their properties will enable prediction of their fate in the environment (Oberdörster et al., 2005; Westerhoff et al., 2011).

2.1.1 Engineered nanomaterials

ENMs are materials that are manufactured for application in various industrial and consumer products due to their wide range of properties (U.S. Environmental Protection Agency, 2010; Morimoto et al., 2010). ENMs have been categorised by the International Organization for Standardization (ISO) as materials that include nanoparticles, nanotubes and nanostructured materials with internal or external dimensions in the nanoscale, having at least one dimension between 1–100 nm (Crosera et al., 2009; Davis et al., 2010; Morimoto et al., 2010; Water Rearch Australia, 2013). The advancement in the capabilities of nanotechnology has offered manufacturers a new technology with a potential to improve their products in a wide variety of fields (Crosera et al., 2009; Musee, 2011). ENMs have been applied in nanotechnology-enabled products and commercialised through many consumer products (e.g. paints, plastics, inks, paper, cosmetics and food-stuffs). In addition, ENMs are used in medicinal products (e.g. pharmaceuticals) and for environmental purposes (e.g. photocatalysts for wastewater treatment and novel membrane structures for water filtration) (Mauter and Elimelech, 2008; Musee, 2011; Musić et al., 1997; Porkodi and Arokiamary, 2007; Water Rearch Australia,

2013). **Table 1** lists different types of nanomaterials and their typical applications, as published by the Organization for Economic Co-operation and Development (OECD) in 2010.

Table 1 Selected list of ENMs and their various applications (Water Rearch Australia, 2013)

Nanomaterials	**Typical Application**
Fullerenes (C_{60})	Cosmetics
Single- and multi-wall carbon nanotubes (SWCNTs and MWCNTs)	Composite materials, textiles, solar cells, displays, hydrogen storage, desalination, electronics
Silver nanoparticles (Ag)	Textiles, household products (antibacterial)
Iron nanoparticles (Fe)	Soil remediation
Titanium dioxide (TiO_2)	Cosmetics, coatings, pigments, food, photocatalysis
Aluminium oxide (Al_2O_3)	Printing, coatings, fuel catalysts
Cerium oxide (CeO_2)	Polishing, fuel catalysts
Zinc oxide (ZnO)	Cosmetics
Silicon dioxide (SiO_2)	Coatings, construction, composite materials
Dendrimers	Drug delivery, printing, composite materials
Nanoclays	Coatings, food packaging
Gold nanoparticles (Au)	Medical diagnostics, therapy

ENMs eventually find their way into the environment either during production, when in use or at the disposal stage (Limbach et al., 2008; Musee, 2011; Reijnders, 2009). According to Sharma (2009), the production of ENMs is expected to rise from 400 to 58 000 tons from 2011 to 2020, with an estimated profit of US$1 trillion by 2015 due to the application of these materials across many industries.

Many studies have been undertaken to investigate how ENMs are released into WWTPs and eventually into aquatic systems and the environment. It has also been reported that TiO_2 nanoparticles are released from wall paint, and new and aged facade paints, by natural weathering (Kaegi et al., 2008). In the case of SiO_2, tribological studies show that the nanoparticles are released due to friction from SiO_2/acrylate nanocomposites (Reijnders, 2009). It was predicted that silver nanoparticles can find their way into aquatic systems and the environment from antibacterial coatings and composites used in food nano-based applications and agriculture (Köhler et al., 2008; Nowack et al., 2012). However, the release of CNTs from synthetic textiles (e.g. pure CNT yarns interwoven with natural or synthetic polymer yarns, natural or synthetic fibres coated with a layer of pure CNTs and synthetic polymer fibres integrated with CNTs) was difficult to evaluate due to lack of understanding of the degradation processes of the composite materials (Köhler et al., 2008; Nowack et al., 2012).

Even though the degradation processes are not fully understood, Köhler et al. (2008) reported that the release of CNTs could result from the degradation of the matrix material during the

use phase of synthetic textile fibres. The degradation is reported to be caused by chemical and physical effects such as chemicals, water, high temperature, wear and tear, mechanical stress and UV-radiation (Köhler et al., 2008). Basically, the release of nanomaterials into effluents from domestic and industrial wastewaters is influenced by wear of the products that possess these nanomaterials (Musee, 2011; Reijnders, 2009). When these nanoparticles find their way into WWTPs and aquatic systems, their fate, behaviour and transport depends on their physicochemical properties and parameters of the media in which they occur (Joner et al., 2007; Musee, 2011; Oberdörster et al., 2005).

2.1.1.1 Physicochemical properties

The behaviour, transport, and toxicity of ENMs depends on their physicochemical (physical-chemical) properties, a subject that is often neglected during studies on toxicity, fate and behaviour in the environment (Joner et al., 2007; Luyts, Napierska et al., 2013). Parameters such as the pH, ionic strength, type of electrolytes and natural organic matter (NOM) of the influent coupled with the physicochemical properties of the ENMs determine their behaviour and transport, irrespective of whether they are bound or transported in soils or sediments (Joner et al., 2007; Sharma, 2009). Therefore, these abiotic factors should also affect their fate and behaviour in WWTPs as they significantly affect their sedimentation rates (Keller et al., 2010). Just as Oberdörster et al. (2005) proposed a list of physicochemical properties that are indispensable for toxicity studies, the same physicochemical properties are important in fate and behaviour studies. Physicochemical properties that were recommended as key characteristics were: size distribution, agglomeration state, shape, crystal structure, chemical composition, surface area, surface chemistry, surface charge and porosity.

2.1.1.1.1 Effect of abiotic factors on ENMs

a) **pH**: According to Dunphy-Guzman et al. (2006), pH affects the charge of the surfaces of the titania nanoparticles. The transport and aggregation of nanoparticles will differ depending on their point of zero charge (pH_{zpc}), which is affected by particular pH values (Dunphy-Guzman et al., 2006).
b) **Ionic strength**: An increase in the ionic strength of a solution in which particles are suspended leads to aggregation, as the diffuse layer associated with the particles is compressed. This decreases the particle's zeta potential and diminishes inter-particle repulsions, thus allowing aggregation (French et al., 2009).
c) **Type of electrolyte**: The presence of electrolytes will balance and screen surface charges and may induce destabilisation and aggregation of nanoparticles (Keller et al., 2010; Li, 2011).

d) Natural organic matter (NOM): When NOM is adsorbed on the surface of nanoparticles, it shields the surface charges of the nanoparticles. This interaction affects the balance between attractive and repulsive forces, thus influencing their behaviour by controlling aggregation and attachment to environmental surfaces (Keller et al., 2010).

2.1.1.1.2 Effect of physicochemical properties on toxicity

a) Size and surface area: Most studies show that particle size influences the toxicity of a material. There exists an inverse relation between size and toxic potency (Luyts et al., 2013). Kaewamatawong et al. (2005) reported that nanoparticles of silica had a greater ability to induce lung inflammation and tissue damage in mice. In this study, the acute pulmonary toxicity of amorphous silica nanoparticles (14 nm) was compared to that of fine silica particles (213 nm). Size also influences the bioavailability and toxicokinetics of nanoparticles. Choi et al. (2010) studied the role of diameters of instilled nanoparticles using a rat model; specifically, the translocation of nanoparticles rom the lungs to the extrapulmonary regions of the rat body was studied. The study concluded that nanoparticles with a hydrodynamic diameter smaller than 34 nm translocate much more rapidly from the lungs to the mediastinal lymph nodes; nanoparticles with a hydrodynamic diameter <6 nm were found to travel rapidly from the lungs to lymph nodes and the bloodstream and eventually end up being cleared by the kidneys.

b) **Geometry/shape**: The shape or geometry of nanoparticles governs their toxicity in terms of their uptake mechanism and distribution in animals (Luyts et al., 2013). In terms of uptake, several models have been proposed. **Figure 1** illustrates a model proposed by Champion and Mitragotri (2006).

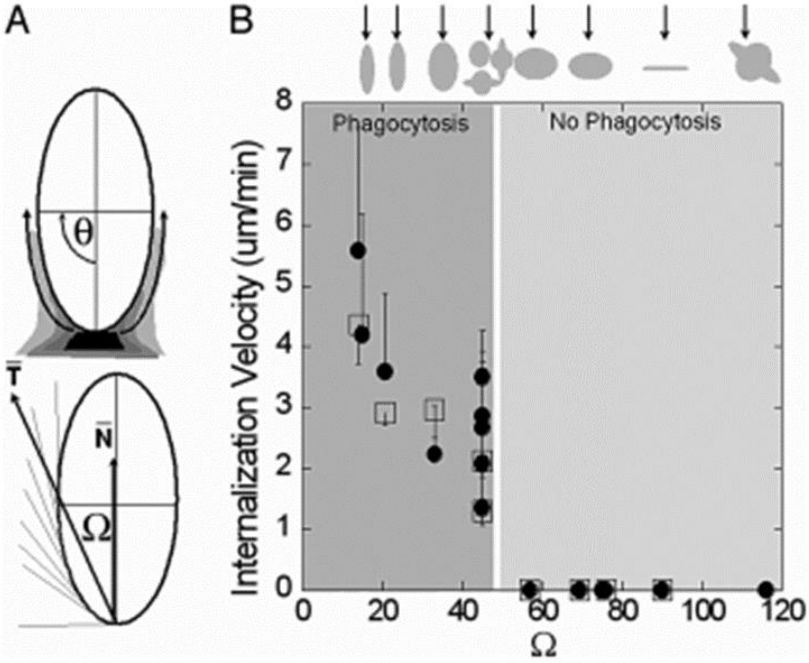

Figure 1 How local particle geometry determines phagocytosis by macrophages

(A) denotes the spreading of the macrophage membrane around the surface of a disk-shaped NP. This process occurs in a tangential fashion where *T* is the average of tangential angles $\theta = 0$ to $\theta = \pi/2$. Ω represents the angle between *N* (the normal at the area of initial particle–cell contact) and *T*. (B) is the internalisation velocity (the course travelled by the membrane over internalisation time) as a function of Ω. Each dot represents a different NP shape, size or aspect ratio and the bars represent SD. The arrows above the differently shaped NPs indicate the attachment site that corresponds to Ω on the x axis in the plot. When $\Omega \leq 45^{o}$, the NPs are internalised, proven by the positive internalisation velocity. Above this critical angle, no internalisation takes place and the cell membrane spreads over the particle (Champion & Mitragotri, 2006; Luyts et al., 2013)

Champion and Mitragotri (2006) used polystyrene nanoparticles of many sizes and shapes to study the role of target geometry in phagocytosis. Based on their observation, they proposed the model (see **Figure 1**) using two variables that influence the phagocytosis. These variables are the tangent angle (Ω) at the point of initial cell contact and the ratio of particle volume to macrophage volume (V*). It was concluded that the phagocytosis was successful when $\Omega \leq 45^{o}$ and $V^* \leq 1$; phagocytosis was not initiated when $\Omega > 45^{o}$ and not completed when $V^* > 1$. This study illustrates the influence and importance of geometry on the uptake of nanoparticles. Furthermore, shape or geometry may be used to explain physical damage that is caused by nanoparticles. According to Luyts et al. (2013) it is comprehensible that nanocrystal

needles can cause cellular and/or tissue damage as opposed to crystal deposition in tissues, which results in tissue damage and strong inflammation.

c) **Surface charge**: Several researchers have tried to explain the correlation between nanoparticle surface charge and toxicological endpoints by considering the effects of nanoparticles' charge on cellular uptake, translocation of nanoparticles to different tissues and cytotoxicity associated with the nanoparticles. Several *in vitro* and *in vivo* studies give credence to the dependence of surface charge on toxicity; these studies have in fact shown that a positive surface charge has a major effect on the toxicological properties of the nanoparticles. Klesing et al. (2010) have shown that, unlike their anionic (-26 mV) counterpart, calcium phosphate-PEI core-shell nanoparticles (+32 mV) loaded with photoactive dye caused cell death in HIG-82 and J774A.1 cells after cellular uptake. Liu et al. (2011) have also illustrated that positively charged polystyrene nanoparticles displayed higher cytoxicity in HeLa and NIH 3T3 cells when compared with negatively charged particles. Nanoparticles with a non-cationic surface charge were shown to travel rapidly from lungs to mediastinal lymph nodes in a rat model (Choi et al., 2010).

2.1.1.2 Importance of characterisation of ENMs

The physical and chemical properties of ENMs are important when analysing ENMs in a particular matrix. Apart from concentration and composition, the chemical characteristics of ENMs on any functional layer on the particle surface is important. Many techniques, including microscopic approaches and spectroscopic and complementary techniques, can be employed to provide information on properties of the ENMs. These techniques should be effective and sensitive enough to measure low concentrations while simultaneously minimising disturbance of samples to ensure that laboratory characterisation produces results from an unperturbed environmental state. **Table 2** gives a summary of the characteristics of nanoparticles as well as analytical techniques that are suitable for their characterisation. The characterisation of the physicochemical properties of ENMs is a necessary activity and each property is important in terms of explaining the toxicity, fate and behaviour of ENMs. **Table 3** summarises the properties of nanoparticles and respective their importance (Tiede et al., 2008).

Table 2 Properties of nanoparticles and examples of analytical methods that are potentially suitable for their measurement (Tiede et al., 2008)

Nanoparticle properties	**Microscopy and related techniques**	**Spectroscopic and related techniques**	**Other techniques**
Aggregation	STEM, TEM, SEM, AFM, STM	XRD, SANS	Zeta potential
Chemical composition	AEM, CFM	NMR, XPS, Auger, AES, AAS, MS, XRD, EBSD	
Mass concentration	AEM, CFM		Gravimetry, thermal analysis
Particle number concentration			Particle counter, CPC
Shape	STEM, TEM, SEM, AFM, STM		
Size	STEM, TEM, SEM, AFM, STM		DMA
Size distribution	STEM, TEM, SEM, AFM, STM	SPMS, SAXS	UCPC, SMPS
Dissolution			Voltammetry, diffuse gradients in thin films
Speciation		XAFS, XRD	Titration
Structure	STEM, TEM, SEM, AFM, STM	XRD, SANS	
Surface charge			Zeta potential
Surface chemistry	AEM, CFM	XPS, Auger, SERS	

Table 3 Properties of nanoparticles and their respective importance of measurement (Tiede et al., 2008)

Property	Importance of measurement
Aggregation	Nanoparticles that have a tendency to aggregate may keep their functionality; however, the increase in size could lead to a decrease in uptake
Elemental composition	Different particle composition leads to different behaviour/impact, e.g. Cd versus Fe
Mass concentration	Normally, increased contaminant concentration leads to an increase in toxicity/impact, but this is not always applicable to nanoparticles
Particle number concentration	Nanoparticles have low mass concentrations, but show a high percentage of total particle numbers
Shape	Different particle shapes (e.g. spherical, tubular) can possess different affinities or accessibilities, e.g. transport through membranes into cells, different antibacterial behaviour
Size and size distribution	Nanoparticles are defined and classified according to their size, and size is one of the primary properties describing transport behaviour
Solubility	Soluble nanoparticles – their ionic form can be harmful or toxic (e.g. ZnO versus Zn^{2+})
Speciation	Different species can have different behaviour, toxicity, impact (e.g. C_{60} versus C_{70}, ENP complexes with natural organic matter or oxidation state)
Structure	The structure can influence stability or behaviour (e.g. rutile or anatase as possible crystal structures of TiO_2)
Surface area (and porosity)	Increase in surface area increases reactivity and sorption behaviour
Surface charge	Surface charge influences particle stability, especially in dispersions
Surface chemistry	Coatings can consist of different chemical compositions and influence particle behaviour or toxicity (e.g. quantum dots with CdSe core and ZnS shell)

2.1.2 Titanium dioxide nanoparticles

Although titanium (Ti) is the seventh most abundant metal on earth, it is the ninth most abundant element. Ti has reserves that exceed 600 million tons; however, it is estimated that annual production of Ti metal and TiO_2 is only only 90 000 tons and 4.3 million tons, respectively (Kiser et al., 2009). TiO_2 is available in the environment through both natural and man-made sources. Minerals like rutile (TiO_2) and ilmenite ($FeTiO_3$) are the main natural sources of TiO_2; they are constituents of plantonic and metamorphic rocks and are also found as clear minerals in beach sands (Sharma, 2009).

TiO_2 naturally occurring in soil, and synthetic TiO_2, are used in commercial products that have been utilised for years, most of which are used in nano-based products (Kiser et al., 2009; Musić et al., 1997; Sharma, 2009; Westerhoff et al., 2011). TiO_2 is used as a white pigment in products such as paints, plastics, inks, paper, cosmetics, food-stuffs, pharmaceuticals and

sunscreens (Kiser et al., 2009; Musee, 2011; Musić et al., 1997; Westerhoff et al., 2011). Other applications of TiO_2 include water purification and photoelectric systems such as nanolasers, diodes, biosensors, solar cells and drug delivery systems in medicine (Chaüque, 2012; Porkodi & Arokiamary, 2007). The increase in applications is due to the many properties that TiO_2 possesses, including optical, chemical and mechanical properties, yet these parameters are dependent on the crystalline phase in which TiO_2 exists (Bersani et al., 1998; Parra et al., 2008; Qu et al., 2013). These crystalline phases are anatase, rutile and brookite, with anatase being the most extensively used in many applications, especially photocatalysis (Parra et al., 2008). The desirable properties of TiO_2 are high chemical stability, low human toxicity, low cost, photocatalytic activity in UV and possible visible light range (Qu et al., 2013).

TiO_2 nanoparticles are synthesised via many methods, including hydrothermal synthesis, solvothermal synthesis, sol-gel synthesis, direct oxidation synthesis, chemical vapour deposition synthesis, electrodeposition synthesis, sonochemical synthesis, and microwave synthesis (Byranvand et al., 2013). Among these methods, the sol-gel method is the most versatile and easy to use. Nanoparticles synthesised by sol-gel have high surface areas; an additional advantage associated with this method is that meso- to macroporous nanoparticles can be produced. Metastable phases that are normally impossible to achieve can be obtained at low temperatures due to the reactivity and versatility of the reactants used in the alkoxide-based sol-gel method (Parra et al., 2008). Thus the sol-gel method makes it possible to control the crystalline phase of the TiO_2 nanoparticles, the number of defects and the size of the crystals (Bersani et al., 1998).

2.1.2.1 TiO_2 in wastewater treatment systems and aquatic environments

2.1.2.1.1 Photocatalytic degradation of dye

Photocatalysis using TiO_2 has been applied in many photocatalytic mechanisms due to TiO_2 being a suitable semiconductor (Saien and Soleymani, 2007). The use of TiO_2 as the most favoured semiconductor photocatalyst is linked to its high efficiency, low cost, physical and chemical stability, widespread availability and non-toxic properties (Min, Wang and Han, 2007; Paulauskas et al., 2013; Tan et al., 2011). Furthermore, the use of TiO_2 in wastewater remediation is based on the following reasons (Saien and Soleymani, 2007):

i. the process occurs under ambient conditions;
ii. the formation of photocatalysed intermediate stable products is avoided, unlike in direct photolysis techniques;
iii. there is complete oxidation of substrates to CO_2;
iv. has a high turnover and is inexpensive;

v. it offers great opportunity as a technology that can be industrialised to purify wastewaters.

The photodegradation of organic species by oxidation proceeds through the widely accepted mechanism, which is illustrated in equations [1-4]. When a photocatalyst (e.g. TiO_2) is illuminated with a photon of energy equal to its band gap, electrons are promoted from the valence band to the conduction band (e_{cb}^-) while generating energised holes (h_{vb}^+) in the valence band (Gúmúş & Akbal, 2011; Leung et al., 2007; Tan, Wong & Mohamed, 2011). The species that are absorbed on the surface of the photocatalysts may participate in redox reactions with the electrons and holes migrating to the surface of the photocatalyst. The holes may react with H_2O or OH^- to produce the hydroxyl radical while the electrons are picked up by oxygen to generate superoxide radical anions ($O_2^{\bullet -}$) (Faisal, Tariq & Muneer, 2007; Gúmúş & Akbal, 2011).

$$TiO_2 + h_v = e_{cb}^- + h_{vb}^+ \quad \textbf{[1]}$$

$$e_{cb}^- + O_2 = O_2^{\bullet -} \quad \textbf{[2]}$$

$$h_{vb}^+ + H_2O = {}^{\bullet}OH + H^+ \quad \textbf{[3]}$$

$$h_{vb}^+ + OH^- = {}^{\bullet}OH_{ad} \quad \textbf{[4]}$$

The hydroxyl radicals and superoxide radical anions have been suggested to be the primary oxidising species in the photocatalytic process leading to bleaching of the dye (Faisal Tariq & Muneer, 2007; Gúmúş & Akbal, 2011; Julkapli et al., 2014). **Figure 2** illustrates the generation of electrons and holes that lead to the photocatalytic degradation of organics (e.g. dye pollutants) in wastewater.

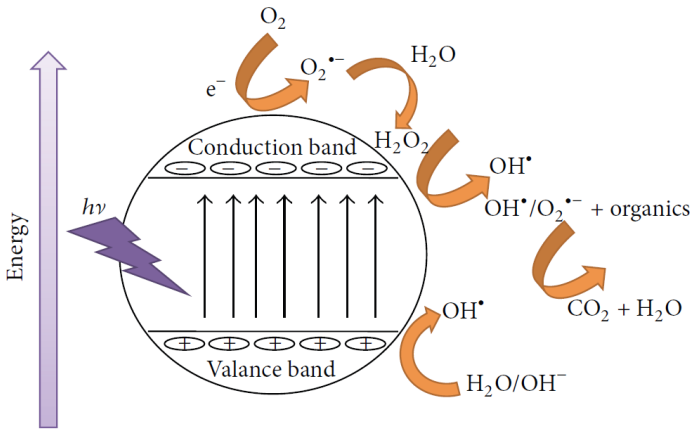

Figure 2 Photocatalytic mechanism and degradation process (Julkapli et al., 2014)

Although TiO_2 has high photoactivity and has been used as a photocatalyst for the treatment of organic and dye pollutants (Ghaly, Farah & Fathy, 2007), various factors limit its application as a photocatalyst (Min et al., 2007; Ni et al., 2007). A variety of strategies have been adopted with a view to minimising limiting factors such as the large band gap, high electron-hole recombination rate and the sole utilisation of the UV region of the magnetic spectrum at which irradiation of TiO_2 is carried out. Among these strategies, chemical modification of TiO_2 by doping has led to the successful separation of the electron-hole pair, reduction of recombination, and utilisation of visible light, which have in turn led to the overall improvement of photocatalytic activity of the TiO_2 (Ni et al., 2007; Pelaez et al., 2012).

Chemical modification of TiO_2 by doping has been carried out using metals (Cr, Co, V, Cu, Pt, Au, Ni, Mn, Nb, W and Fe) and non-metals (F, C, S, B and N), with non-metal doping showing great promise in achieving visible light active photocatalysis (Cong et al., 2007; Ni et al., 2007; Pelaez et al., 2012; Sacco et al., 2012). This is because metal doping can result in thermal stability and an increase in carries trapping, which in turn leads to a decrease in the photocatalytic efficiency (Sacco et al., 2012). Furthermore, nitrogen has been reported to be the most promising dopant among the non-metals (Fujishima, Zhang & Tryk, 2008; Pelaez et al., 2012). When TiO_2 is doped with nitrogen, photoactivity is improved due to the decrease in the band gap caused by mixing of N 2p states with O 2p states on top of the valence band, or the generation of a N-induced midgap level (Asahi et al., 2001; Cong et al., 2007). The ability of nitrogen to lower the band gap, which improves visible light activity, provides a good opportunity for the extensive application of TiO_2 such as oxidation of CO, ethanol, gaseous 2-propanol, acetaldehyde, and NO_x as well as the degradation of dyes such as methylene blue (Cong et al., 2007).

Several research groups have reported limited success in working towards the decomposition of dyes in wastewater using visible light activated doped-TiO_2. Asahi et al. (2001) reported substantial photocatalytic activity of N-TiO_2 towards the decomposition of methylene blue under 500 nm wavelength illumination. In the same study, the photocatalytic activity of N-TiO_2 was shown to be superior to that of pristine TiO_2. Dlamini et al. (2011) investigated the photodegradation of bromophenol blue (BPB) using a fluorinated TiO_2 composite and the fluorinated TiO_2 catalyst was found to degrade BPB efficiently; this is because the fluorinated TiO_2 was found to induce the production of excess free radicals whereas the pure TiO_2 did not.

2.1.2.1.2 Behaviour of TiO_2

Before industrial effluent can be released, WWTPs play an important role in minimising any pollutants that might find their way into the aquatic environment (Chaüque, 2012). However, WWTPs were found not to be fully effective in minimising the leaching of ENMs into aquatic environments (Kim, 2014; Kiser et al., 2009; Musee, 2011; Westerhoff et al., 2011). Current available data on the removal of ENMs by WWTPs, and on the adverse effects of ENMs, indicate that little is understood about their fate and behaviour before they even reach aquatic systems (Brar et al., 2010; Chaüque, 2012; Kiser et al., 2009). ENMs can be released through washing from consumer products into sewage (e.g. TiO_2 and ZnO in sunscreens and UV-absorber lotion) and various studies have confirmed the movement and presence of ENMs into WWTPs (Kim, 2014). In the USA, the occurrence and presence of ENMs in WWTPs was confirmed through the analysis of titanium (Ti) in raw sewage and treated effluents from ten large scale WWTPs (Westerhoff et al., 2011).

Studies aimed at the removal of ENMs during water treatment provide an understanding of the fate and behaviour of ENMs in WWTPs and aquatic environments. Chaüque (2012) monitored physicochemical parameters and the behaviour of ZnO nanoparticles in a simulated wastewater treatment plant (SWWTP) fed with raw wastewater from Johannesburg Water (Gauteng, South Africa). The study reported a potential release of engineered nanoparticles (ENPs) with an increase in ENP concentration and larger fractions of ENPs associated with sludge. Of interest in terms of the fate and behaviour of nanoparticles, the removal efficiency of ZnO ENPs was reported to be directly proportional to the ionic strength and pH of the wastewater investigated. The fate of nano-CeO_2 (cerium dioxide) during wastewater treatment was investigated using a laboratory-scale activated sludge system (Gómez-Rivera, 2012; Field, 2012). The study reported 96.6% Ce removal by activated sludge treatment with effluent concentrations of CeO_2 nanoparticles (<200 nm) averaging 0.11 mg Ce/L. The CeO_2 was said to be mediated by agglomeration or sedimentation of larger particles and by sludge biosorption. Kaegi et al. (2011) studied the behaviour of metallic silver nanoparticles in a pilot wastewater treatment plant. Using a mass balance and previously measured Ag concentrations, the study concluded that 5% of added Ag left the WWTP via effluent, 85% ended up in sludge and 5% remained in the WWTP. These studies suggest that TiO_2 is removed with the sludge since TiO_2 adsorbs on the biosolids during treatment of wastewater (Kiser et al., 2009). It is therefore possible that the TiO_2 ENMs have an effect on the microbes employed for the removal of organic pollutants from wastewater when an aerobic-activated sludge process is used, thus inducing a holistic effect on the functionality of the WWTPs.

Biological manipulation to remove wastewater contaminants utilises microorganisms for remediating industrial and municipal wastewater. The process depends on the availability of contaminants that feed the bacteria, which leads to the breaking down or complete removal of the contaminants from the wastewater. The microbe-based treatment method is beneficial for plant treatment efficiency due to its low cost, ability to reduce many contaminants, and its versatility (Musee, 2011). The functionality and performance of the WWTP is dependent on the survival of the microorganisms (Musee, 2011; Wagner et al., 2002). Thus, it is important to assess the possible effects of ENMs on the WWTPs (Klaine et al., 2008; Musee, 2011). Musee (2011) has reported that TiO_2 nanoparticles are able to alter the nitrogen-fixing activity of *Anabaena variabilis*. Work undertaken by Klaine et al. (2008) has also reported that TiO_2 nanoparticles prevent membrane fouling in wastewater treatment by inhibiting *Escherichia coli* (*E. coli*) when the system was placed under ultraviolet illumination. The antibacterial effect of TiO_2 nanoparticles on *Psuedomonas* species was illustrated by Ozaki (2013). The bacteria mentioned above are part of the microbial consortia found in WWTPs. To this end, it is paramount to study the fate and behaviour of TiO_2 nanoparticles with a view to understanding fully the potential adverse effects of the nanoparticles on the bacteria found in the WWTPs. Lessons derived from understanding the effects of the nanoparticles on the bacteria would aid in the development of a technology that is effective in the removal of contaminants from wastewater (Klaine et al., 2008; Musee, 2011; Ozaki, 2013).

2.1.2.2 Stability of TiO_2 nanoparticles

Understanding the stability of ENMs in WWTPs and in aquatic environments helps in understanding whether the ENMs will settle out from wastewater, then sediment in aquatic environments, as this is linked to agglomeration/aggregation of ENMs (Chaüque, 2012). Understanding stability and how the ENMs become unstable and thus agglomerate or aggregate is crucial when determining the fate and behaviour of ENMs in WWTPs and the aquatic environment (Chaüque, 2012; Sharma, 2009). The stability of ENMs is greatly affected by the medium in which the ENMs are contained (Chaüque, 2012). Factors that influence the stability of TiO_2 nanoparticles in WWTPs include pH, ionic strength, ionic composition and NOM (Chaüque, 2012; Keller et al., 2010; Kiser et al., 2009).

During the agglomeration/aggregation of TiO_2 nanoparticles, pH is particularly important (Dunphy-Guzman et al., 2006; Sharma, 2009). Sharma (2009) reported that agglomeration/aggregation size increases when the pH nears point of zero charge (pH_{zpc}); this tendency is generally observed during the settling of particles. The electro-repulsion of particles seemed to constitute the basis for understanding the causes of agglomeration/aggregation. When the media in which the particles are contained approaches

the pH_{zpc}, the electro-repulsion forces between nanoparticles decreases and the nanoparticles agglomerate/aggregate (Sharma, 2009). French et al. (2009) have also demonstrated that TiO_2 nanoparticles form agglomerates/aggregates at specific conditions of pH and ionic strength. Furthermore, the relative size of aggregates reportedly changed upon variation of the pH (Pettibone et al., 2008). Apart from pH, ionic strength and the nature of the electrolyte(s) in aqueous suspension affect the agglomeration/aggregation of TiO_2 nanoparticles. Using dynamic light scattering (DLS), 4-5 nm TiO_2 nanoparticles were shown to form stable aggregates with an average diameter of 50–60 nm at pH~4.5 in a NaCl suspension of an ionic strength of 0.0045M. When the ionic strength was increased to 0.0165M, keeping the pH constant, the TiO_2 nanoparticles formed micron-sized aggregates within 15 min. When the electrolyte was changed to $CaCl_2$ at an ionic strength of 0.0128M, the formation of aggregates occurred within 5 min at pH 4.8; this was way quicker than when NaCl was used as an electrolyte at the same ionic strength and pH (French et al., 2009).

NOM (natural organic matter) inevitably interacts with nanomaterials in wastewater to form complexes. NOM is the compounds generated by physical, chemical and biological activities from plants, animals and microorganisms, including their waste and metabolic products, which results in a diverse mixture of structurally complex compounds (Kim & Yu, 2005; Nkambule, 2012). NOM can be further classified into large groups, namely humic substances, microbial by-products and colloidal NOM (Nkambule, 2012). These compounds have diverse functional groups that can interact and affect the stability of nanomaterials. When nanomaterials become coated with NOM, they become negatively charged and this has an impact on their fate and transport in the aqueous environment (Yang, Lin & Xing, 2009). Adsorption of NOM on nano-oxides enhances their suspension in water (Pettibone et al., 2008; Yang, Lin & Xing, 2009; Zhang et al., 2009). To determine the fate, behaviour and transport of nanoparticles, investigations were carried out to assess how NOM affects the stability of the nanoparticle. Furthermore, the effect of NOM on the stability of the nanoparticles was correlated to the functional groups present in NOM, which ultimately determine the uptake and distribution of nanoparticles from aqueous media (Chaüque, 2012). The effect of NOM and divalent cations (Ca^{2+}) on the stability of engineered metal oxide nanoparticles (including TiO_2) has been investigated (Zhang et al., 2009). The study concluded that NOM plays an important role in influencing the stability of nanoparticles in water, and it does this by increasing the surface potentials of the nanoparticles after imparting a negative charge to the nanoparticle surface. This means that NOM stabilises nanoparticles in water, thus reducing their agglomeration/aggregation. However, it has been demonstrated that, in the presence of Ca^{2+}, agglomeration/aggregation is induced; this is because the divalent cation neutralises the negative charges that were induced on the nanoparticles by the NOM. Therefore, the ionic

strength of water also plays an important role on how NOM affects the agglomeration/aggregation of nanoparticles (Zhang et al., 2009).

2.1.2.3 Toxicity of TiO_2 nanoparticles

Nanoparticles differ from microparticles made up of the same material, in terms of chemical, optical, magnetic, biological and structural properties. It is noteworthy that the physicochemical characteristics of nanoparticles are closely associated with biological effects that give them their toxicological profile (Lavicoli et al., 2011). Therefore, a proper characterisation of nanomaterials, combined with an understanding of the processes that take place on the surface of nanoparticles when they are in contact with living systems, is important in understanding the possible toxicological effects.

Numerous *in vitro* (on different cell lines) and *in vivo* (using mice/rodents) toxicological studies of TiO_2 nanoparticles have been conducted on bacteria (Chaüque, 2012; Cherchi & Gu, 2010; Luyts et al., 2013; Maness et al., 1999; Musee, 2011). Musee (2011) and Maness et al. (1999) reported that the antimicrobial toxicity of TiO_2 nanoparticles is due to the production of free radicals. The toxicity was further confirmed to follow a two-step mechanism: the outer cellular membrane is first oxidatively destabilised, followed by free radical attack of the cytoplasmic membrane (Musee, 2011; Sunada, Watanabe & Hashimoto, 2003). Other investigations of the routes of bacterial toxicity of TiO_2 nanoparticles have also reported the generation of hydroxyl radicals, oxidative toxicity and destabilisation of cellular membrane integrity (Musee, 2011). As physicochemical characteristics have been associated with toxicity, Other studies have reported that the toxicity of TiO_2 nanoparticles is influenced by physicochemical properties like shape and size (Musee, 2011; Simon-Deckers et al., 2009). An investigation by Simon-Deckers et al. (2009) confirmed that the toxicological impact of metal oxide nanoparticles (TiO_2 included) and carbon nanotubes on bacteria (*Cupriavidus metallidurans* and *E. coli*) is dependent on size, composition, surface charge and shape.

Wastewater treatment via the activated sludge process depends on bacteria as the working force for the breakdown of contaminants. The bacteria need to remain unaffected by other contaminants in the wastewater for the treatment to be completely efficient. This has resulted in investigations on the antibacterial activity of SiO_2, TiO_2 and ZnO nanoparticles (Adams et al., 2006; Chaüque, 2012). A study on the comparative eco-toxicity of nanoscale TiO_2, SiO_2, and ZnO water suspensions was undertaken using Gram-positive *Bacillus subtilis* (*B. subtilis*) and Gram-negative *E. coli* as test organisms. TiO_2 was found to be the second most active

after SiO_2, and *B. subtilis* was the most susceptible to the nanoparticles under investigation, with antibacterial activity increasing with particle concentration (Adams et al., 2006). The susceptibility of Gram-positive bacteria towards TiO_2 has since been confirmed by other studies (Fu, Vary & Lin, 2005).

Many studies on the toxicity of TiO_2 nanoparticles to human and animal cells have been reported and reviewed, with suggestions made on future areas to be investigated. Gurr et al. (2005) reported induced oxidative DNA damage, lipid peroxidation, and micronuclei formation, as well as increased hydrogen peroxide and nitric oxide production in a human bronchial epithelial cell line (BEAS-2B cells) by anatase TiO_2 nanoparticles (sized 10 and 20 nm), in the absence of photoactivation. It was concluded that the smaller the particles, the easier for oxidative damage to be induced, as treatment with anatase particles 200 and >200 nm did not induce oxidative stress in the absence of light. Furthermore, anatase TiO_2 has been reported to be more toxic than the other polymorphs of TiO_2 due to its high photoactivity (Gurr et al., 2005; Kakinoki et al., 2004; Sayes et al., 2006; Warheit et al., 2007). Sayes et al. (2006) reported anatase to be 100 times more toxic than rutile when human dermal fibroblasts (HDF) and human lung epithelial cells (A549) were used. The anatase TiO_2 nanoparticles were shown to decrease the mitochondrial activity (cellular viability) and enhanced interleukin 8 (IL-8) in both HDF and A549 cell lines. Anatase has also been reported to be more potent than a mixture of anatase and rutile (Sayes et al., 2006).

In vivo studies indicate that ultrafine anatase/rutile TiO_2 nanoparticles are more toxic than fine TiO_2 nanoparticles on a mass basis, which is attributable to the greater surface area associated with ultrafine particles (Bermudez et al., 2004; Warheit et al., 2007). According to Warheit et al. (2007), 80/20 anatase/rutile P25 ultrafine-TiO_2 nanoparticles caused more lung inflammation, cytotoxicity, cell proliferation and histopathological responses than rutile R-100 fine-TiO_2 and ultrafine rutile TiO_2 particles after intra-tracheal instillation of the different nanoparticles in rats. However, upon exposure of the rats to different concentrations of pigmentary TiO_2 particles, the responses were found to be unique to a particular rodent species (Bermudez et al., 2002).

2.1.3 Wastewater treatment plants

WWTPs have played an important role in wastewater recycling since their introduction to human civilisation in Britain in the 20th century. Wastewater treatment processes employ tailored methods for specific treatment depending on the application of the treated water.

These applications include disposal to water systems for restoring anthropogenic water usage, reinforcing the public water supply and irrigation in agriculture (Chaüque, 2012). Thus, WWTPs will vary in the treatment applied depending on the characteristics of the influent water and depending on the target water quality effluent.

The difference in the composition of wastewater depends on the type of community in which it originates. Composition of wastewater includes suspended solids, sediments, minerals, toxic compounds, inorganic chemicals, dissolved and suspended organic materials, nutrients, pathogens and parasites (Chaüque, 2012; Sonune & Ghate, 2004). **Table 4** illustrates the general profile of raw wastewater. Basically, wastewater is made up of a combination of solids and liquids from domestic and/or industrial settings. Therefore, wastewater can be classified into two types: domestic and industrial. These solids and liquids are reduced through the breakdown of highly complex organic solids that are able to decay to mineral or stable organic solids in a process called wastewater treatment (Sonune & Ghate, 2004). This process also includes the removal or inactivation of pathogens and parasites in the wastewater (Chaüque, 2012).

Wastewater treatment comprises chemical or biological reactions and physical forces, known as unit processes and unit operations respectively. **Figure 3** illustrates where these unit operations occur in a typical wastewater treatment plant. These unit processes and unit operations can also be categorised according to the respective stages of treatment, known as preliminary, primary, secondary and tertiary treatment. In the preliminary level, wastewater constituents such as rags, sticks, floatables, grit and grease are removed. Primary treatment involves the removal of some suspended solids and organic matter. The treatment can be enhanced by adding chemicals, usually $Al_2(SO_4)_3$, or filtration. Secondary treatment, without nutrient removal, involves removal of biodegradable organic matter and suspended solids. Secondary treatment with nutrient removal removes biodegradable organics, suspended solids and nutrients (nitrogen (N), phosphorus (P), or both N and P). The last treatment stage (i.e. tertiary treatment), incorporates the removal of residual suspended solids and disinfection of the wastewater to remove or inactivate pathogens and parasites. Furthermore, the biological treatment level can be categorised into two: attached growth or biofilm (e.g. biofilters) and suspended growth (e.g. activated sludge and lagoons) (Metcalf & Eddy, 2003; Sonune & Ghate, 2004).

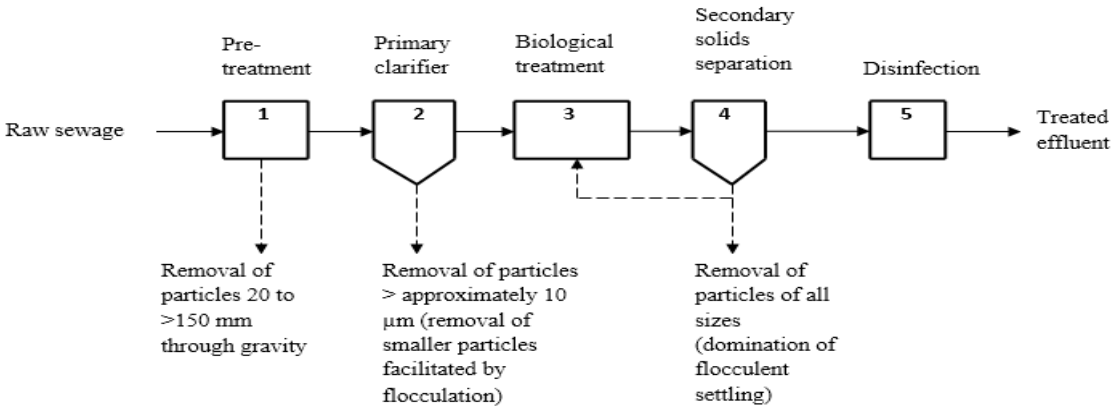

Figure 3 Conventional WWTP process that employs an activated sludge system (Kiser et al., 2009; Metcalf & Eddy, 2003)

Although biological treatment for the removal of wastewater contaminants has been used and developed over many years, it still has its shortcomings. For example, biological methods take much time, and cannot degrade some of the complicated synthetic dyes that are increasing in wastewater (Gúmúş & Akbal, 2011; Pirkarami & Olya, 2014). To overcome such challenges, more efficient methods are constantly being researched and developed. Among the many methods that have been developed for the removal of dye in wastewater, advanced oxidation processes (AOPs) are among the most efficient. AOPs are capable of achieving high oxidation yields from several kinds of organic compounds (Gúmúş & Akbal, 2011). AOPs include ozonation, photocatalysis and photo-fenton (Can et al., 2006; Pirkarami & Olya, 2014).

The basis of AOPs is the generation of very reactive species such as hydroxyl radicals ($OH^{\bullet}$) that are excessively reactive and strong oxidising agents capable of breaking down organic compounds. Photocatalysis has gained popularity due to its ability to completely mineralise, under moderate conditions, the organic contaminants in wastewater into harmless compounds such as CO_2 and H_2O (Guillard et al., 2003; Gúmúş & Akbal, 2011; Saien & Soleymani, 2007). TiO_2 powder is among the most used photocatalysts, used in most cases for the degradation of organic compounds in wastewater under UV illumination (Guillard et al., 2003). Therefore, the main objective of this study is to evaluate the effect of TiO_2 on biological wastewater treatment, and the photocatalytic degradation of dye in wastewater.

Table 4 Typical profile of untreated raw wastewater (Metcalf & Eddy, 2003)

Contaminants	Unit	Concentration		
		Low strength	Medium strength	High strength
Total solids (TS)	mg/L	390	720	1230
Total dissolved solids (TDS)	mg/L	270	500	860
Fixed	mg/L	160	300	520
Volatile	mg/L	110	200	340
Total suspended solids (TSS)	mg/L	120	210	400
Fixed	mg/L	25	50	85
Volatile	mg/L	95	160	315
Settleable solids	mg/L	5	10	20
Biochemical oxygen demand, 5-d, 20°C (BOD, 20°C)	mg/L	110	190	35p
Total organic carbon (TOC)	mg/L	80	140	260
Chemical oxygen demand (COD)	mg/L	250	430	800
Nitrogen (total as N)	mg/L	20	40	70
Organic	mg/L	8	15	25
Free ammonia	mg/L	12	25	45
Nitrites	mg/L	0	0	0
Nitrates	mg/L	0	0	0
Phosphorus (total as P)	mg/L	4	7	12
Organic	mg/L	1	2	4
Inorganic	mg/L	3	5	8
Chlorides	mg/L	30	40	90
Sulphate	mg/L	20	30	50
Oil and grease	mg/L	50	90	100
Volatile organic compounds (VOCs)	µg/L	<100	100-400	>400
Total coliform	No./100 mL	10^6-10^8	10^7-10^9	10^7-10^{10}
Faecal coliform	No./100 mL	10^3-10^5	10^4-10^6	10^5-10^8
Cryptosporidium oocyts	No./100 mL	10^{-1}-10^0	10^{-1}-10^1	10^{-1}-10^2
Giardia lamblia cysts	No./100 mL	10^{-1}-10^1	10^{-1}-10^2	10^{-1}-10^3

2.1.3.1 Activated sludge wastewater treatment

Activated sludge (AS) treatment of wastewater employs microorganisms that biologically degrade organic matter. The AS is a confluence of microorganisms that form solids when they are used for wastewater treatment using the AS treatment process. The AS includes aerobic and anaerobic microorganisms (autotrophic or heterotrophic), accumulated food materials, and waste products from aerobic decomposition. AS wastewater treatment is a technology that produces an extremely high quality effluent (Chaüque, 2012; Grady et al., 2011; Spellman, 2003). The AS process includes bacteria and other microorganisms such as fungi, protozoa, and rotifers consisting of human and animal viruses (Chaüque, 2012; Musee, 2011). The growth of the different types of microorganisms depends on the environmental conditions that are unique to that particular microorganism; different microorganisms grow under different environmental conditions. Therefore, the type of wastewater to be treated will in all likelihood influence the process design and mode of operation of the treatment plant.

During aerobic wastewater treatment using the AS process, the influent is mixed with the AS and oxygen is pumped into the wastewater liquor by mechanical mixing in order to create a biological floc that changes the organic matter in the wastewater into a flocculent microbial suspension. The flocs are able to settle out of the wastewater in the clarifier due to gravity. The AS process is capable of treating influents from both domestic settings and industrial settings such as pulp and paper mills, textile factories, food industries, butcheries, coal gasification wastes, petrochemical by-products, and oil refinery wastes (Chaüque, 2012). Specific groups of bacteria catalyse the reactions involved in the treatment of the different types of contaminants found in these influents.

2.1.3.1.1 Bacterial removal of contaminants

Benefits associated with the use of bacteria-based treatment processes include low cost and the ability to transform various contaminants and thereby reduce their concentrations. However, the ability to completely remove pollutants and the ability of the microbes to function in constantly changing physical and chemical conditions in wastewater are the greatest advantages for the treatment of different kinds of influent compositions. The removal of contaminants exploits a combination of microbiological treatment processes, mainly aerobic, anoxic and anaerobic, depending on the wastewater quality and effluent quality limits. This offers a maximum treatment efficiency compared to chemical and physical processes that are costly, difficult, and time consuming (Grady et al., 2011). Microbiological treatment processes can be tailored to remove organic contaminants, inorganic contaminants, metal ions and endocrine disrupting chemicals (EDCs).

2.1.3.1.1.1 Removal of organic contaminants

Organic contaminants include dyes, pesticides, fuels, antibiotics, solvents and chlorinated phenolics. These xenobiotic contaminants should be removed from wastewater as they are by design expected to modify biological functions, and are said to be toxic, mutagenic, carcinogenic and teratogenic. Bacteria in the WWTPs can partially or completely break down the organics through aerobic or anaerobic processes (Musee, 2011). Sinha et al. (2009) reported thirty-two genera of bacteria that can break down organic compounds such as polyaromatic hydrocarbons (PAHs), phthalate compounds, halogenated organic compounds, azo dyes and pesticides. These bacteria include genera such as *Bacillus*, *Arthrobacter*, *Pseudomonas*, *Mycobacterium*, *Sphingomonas*, and *Xanthomonas* species.

2.1.3.1.1.2 Removal of inorganic contaminants

Inorganic contaminants include nitrogen and phosphates, which usually occur in high concentrations in wastewater (Musee, 2011). The removal of nitrogen employs a separate stage that involves nitrification and denitrification for the conversion of ammonia to nitrate and nitrate to nitrogen gas. The removal of nitrogen is achieved under anoxic conditions, which is a downstream treatment process occurring before the aerobic zone. The removal of phosphates is through the anaerobic zone, which occurs before the anoxic zone and encourages the growth of specialised phosphorus-storing bacteria (Grady et al., 2011). The following bacteria are used in the removal of nitrogen and phosphates: *Acinobacter*, *Betaproteobacter*, *Nitrosomonas*, *Nitrobacter*, *Nitrospira*, *Gemmatimona*, and *Thiosphaera* (Musee, 2011).

2.1.3.1.1.3 Removal of endocrine disrupting chemicals

According to the World Health Organization/United Nations Environment Programme (2012), EDCs are endogenous substances that disrupt endocrine system functionality, which causes harmful health effects in an organism, and these harmful effects may be further transferred to its progeny or populations. These compounds, which are either naturally occurring or man-made, are constituents of a variety of materials, including pesticides, metals, additives or contaminants in food, and personal care products. EDCs are linked to altered reproductive function in humans (both males and females), an increase in breast cancer cases, slow neurodevelopment in children and changes in immune function (DWA, 2010; World Health Organization/United Nations Environment Programme, 2012). Examples of EDCs include diethylstibestrol, dioxin and dioxin-like compounds, polychlorinated biphenyls (PCBs) and pesticides such as dichlorodiphenyltrichloroethane (DDT). Bacteria can degrade EDCs by reducing the endocrine disruptor activity in the wastewater in various different conditions (Musee, 2011). Andersen et al. (2003) reported a decrease in oestrogen activity caused by high levels of bacterial denitrification in a WWTP. Complete and/or partial breakdown of various organic EDCs utilising bacteria in wastewater have been reported (Musee, 2011; Roccaro et al., 2013). When physical and chemical phases are compared to bacterial removal of EDCs, bacterial removal is said to be more efficient (Liu, Kanjo & Mizutani, 2009). Furthermore, improved reduction of endocrine disruptors caused by increased residential time in bacterial treatment has been reported (Svenson, Allard & Ek, 2003).

2.1.3.1.1.4 Removal of metal ions

Metal ion removal is carried out by bacteria that change the redox state of the metal ion through biosorption or bioaccumulation. Although metal ions are important for metabolism, they can be detrimental to aquatic organisms at elevated levels. It is thus paramount that WWTPs reduce the metal content to acceptable levels before effluent is released to the environment (Musee, 2011). One mechanism by which metal ions are removed from wastewater involves the use of electron receptors during anaerobic respiration. For example, *E. coli* and *Thiobacillus ferrooxidans* were reported to remove Hg^{2+} by altering it to Hg (White, Sayer & Gadd, 1997). Biological materials (e.g. dead bacterial cells, protozoans, yeasts, fungi and plants) are said to play an important part in heavy metal removal. The use of bioflocculants for the removal of metal ions is receiving more attention as they contain organic groups to which the metal ions bind. This method is viewed as economical compared to physical and chemical methods. Lin and Harichund (2011) produced bioflocculants from *Herbaspirillium*, *Paenibacillus*, *Bacillus*, and *Halomonas* species for the treatment of industrial wastewater. This bioflocculants were shown to simultaneously and effectively remove several heavy metals; for example, 95% of Cr^{2+} and 94% of Ni^{2+} ions in biavin medium blue dye effluent were removed by bioflocculants (Lin & Harichund, 2011).

2.1.3.1.2 Performance characteristics of an activated sludge system

2.1.3.1.2.1 Floc formation

Flocculation in wastewater treatment is an important requirement that assists in the formation of aggregates (flocs) from the finely divided and chemically stable particles. This mechanism enables the formation of larger particles from unstable particles so that they can be removed readily when they settle in the secondary settling tanks (Grady et al., 2011; Metcalf & Eddy, 2003). However, in the aeration tanks, mixing keeps the flocs small and prevents them from settling to ensure increased removal of suspended solids and BOD. The mixing increases the surface area for bacterial cells to utilise more food (organic material) and oxygen for efficient removal from wastewater (Chaüque, 2012; Metcalf & Eddy, 2003). Factors that influence floc formation include oxygen, pH, temperature, and substrate concentration (e.g. organic material and nutrients) (Davies, 2005; Spellman, 2014).

a) **Dissolved oxygen:** Growth of microorganisms is dependent on the availability of oxygen; low oxygen levels in the aeration tank limit respiration, and this ultimately stagnates growth. For bacterial flocs, oxygen concentration is not limiting above about 1.5–2.0 mg/L. Below this concentration, floc formation is inhibited; this because

filamentous bacteria are more tolerant to low oxygen concentrations than floc-forming bacteria thus resulting in filamentous bulking (Davies, 2005).

b) pH: Injury to activated sludge microorganisms is high when pH varies widely. An ideal range at which pH can be kept for the mixed liquor is 6.0–8.0. When variations in pH are outside this range, microbial activity will be reduced, thus affecting floc formation (Spellman, 2003).

c) Temperature: The growth rate of bacteria increases with temperature, with the rate doubling for every 10ºC temperature increase. However, understanding the bacteria in flocs is paramount, as bacteria have a genetically determined feasible temperature range. In activated sludge, the feasible temperature range for carbonaceous bacteria is about 0–30 ºC, while for thermophilic bacteria it is about 30–60ºC (Davies, 2005).

d) Substrate concentration: Although the main substrate for microorganisms is organic material, nutrients (nitrogen and phosphorus) are also important for growth. Without these nutrients, poor bacterial growth results and this ultimately leads to poor organic matter degradation in wastewater. Thus, to optimise carbonaceous treatment in influents deficient in nitrogen and phosphorous, these nutrients are added. For phosphorous and nitrogen not to limit growth, the ratio of C:N:P should be 100:5:1, which is the optimum ratio in the mixed liquor (Davies, 2005).

2.1.3.1.2.2 Food to microorganism ratio (F/M)

The food to microorganism ratio is used to monitor activated sludge processes, calculated based on the amount of food (BOD and/or COD) available per microorganisms which are measured as volatile suspended solids (Spellman, 2003). The F/M ratio is a process parameter used to characterise process designs and operating conditions (Metcalf & Eddy, 2003). To optimise the growth rate of microorganisms, the F/M ratio would provide valuable information. A high F/M ratio would show rapid microorganism growth (Chaüque, 2012).

2.1.3.1.3 Testing of the effects of ENMs on biological wastewater treatment

An understanding of the fate of ENMs in WWTPs is very important for environmental risk assessment. The effects of ENMs on biological WWTPs can be assessed using many approaches. Studies have been conducted through the monitoring of full-scale sewage treatment plants, through dosage to medium-scale pilot sewage treatment plants or by laboratory testing (Gartiser et al., 2014). Kaegi et al. (2011) studied the behaviour of metallic silver nanoparticles in a pilot WWTP by spiking the wastewater with the metallic silver nanoparticles to achieve an influent concentration of 2.4 mg/L. It was found that silver nanoparticles were adsorbed onto the wastewater biosolids both in the effluent and sludge.

About 85% of the added silver was found in the surplus sludge while 5% was found in the effluent and 5% remained in the effluent. For the period after the high initial dosing phase, an excellent mass closure of 99% was obtained. Considering laboratory-scale sewage treatment plants, Gomez-Rivera et al. (2012) studied the clearance of CeO_2 oxide mixed with primary treated municipal wastewater at a concentration of 55 mg Ce/L. it was observed that about 97% of the CeO_2 nanoparticles was cleared during a 63-days-long treatment. The fate and behaviour of the CeO_2 nanoparticles was found to be influenced by the pH of the wastewater. The stability of the suspensions was better achieved in synthetic wastewater prepared according to OECD 303A than in wastewater. For full-scale sewage treatment plants, Westerhoff et al. (2011) monitored and found the removal of titanium in ten full-scale sewage treatment plants to be 96–99%. In the effluents, the titanium oxide nanoparticles detected from the ten full-scale treatment plants ranged from <2 to 20 µg/L.

Testing protocols for ENMs have not been developed, but standardised test protocols such as the OECD guidelines for testing chemicals, 303 A, are being used. These OECD guidelines were designed to determine the elimination and primary and/or ultimate biodegradation of water-soluble organic compounds in a continuously operated test system simulating an activated sludge process (Gartiser et al., 2014). Several studies on the fate and behaviour of ENMs have been conducted using the OECD guidelines, and to also confirm whether the guidelines are suitable for the testing of nanomaterials or not. When the behaviour of nanoscale titanium dioxide in laboratory-scale WWTPs was investigated according to OECD 303, Gartiser et al. (2014) found the guidelines to be applicable for testing of nanomaterials if modifications regarding the dosage, nitrifying conditions and characterisation of nanomaterials were carried out. Additionally, not only did this study show that >95% of the TiO_2 nanoparticles were retained in the sludge and only 3–4% were found in the effluent, no effect on the biodegradation of the organic synthetic wastewater by the nanoparticles was observed. Chaüque (2012) monitored the physicochemical parameters and the behaviour of zinc oxide nanoparticles in a SWWTP that was set up according to OECD 303 A. The results indicated the suitability of the OECD 303 A method for assessment of the fate and behaviour of ZnO ENPs in WWTPs. The OECD system consists of two units, a control and test unit, which are run in parallel under identical conditions and this suits the purpose of the test.

3 EXPERIMENTAL MATERIALS

In order to achieve the objectives stated in section 1.2, the following materials and chemicals were used as received: titanium *tert*-butoxide (≥97% gravimetric; Fluka Analytical, Sigma-Aldrich Co.); *n*-butanol (99.8% anhydrous, Sigma-Aldrich Co.); formic acid (≥95% reagent grade, Sigma-Aldrich Co.); magnesium chloride (Merck); sodium chloride (Associated Chemical Enterprises); calcium chloride (CJ labs); hydrochloric acid (32%, Sigma-Aldrich Co.); and sodium hydroxide (≥98% anhydrous, reagent grade, Sigma-Aldrich Co.).

4 EXPERIMENTAL PROCEDURES

4.1 Synthesis of TiO_2

For the synthesis of TiO_2, a modified sol-gel method, as described by Dlamini et al. (2011), was adopted. A TiO_2 precursor (i.e. titanium *tert*-butoxide) (10 mL) was dissolved in *n*-butoxide (52 mL) and the mixture was stirred for 30 min at room temperature. Formic acid (11 mL) was then added to the homogeneous solution for hydrolyzation and the mixture was stirred for another 4 hr to allow the formation of a white precipitate. An age stage of 2 hr was allowed and the mixture was then dried overnight at 80°C in an oven. The resulting powders were calcined at 500°C in air in a furnace.

4.2 Characterisation of TiO_2

The TiO_2 nanoparticles' morphologies were examined using TEM (JOEL-JEM 2010) at an acceleration voltage of 200 kV, with the nanoparticles deposited on carbon-coated copper grids. For further analysis of the nanoparticles' morphologies, a SEM (TESCAN Vega TC) that uses VEGA 3 TESCAN software was used under nitrogen gas. The crystal phase of the nanoparticles was characterised using powdered X-ray diffraction (XRD) (X'Pert Philips) with a CuKα radiation (0.1540 nm) polychromator beam in 2θ scan range 20 to 80°. The instrument power settings were 40 kV and 40 mA and a step size and step time of 0.0170 (2θ) 87.63 s was used. A Raman Spectrometer (Raman Micro 200, Perkin Elmer) with a single monochromator, a holographic notch filter and cooled TCD was used to record the Raman bands of the nanoparticles, and it was excited using a 514.5 nm Ar^+ line. Brunauer-Emmett-Teller surface area (S_{BET}) was analysed by nitrogen adsorption in a Micrometric ASAP 2020. Prior to analysis, samples were degassed at 100°C. The nitrogen adsorption volume at relative pressure (P/P_0) of 0.980 was used to determine the pore volume. The ultraviolet-visible (UV-Vis) spectra of dye-stuff was recorded using a Shimadzu UV-Vis spectrophotometry.

4.3 Aggregation kinetics and stability studies

TiO_2 nanoparticles, synthesised via the sol-gel method, were used to prepare the suspensions. The different suspensions were prepared using deionised water (DI), monovalent cation electrolyte (NaCl) and divalent cation electrolytes ($CaCl_2$ and $MgCl_2$). The disperse dye-stuff was used as a representation of NOM. Stock solutions of the different aqueous mixtures were prepared for experiments with and without dye-stuff. Information about the dye-stuff was gathered from the feeder company in Cape Town and further scanned on a UV-Vis spectrometer. A concentration of 1 mg/L of the dye-stuff was used for all the dye-stuff experiments.

The ionic strength of the electrolyte solutions was fixed at 0.9 mM for all the electrolyte experiments. This ionic strength is low enough for the electrical double layer not to be too compressed but enough for the particles to show significant agglomeration around pH_{pzc}. At a higher ionic strength, the particles would aggregate at every pH (Romanello & Fidalgo de Cortalezzi, 2013). For all agglomeration measurements, fresh aliquots of 100 mL of the stock solutions were adjusted to the desired working pH. The pH of the aliquots was adjusted in the pH range 2–11 using 6M HCl and 6M NaOH. After the stabilisation of pH, TiO_2 (3 mg) was added to the solution and stirred gently to reach a homogenous suspension. Zeta potential measurements were taken immediately after the pH of the aliquots had stabilised. Size measurements were taken an hour following the preparation of the suspensions. All measurements were conducted in triplicate. Small amounts of the aliquots were put into disposable polystyrene cuvettes for measurement of both parameters. Hydrodynamic diameter (size) measurements were performed by DLS and zeta potential by electrophoretic light scattering (ELS) using a Zetasizer Nano ZS (Malvern).

4.4 Laboratory-scale wastewater treatment plant simulation

As depicted in **Figure 4**, the SWWTP consisted of two units (test and control) which were run in parallel. These activated sludge units consisted of 20 L influent holding tanks, an aeration chamber with a 3 L working volume, and a secondary clarifier (settling tank) with a 1.5 L working volume. The test and control units were run continuously in parallel under identical conditions with a mean hydraulic retention time (HRT) of 6 h and mean sludge retention time (SRT) of 6–10 days until a steady state was reached. A flow rate of 0.5 L/h was set to achieve an HRT of 6 h. The influent was circulated continuously into the aeration chambers using peristaltic pumps (120S/DV, Watson Marlow). Influent in the holding tanks was incessantly stirred to keep its contents in suspension (RW 20 digital stirrers, IKA) and was changed every 24 h. The aeration chambers of both units were aerated using a perforated tube connected to

a compressor that supplied compressed air to maintain dissolved oxygen above 2 mg/L. From the compressor, the air was controlled at 2 bar with a final air flow of 230 mL/min. Compressed air was not only used for maintaining aerobic conditions but to also assist in keeping the sludge flocs in suspension. Compressed air was also essential in maintaining an even distribution of the flocs in the aeration tanks. The mixed liquor was continuously stirred (Eurostar 20 digital stirrer, IKA). Sludge in the clarifiers was recycled continuously to the aeration chambers with a daily sludge wastage. The sludge was pumped using 323S peristaltic pumps (Watson Marlow).

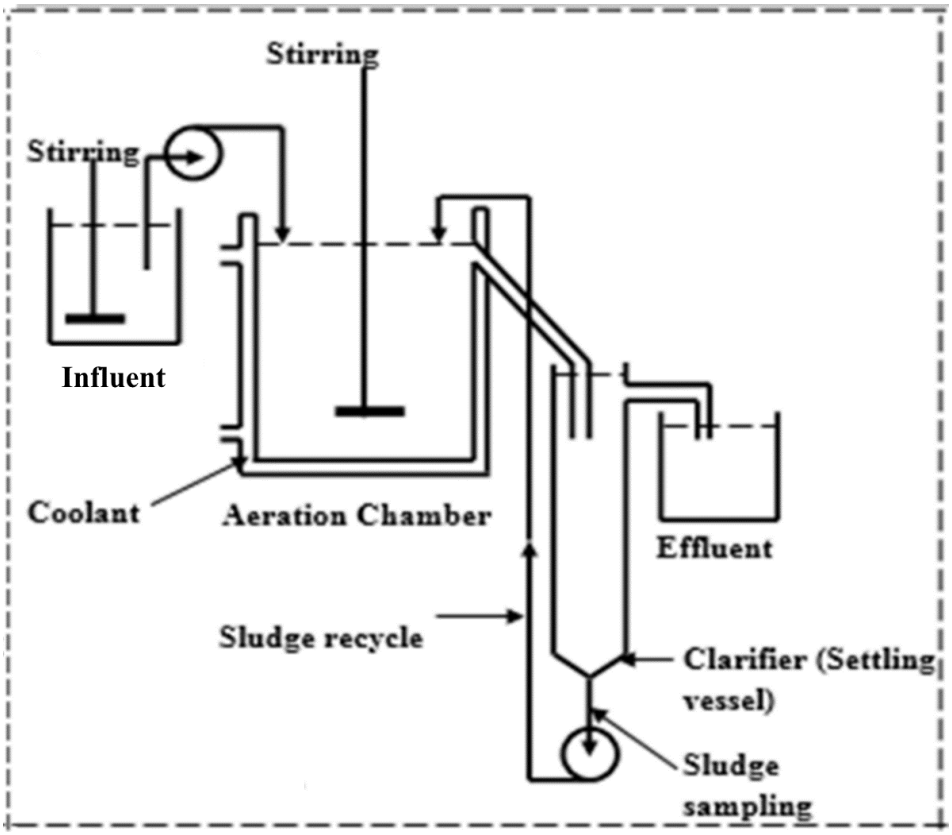

Figure 4 Simulated wastewater treatment plant according to OECD

Return activated sludge (RAS) collected from Pretoria (Daspoort wastewater treatment works) was used as an inoculum for the SWWTP. Before inoculation, 12 L of sludge were aerated for 24 h using compressed air (O20P-ABAC air compressor, Montecarlo) after which the sludge was settled and the supernatant was removed. Secondary influent was then added to the original volume and further aerated for a further 24 h, and the resulting supernatant was reserved. The sludge was then halved and used to inoculate the aeration chambers depicted in **Figure 4**. The reserved supernatant was mixed with secondary influent and used as the influent for the first three days of the first SRT (SRT 1).

4.5 Plant influent

Secondary influent was collected from Pretoria (Daspoort wastewater treatment works), which receives municipal wastewater that is predominantly domestic. Samples were taken weekly to give the wastewater a life span of seven days at 4ºC, in accordance with the OECD 303A guidelines. To formulate the influent for the SWWTP, the Daspoort secondary influent was mixed with synthetic industrial dye-stuff effluent to reach acclimatisation until the system was run with only synthetic industrial dye-stuff effluent. The synthetic industrial dye-stuff effluent was formulated by mixing industrial dye-stuff with synthetic sewage prepared according to OECD 303A guidelines, with an assay tabulated in **Table 5**.

Industrial dye-stuff from textile effluent in Cape Town is composed of a mixture of three disperse dyes: Bemacron Yellow RS (0.855%), Bemacron Br Red (1.9%) and Bemacron Rubine RS (0.104%). Depicted in **Figure 5** are structures of dyes that resemble the mixture of dyes deduced from data received from the feeder company (Mahlalela, Ngila & Dlamini, 2017). The concentration of the dye-stuff was maintained at 50 mg/L. The influent for the SWWTP was varied against activated sludge until 100% synthetic sewage as the major source of carbon and energy for the microorganisms was reached.

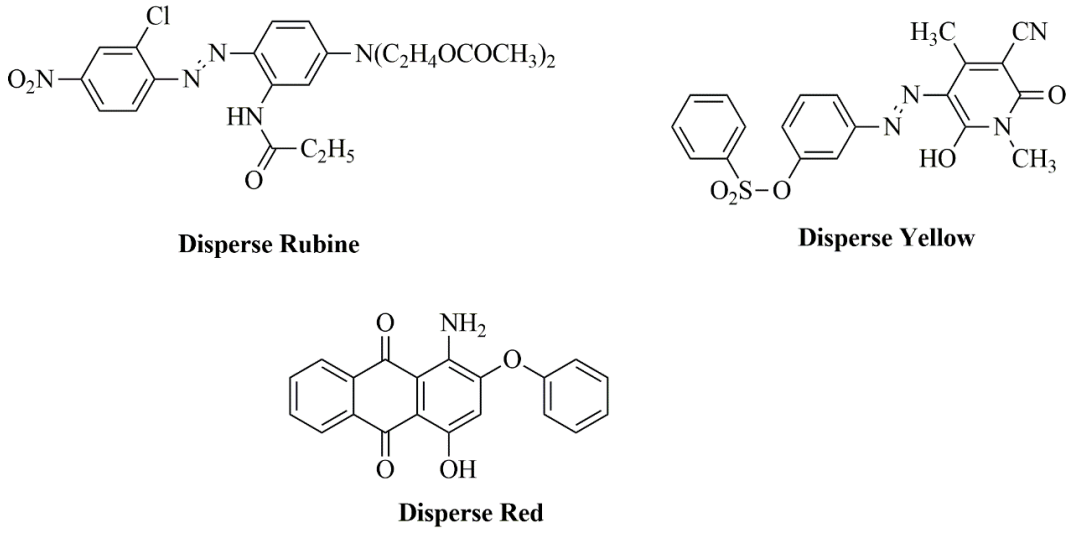

Figure 5 Disperse dye-stuff from industrial plant

Table 5 Composition of synthetic sewage (OECD, 2005)

Constituents	Concentration (mg/L)
Peptone	160
Meat extract	110
Urea	30
Anhydrous dipotassium hydrogen phosphate	28
Sodium chloride	7
Calcium chloride dehydrate	4
Magnesium sulphate heptahydrate	2

4.6 Acclimatisation and test simulation

After inoculation, the SWWTP was fed for three days with 100% secondary influent mixed with the supernatant from the second day of sludge aeration. According to the OECD guidelines, the concentration of the mixed liquor suspended solids (MLSS) should be about 2500 mg/L. Our MLSS was in the range 1000–2500 mg/L. For the remaining seven days of SRT 1, the system was then fed with 100% unmixed secondary influent. To allow the microorganisms to acclimatise to the new source of food (i.e. synthetic industrial dye-stuff effluent), the secondary influent was mixed with the synthesised industrial dye-stuff effluent. The secondary influent was then reduced periodically while gradually increasing the synthesised industrial dye-stuff effluent until the system was run with 100% synthesised industrial dye-stuff effluent. The change in concentration of the influent during the different SRTs for the acclimatisation is shown in **Table 6**.

Table 6 Influent composition for acclimatisation of microorganisms

SRT	Days	Influent composition
1	0–10	100% 2˚ influent
2	11–20	80% 2˚ influent + 20% synthetic industrial dye-stuff effluent
3	21–30	70% 2˚ influent + 30% synthetic industrial dye-stuff effluent
4	31–40	50% 2˚ influent + 50% synthetic industrial dye-stuff effluent
5	41–50	30% 2˚ influent + 70% synthetic industrial dye-stuff effluent
6	51–60	20% 2˚ influent + 80% synthetic industrial dye-stuff effluent
7	61–90	100% synthetic industrial dye-stuff effluent

After reaching 100% synthesised industrial dye-stuff effluent (on day 61), the SWWTP was run with the same concentration for three more SRTs (day 61 to day 90) to reach steady state

before the addition of TiO_2 nanoparticles to the test unit, which commenced on day 91. The TiO_2 suspension concentrations were 5 mg/L, 10 mg/L and 15 mg/L for days 91–100, 101–110 and 111–120, respectively.

4.7 Functionality of the SWWTP

The performance of the SWWTP was monitored by conducting several chemical and physical tests. These tests include influent and effluent chemical oxygen demand (COD), five-day biological oxygen demand (BOD_5), total nitrogen (TN), and total suspended solids (TSS). MLSS and mixed liquor volatile suspended solids (MLVSS) in the aeration tanks were also monitored. Prior to COD, BOD_5 and TN measurements, the samples were filtered using 0.45 µm PVDF filters (Sigma-Aldrich). The spectrophotometer (Spectroquant Pharo 300, Merck) was used for COD, BOD_5 and TN measurements. For the COD determination, a COD kit (1.14541.0001, Merck), which is analogous to a German standard DIN EN ISO 7393, was used. BOD_5 was also determined using a BOD kit (1.00687.0001, Merck,), which conforms to a European standard EN 1899 210. The TN concentration was analysed using kit number 1.14763.0001 (Merck).

The population of the microorganisms during the addition of TiO_2 nanoparticles was ascertained by measuring total plate counts (TPC) as colony-forming units (CFU/mL) using equation **[5]**. Plate count agar (23 g) was suspended in 1000 mL distilled water and was heated to boiling to completely dissolve the agar. The agar solution was then sterilised by autoclaving at 121°C for 15 min. It was allowed to cool to 50°C in a circulating water bath and poured into sterile petri dishes and allowed to cool in a laminar flow cabinet. Distilled water (9 mL) was added to 160 mL test tubes with metal stoppers and autoclaved at 121°C for 15 min. After cooling to room temperature, 1 mL of sampled MLSS from the aeration chambers was added and mixed with a vortex mixer. The mixed sample was further serially diluted until the 10^{-4} dilution after which 0.1 mL was transferred to the prepared agar in the petri dishes. The samples were then evenly spread by alternate rotation and back-and-forth motion of plates of a flat level surface and allowed to solidify. The petri dishes were inverted, and incubated at 25°C for 1–2 days. For these experiments, an agar control was prepared along with the plated samples. All samples were plated in duplicate.

$$CFU / mL = \frac{\text{average number of colonies X total dilution factor}}{\text{volume plated}} \quad \textbf{[5]}$$

The concentration of TSS in the effluents of the SWWTP units served as an indicator of the settleability of the activated sludge in the clarifiers, while the MLSS and MLVSS are an indicator of the growth and life of the microorganisms. The TSS and MLSS were determined

using section 2540D of the Standard Methods for the Examination of Water and Wastewater while the MLVSS were determined following the procedure in section 2540E (Greenberg et al., 1992). All the measured solids (i.e. 100–500 mL of the samples) were filtered through glass microfibre filters (934-AH^{TM}, Whatman) with a pore size of about 0.6 µm. The temperature and dissolved oxygen (DO) in the aeration chambers, and conductivity and pH of the influents and effluents, were also measured (Starter DO 300D, Starter conductivity 300C and Starter pH 300, OHAUS, respectively).

4.8 Sludge analysis after exposure to TiO_2 nanoparticles

To remove excess moisture, waste sludge was filtered and dried overnight in an oven at 50ºC. The dried sludge was then ground to fine powder and viewed under nitrogen gas using a scanning electron microscope (SEM) (TESCAN Vega TC) that uses VEGA 3 TESCAN software. Samples were mounted on stubs and gold coated prior to elemental mapping using energy dispersive X-ray spectroscopy (EDS) coupled to SEM. The dried sludge was further analysed using powdered X-ray diffraction (X'Pert Philips) with CuKα radiation (0.1540 nm) polychromator beam in the 2θ scanning range 20-80° to characterise the crystal phase of the TiO_2 nanoparticles in the sludge. The instrument power settings used were 40 kV and 40 mA at a step size and step time of 0.0170 (2θ) and 87.63s, respectively.

4.9 Analysis of titanium in sludge and effluent using ICP-OES

The effluent and sludge of the test and control units were analysed with an inductively coupled plasma optical - emission spectrometer (ICP-OES) (iCAP 6500 Duo, Thermo Scientific). The sludge (0.25 g) and effluents (5 mL) were digested for 3 h under reflux in 5 mL *aqua regia* (3 mL HCl and 1 mL HNO_3) (Durenkamp et al., 2016). All analyses were performed in triplicate.

5 RESULTS, TREATMENT OF RESULTS AND DISCUSSION

5.1 Characterisation of TiO_2

Figure 6 shows TEM and SEM images of the TiO_2 nanoparticles. The average particle size, estimated using TEM, was found to be 12 nm (SD = ±2); this value is comparable to the XRD estimates, thus signifying a uniform average size distribution. Both TEM and SEM results show that the particles were agglomerated and appear to be spherical in shape. The BET surface area and pore volume of the nanoparticles was found to be 55.7 m^2/g and 0.1141 cm^3/g, respectively.

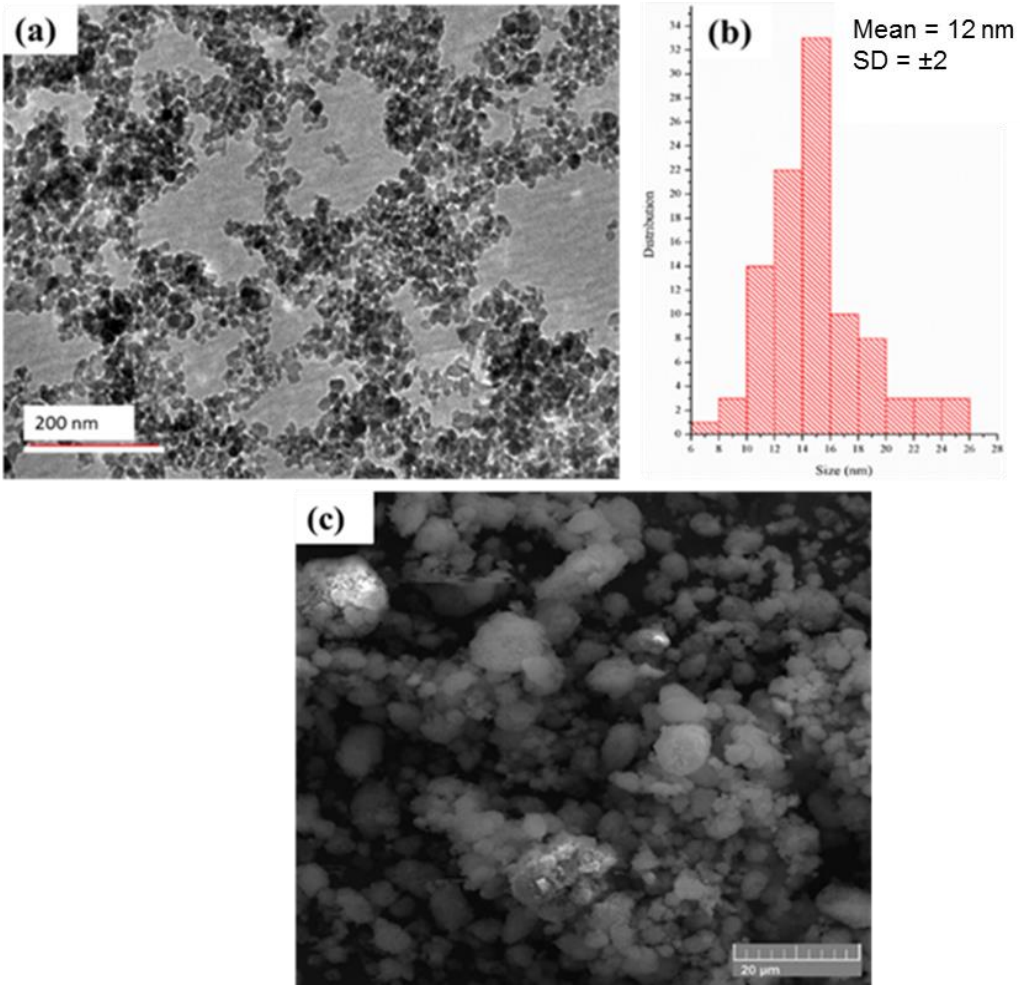

Figure 6 (a) TEM image of TiO_2 nanoparticles with its (b) histogram and (c) SEM image of the TiO_2 nanoparticles

The XRD pattern of the TiO_2 nanoparticles, which is shown in **Figure 7**, indicates peaks that correspond to crystal planes (101), (004), (200), (105), (211), (204), (116), (220), and (215)

(Vijayalakshmi & Rajendran, 2012; Wei et al., 2013; Azella, 2011). The nanoparticles under investigation were confirmed by the JCPDS-01-073-1764 card as being anatase. The well-defined peaks show that the nanoparticles are in fact crystalline. To confirm the average particle size determined by TEM, the crystalline size was commuted using the Debye-Scherrer equation shown in equation **[7]**

$$D = K\lambda/\beta\cos\theta \qquad \textbf{[7]}$$

where D is the crystal size; λ is the wavelength of the X-ray radiation (λ = 0.1540 nm) for CuKα; K = 0.89; θ is the Bragg's diffraction angle; and β is the full width half-maximum height using (101) peaks (Ba-Abbad et al., 2012; Vijayalakshmi & Rajendran, 2012) The calculated crystalline size for the TiO_2 nanoparticles was found to be 15 nm.

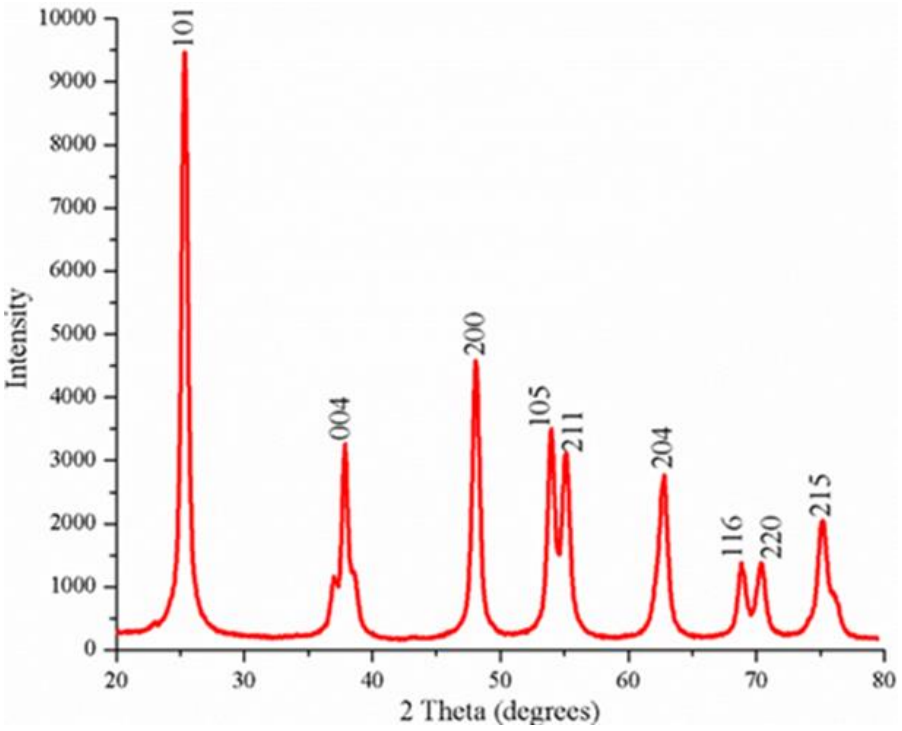

Figure 7 XRD patterns of TiO_2 nanoparticles

In order to confirm the phase of the TiO_2 nanoparticles, Raman spectroscopy was used to elucidate their structural nature. Positions and widths of the bands were also correlated with their vibrational and structural characteristics using Raman spectroscopy (Cong et al., 2007; Priyanka et al., 2014). **Figure 8** shows Raman bands of the TiO_2 nanoparticles and further confirms that the nanoparticles were indeed the anatase phase of titania as indicated by the XRD results. The presence of the four bands (i.e. 144 (E_g), 395 (B_{1g}), 514 (A_{1g}), 514 (B_{1g}) and

639 cm^{-1} (E_g)) in the Raman spectrum of the TiO_2 nanoparticles serves as evidence of the anatase phase corresponding to the size modes expected for a tetragonal structure.

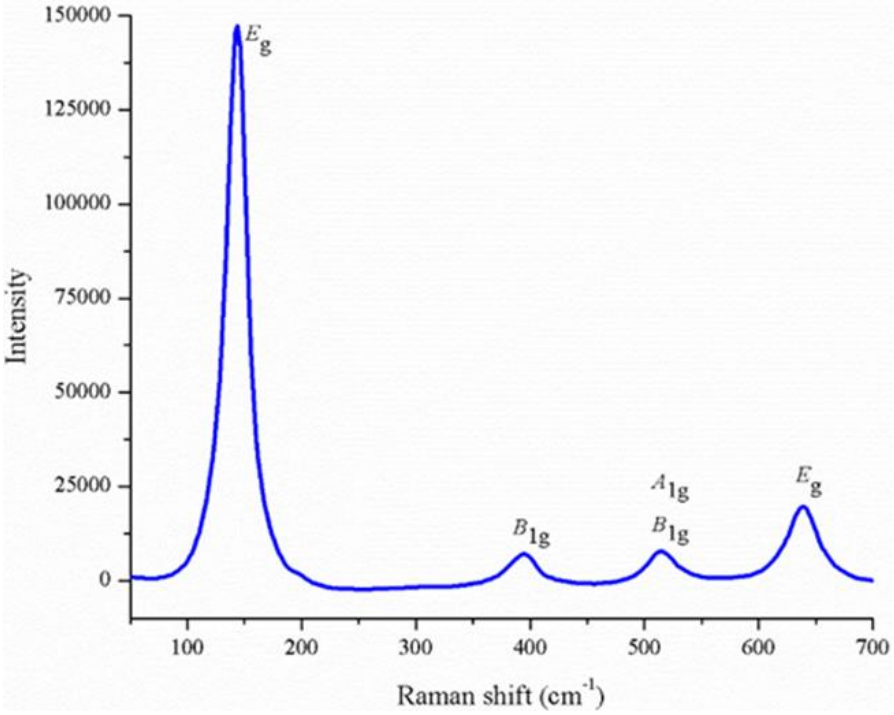

Figure 8 Raman bands of TiO_2 nanoparticles

The N_2 adsorption-desorption isotherm and pore size distribution curves of the TiO_2 nanoparticles is illustrated in **Figure 9**. The TiO_2 nanoparticles were found to be mesoporous as they exhibited an isotherm characteristic type IV with a hysteresis loop of type H1 at a relative pressure 0.45–0.90. The type H1 hysterisis loop is known to correspond to porous materials that have agglomerates (Sing, 1985). This serves as further confirmation of the agglomerated nature of the particles, which was observed on TEM and SEM images (**Figure 6**). The average pore size, which is related to the particle crystalline size 10–20 nm, appears to be in good aggrement with results of XRD analysis.

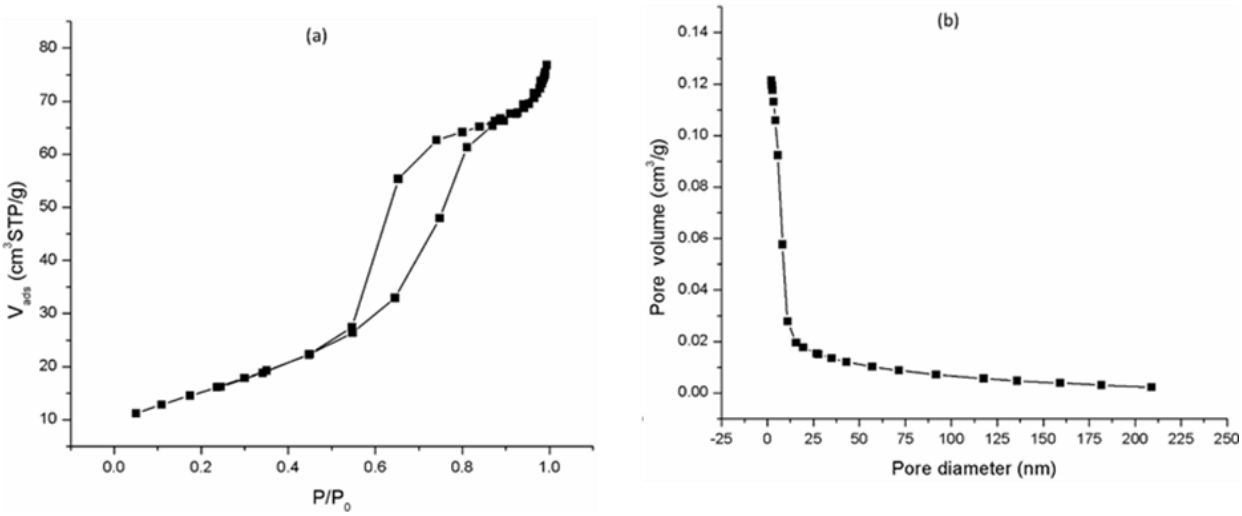

Figure 9 (a) N_2 adsorption-desorption isotherms and (b) pore size distribution curves of the TiO_2 nanoparticles

5.2 Characterisation of dye-stuff

The disperse dye-stuff from textile effluent from Cape Town was a mixture of dyes composed of Bemacron Yellow RS (0.855%), Bemacron Br Red EFBL (1.9%) and Bemacron Rubine RS (0.104%). At pH 4.77, the particle size distribution (DLS) and zeta potential (ELS) of the dye-stuff solution was found to be 648.8 nm and -26.2 mV, respectively. A UV-Vis spectrum of the dye-stuff, which is illustrated in **Figure 10**, indicates the presence of multiple chromophores in the dye-stuff.

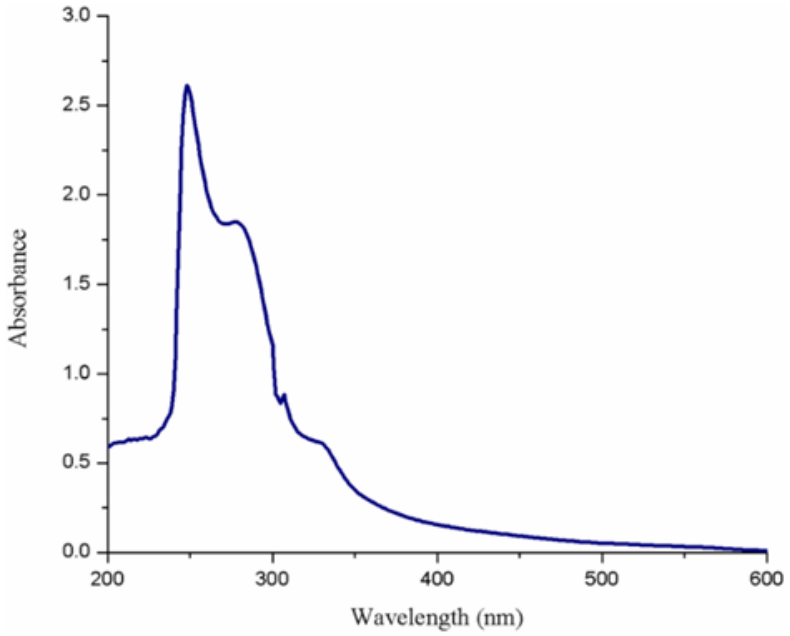

Figure 10 UV-Vis spectrum of the dye-stuff

5.3 Aggregation kinetics and stability studies

5.3.1 Theory

Hydrodynamic diameter (size) measurements were performed by DLS, and zeta potential (surface charge) by ELS using a Zetasizer Nano ZS (Malvern). Dynamic light scattering is based on moving particles undergoing Brownian motion due to random collisions between the solvent molecules and the particles. Fluctuations in scattered light which exist because of the particles in motion are auto-correlated and evaluated in DLS to determine the intensity weighted average diffusion coefficient (m^2/s), D, of the particles (Jiang et al., 2009). The hydrodynamic diameter (d_p) can be calculated from the diffusion coefficient using the Stokes-Einstein equation **[8]**.

$$d_p = kT/3\pi\eta D \qquad \textbf{[8]}$$

where *k* is the Boltzmann constant (J/K), *T* is the absolute temperature (K) and *η* is the viscosity of the medium (kg/ms). Particles in solution exist in different particle sizes and this compels size distribution as a description of the dispersion. The size distribution is determined by fitting the correlation curve to a multiple exponential form (Jiang, Oberdörster & Biswas, 2009).

Electrophoretic light scattering is used to measure zeta potential, which is a potential at a notional boundary that surrounds the electrical double layer within which the liquid moves together with particles. Charged particles in the dispersion move towards the electrode of opposite polarity when an electric field is applied across the dispersion, a phenomenon called electrophoresis. The frequency that is shifted from a laser beam after the light is scattered by the moving particles is measured in order to determine electrophoretic mobility, *U* ($m^2/V•s$), when the laser wavelength and the scattering angle is known (Jiang et al., 2009). Using the Smoluchowski equation **[9]**,

$$U = \varepsilon\zeta/\mu \qquad \textbf{[9]}$$

zeta potential, ζ (mV), can be computed from the electrophoretic mobility where ε is the dielectric constant of the solution and the viscosity of the solution is μ (Romanello & Fidalgo de Cortalezzi, 2013; Jiang et al., 2009).

As an indirect measurement, the rate of agglomeration was calculated from the slope of mean diameter versus time plots. The mean diameter measured at 30-second intervals for 201 seconds was plotted against time (**Appendix 1-8**). Residual plots were drawn to investigate a better method for analysing the data, and the regression curve analysis was chosen as the

method to analyse the data. All the mean diameter and zeta potential measurements were done in triplicate.

5.3.2 Results and discussion

The zeta potential of TiO_2 nanoparticles as a function of pH in different suspensions with no dye-stuff added is shown in **Figure 11(a)**. The point of zero charge (pH_{pzc}) of TiO_2 was ≈5 for the DI suspension, which is comparable to reported values (Chong et al., 2010; Jiang et al., 2009). The zeta potential of the TiO_2 nanoparticles was found to be positive at low pH and negative at higher pH. The positive zeta potential was caused by the acceptance of protons by oxygen atoms on the surfaces of the TiO_2 nanoparticles at acidic pH. However, at basic pH, hydrogen ions are lost from the surfaces of the nanoparticles thus creating a negative zeta potential (Chong et al., 2009; Grzechulska & Morawski, 2002). In suspensions with NaCl, $CaCl_2$ and $MgCl_2$ electrolytes, the respective pH_{pcz} values of ≤4, ≥5 and ≈7 for the TiO_2 nanoparticles were noted. At basic pH range, it was also noted that the TiO_2 nanoparticles in NaCl solution behaved in a similar manner to the DI suspensions; in contrast, the nanoparticles in $CaCl_2$ and $MgCl_2$ solutions behaved differently. Ion adsorption is one of the several mechanisms that influence surface charge. At basic pH, the zeta potential of the TiO_2 nanoparticles for $CaCl_2$ and $MgCl_2$ was maintained at about -5 mV. As for DI, it was found that the negative zeta potential of TiO_2 nanoparticles increases (to around -20 mV) with pH for NaCl suspension. Therefore, the divalent cations (Ca^{2+} and Mg^{2+}) screened the surface charges from acquiring negative values, thus reducing the overall surface charge (Romanello & Fidalgo de Cortalezzi, 2013). The presence of the dye-stuff used in the different suspensions kept the TiO_2 nanoparticles' zeta potentials at negative values for the entire pH range (**Figure 11(b)**). The zeta potential of the dye-stuff of -26.2 mV contributed towards the zeta potential of the TiO_2 nanoparticles remaining negative as the particles of the dye-stuff was being adsorbed on their surface.

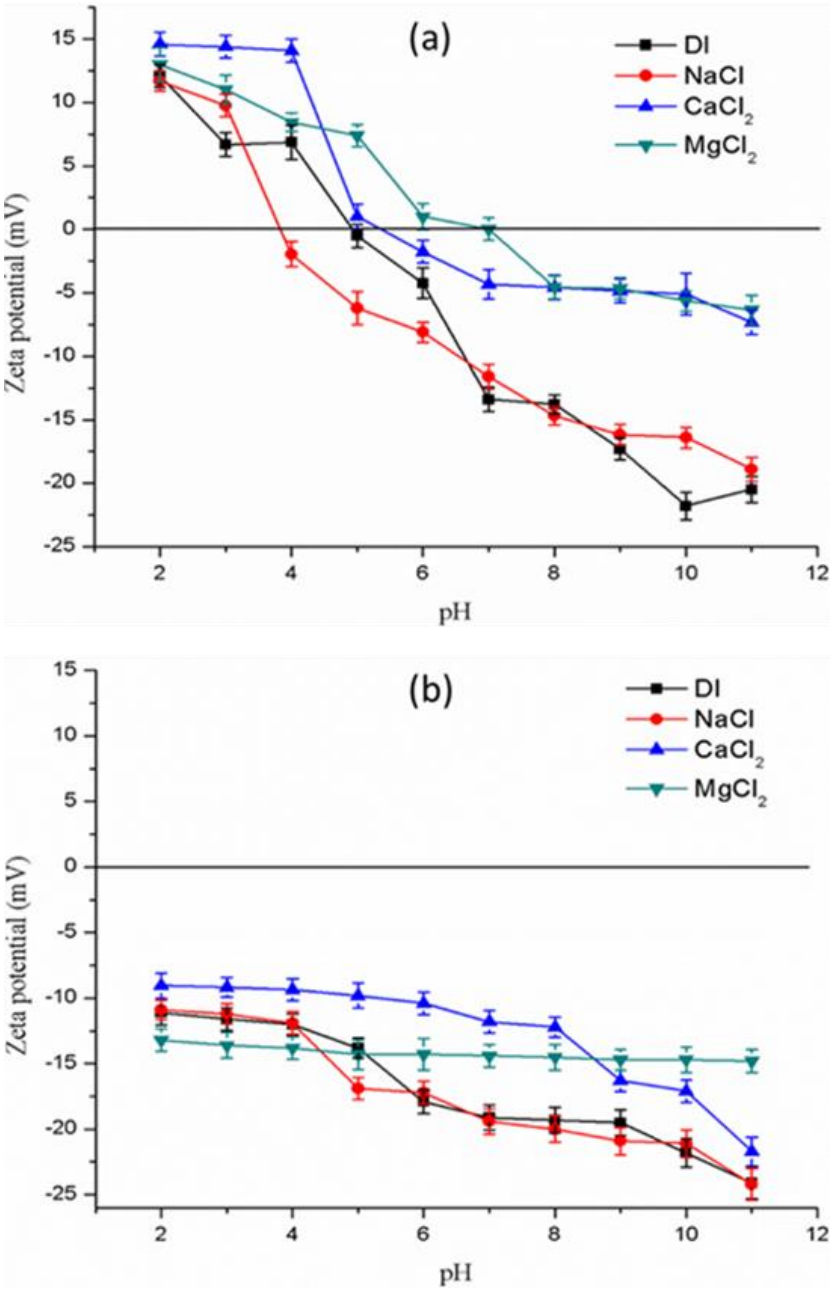

Figure 11 Zeta potential as a function of pH in different solutions with 0.9 mM ionic strength, (a) no dye added and (b) with 1 mg/L dye

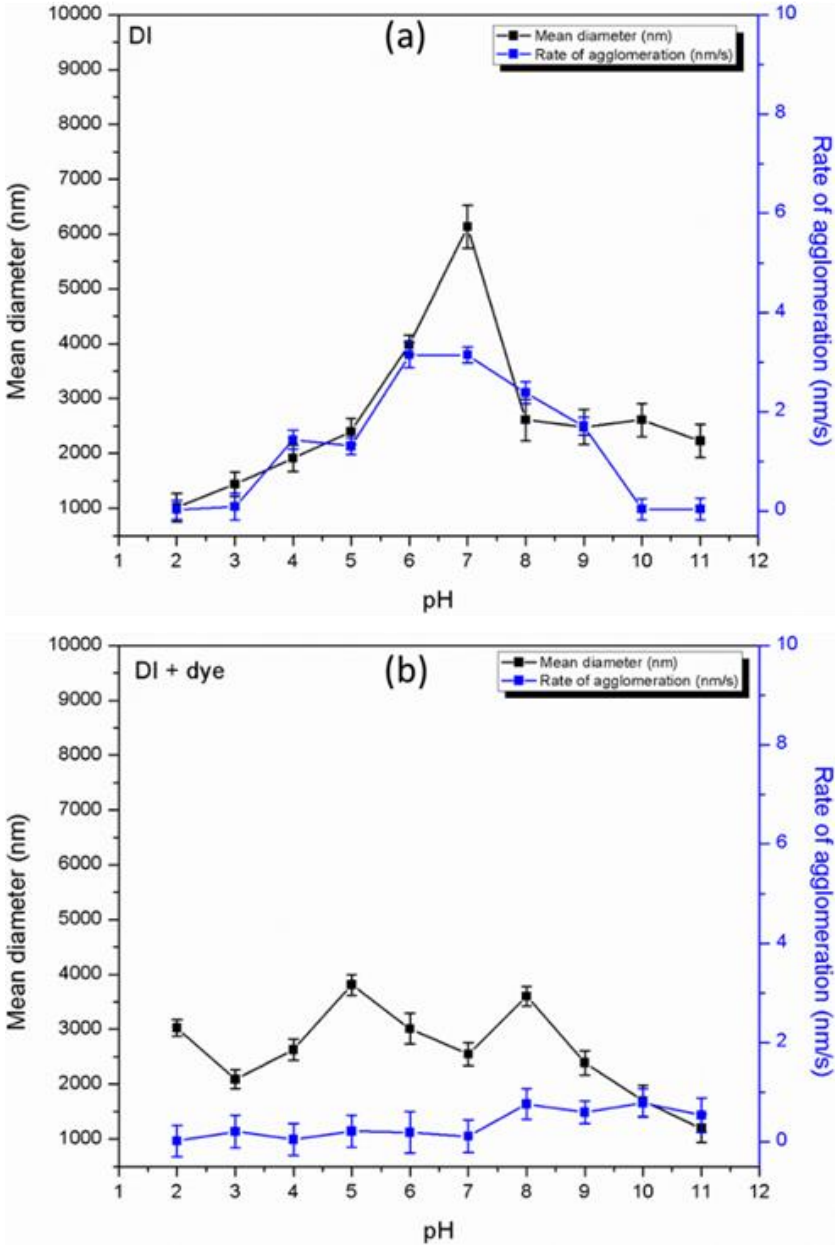

Figure 12 Mean diameter and rate of agglomeration in DI (a) no dye added and (b) with dye added

A strong relationship between the zeta potential and the mean diameter was observed. In **Figure 12(a)**, it was observed that the mean diameter for the TiO_2 nanoparticles in dispersed DI was at a maximum when the pH was similar to the pH_{pzc}. Around the pH_{pzc} of the TiO_2 nanoparticles, reduced repulsions between the particles is experienced. At the extreme pH ranges, the nanoparticles became highly positive (acidic pH) and highly negative (basic pH); and this promoted dispersion of nanoparticles due to electrostatic repulsion between the like-charged nanoparticles thus leading to lower mean diameters. The relationship between zeta potential and mean diameter was further confirmed by the rate of agglomeration, which also peaked at around the pH_{pzc}. of the TiO_2 nanoparticles. It can also be noted that the maximum agglomeration rate of the TiO_2 nanoparticles shifted slightly relative to its pH_{pzc}. This pH shift was attributed to the absence of a buffer in the solution. A similar pattern was reported in a similar study (Romanello & Fidalgo de Cortalezzi, 2013). A reduction in the mean diameter and decrease in rate of agglomeration (**Figure 12(b)**) was observed across the pH range when the dye was added. The decrease in agglomeration was due to the presence of electrostatic repulsions between the nanoparticles, which was induced by the negative zeta potential of the dye-stuff on the surfaces of the TiO_2 nanoparticles. This surface coating increased the steric stabilisation effect.

Ionic strength is one of the factors that govern agglomeration as it influences the magnitude of the electrical double layer (EDL). The thicker the EDL, the higher the dispersion of the particles in solution since thickness intensifies the particle–particle repulsions. An increase in ionic strength suppresses the EDL thus resulting in the agglomeration of particles in the solution. However, the extent to which the reduction in EDL occurs is influenced by the charge of ions (monovalent ions compared to divalent ions); this phenomenon is called the Derjaguin-Landau-Verwey-Overbeek (DLVO) theory. The results obtained from the NaCl experiments were comparable to those of DI. **Figure 13** shows the mean diameter, rate of agglomeration and the interaction energy plots of NaCl experiments, as influenced by a change in pH. Agglomeration was found to be high around the point of zero charge. A similar pH shift, as in the DI experiments, in the agglomeration rate was also observed (see **Figure 13(a)**). According to the interaction energy plots (see **Figure 13(b)**), the repulsion interaction energy (V_r) for NaCl suspension is high at pH 2 and pH 10 and significantly lower at pH_{pzc} ≤4. Around pH_{pzc}, the attractive forces (V_a) (i.e. the attractive van der Waals interaction) were more dominant and this gave rise to a high agglomeration rate. The dip observed around pH 6 may be due to the settling of larger agglomerates from the suspension.

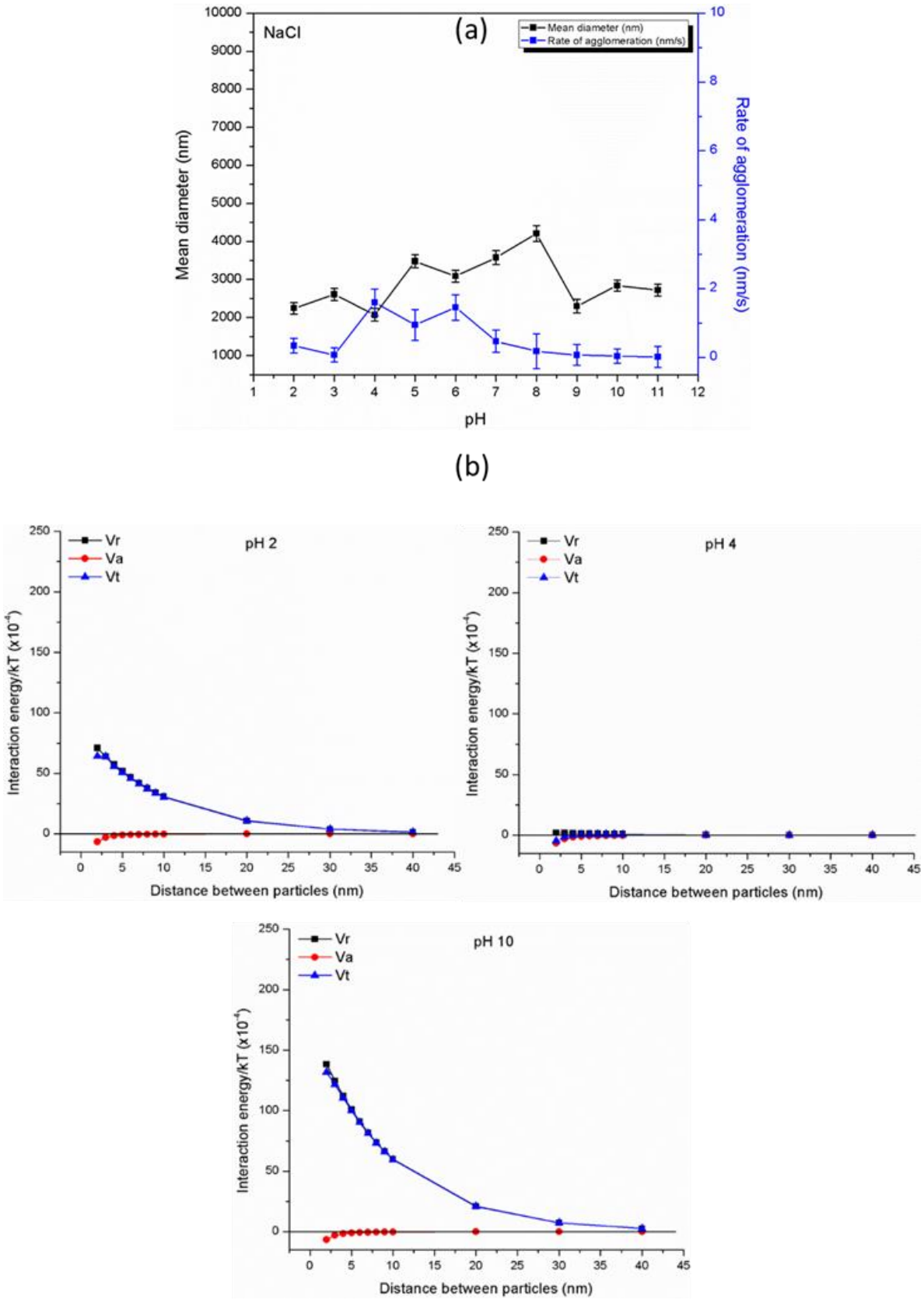

Figure 13 (a) Mean diameter and rate of agglomeration and (b) interaction energy plots at pH 2, pH 4 and pH 10 for NaCl no dye

As shown in **Figure 14(a)**, the suppression of the EDL and its impact on agglomeration was clearly visible in the experiments carried out with $CaCl_2$. For TiO_2 nanoparticles suspended in $CaCl_2$, both the largest agglomerates and the highest rate of agglomeration were observed. In addition, TiO_2 nanoparticles were dispersed at low pH and aggregated in the high pH range above their pH_{pzc} when Ca^{2+} and Mg^{2+} were used. This means that at basic pH there is an electrostatic interaction between the highly negatively charged nanoparticles, which causes the divalent cations to neutralise and the surfaces of the TiO_2 nanoparticles to be negative, and this in turn decreases the thickness of the EDL. DLVO measurements also affirmed the significant decrease in repulsive forces, leading to an overall increase in the attractive van der Waals forces. This is evident in the increase in particle agglomeration at pH 10 (see **Figure 14(b)**). A dip in the mean diameter at pH 8 was observed; the explanation is similar to the dip observed for NaCl at pH 6. At pH 2, where the TiO_2 nanoparticles are positively charged, thus indicating an increase in repulsive forces (see **Figure 14(b)**), a greater dispersion of the nanoparticles is observed. Similar results were observed for $MgCl_2$. On the contrary, the Mg^{2+} cation was less effective at fully suppressing the EDL, as the mean diameters of the agglomerates observed were slightly less than those observed for the $CaCl_2$ suspensions. The ineffectiveness of the Mg^{2+} cation to suppress the EDL is due to the smaller size associated with the Mg^{2+} cations. Therefore, Mg^{2+} has a slightly larger hydrated radius, which reduces its interaction with the negatively charged TiO_2 nanoparticles in solution.

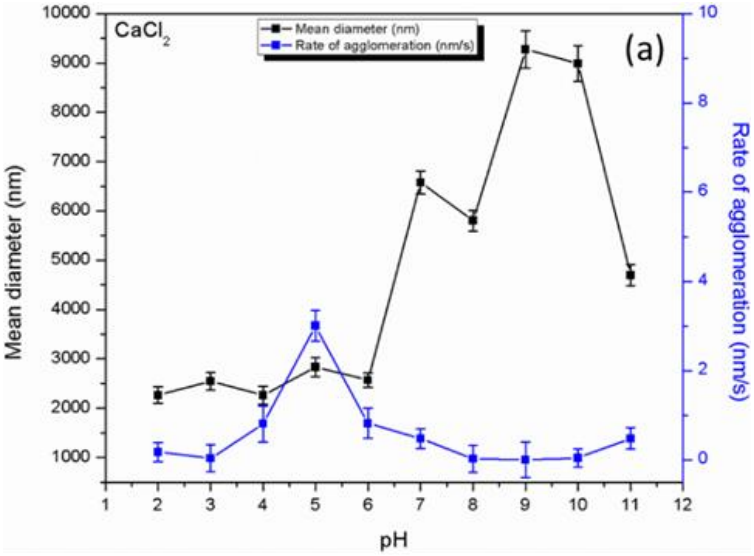

(b)

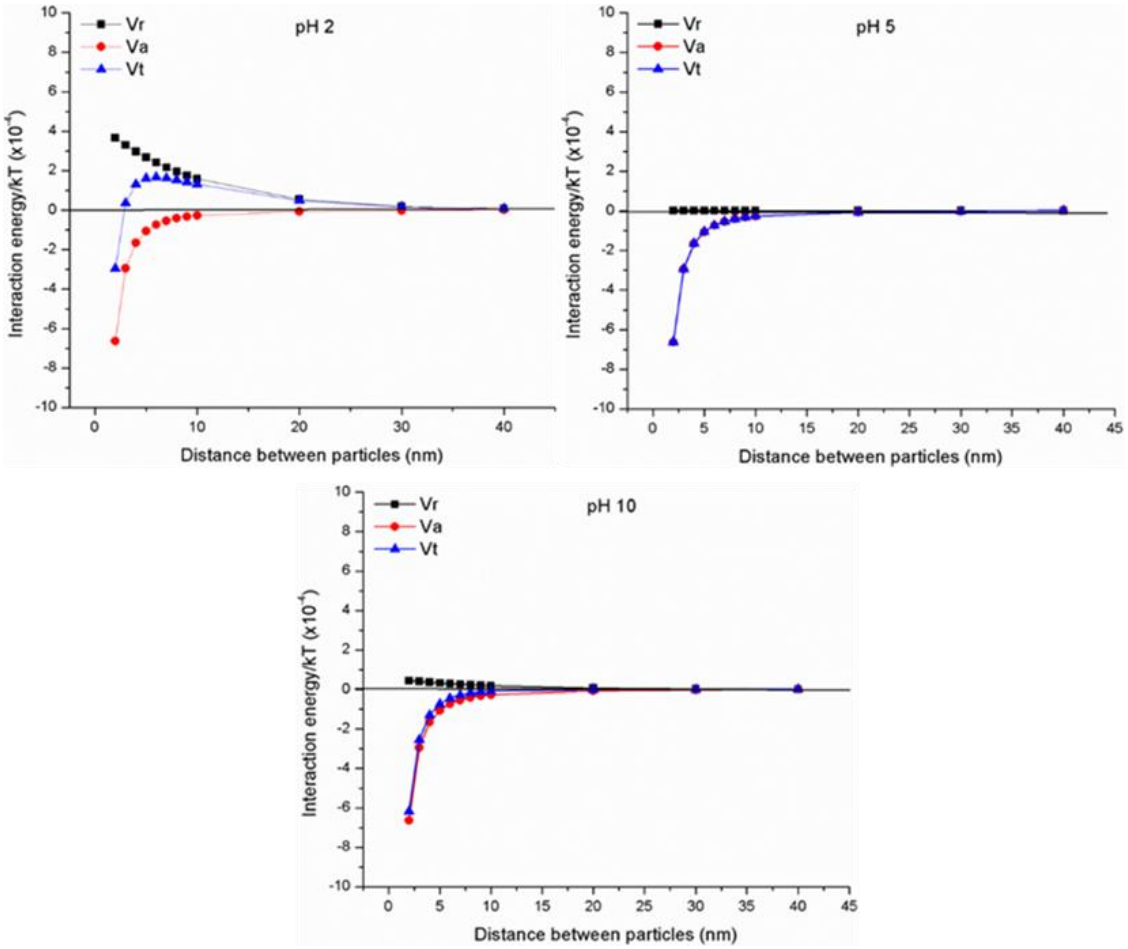

Figure 14 (a) Mean diameter and rate of agglomeration and (b) interaction energy plots at pH 2, pH 5 and pH 10 for $CaCl_2$ no dye

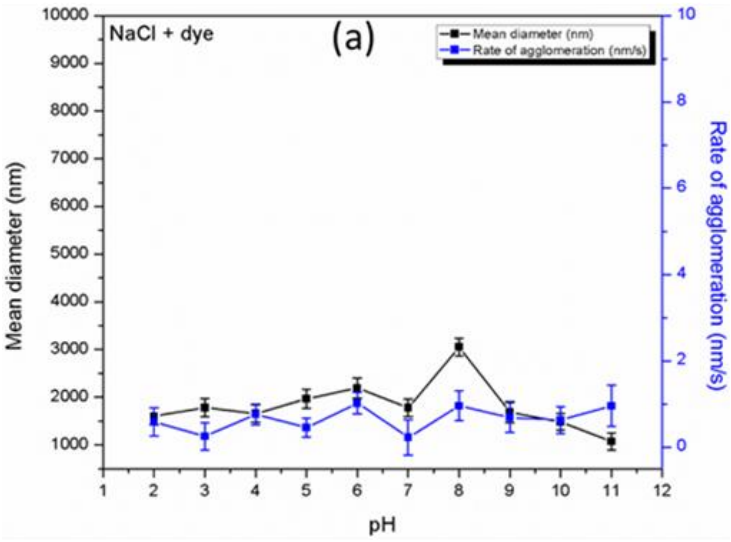

(b)

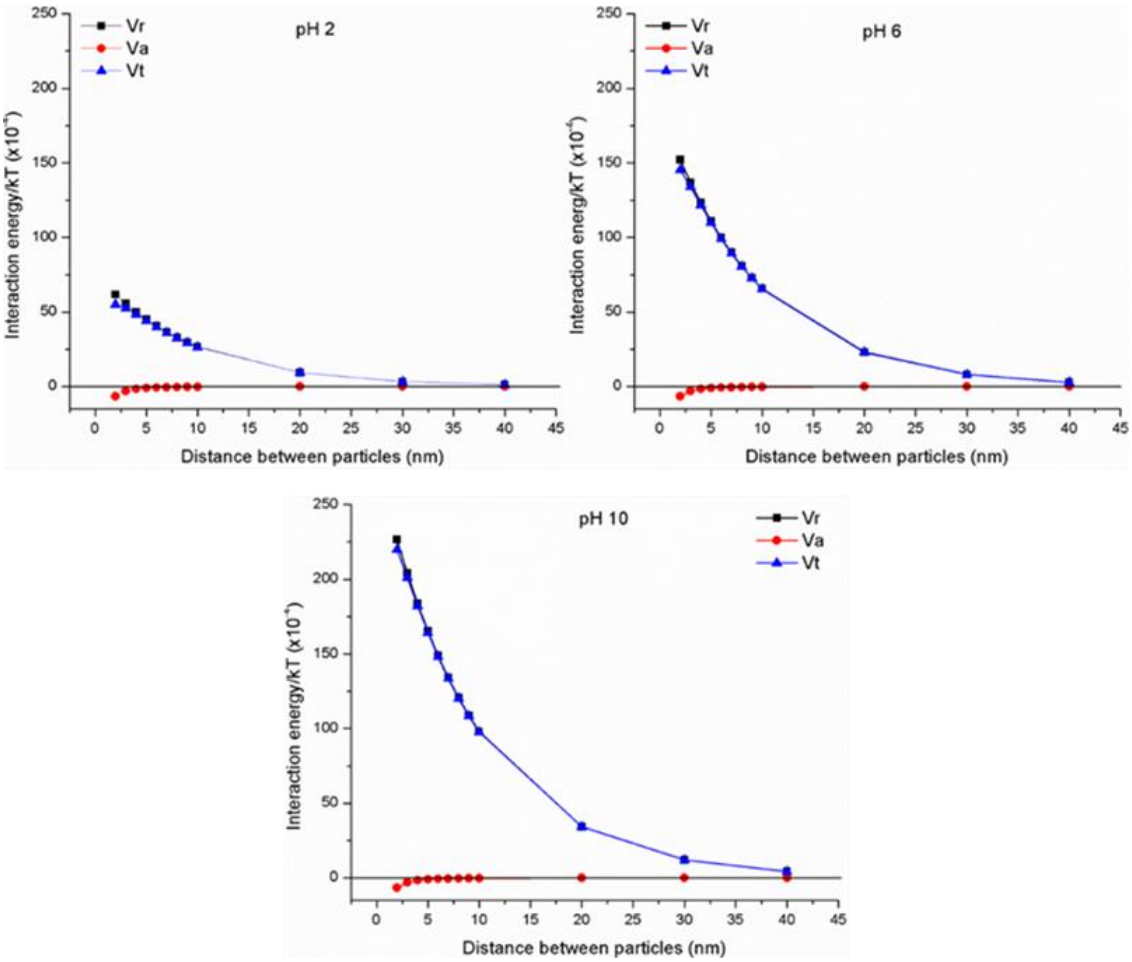

Figure 15 (a) Mean diameter and rate of agglomeration and (b) interaction energy plots at pH 2, pH 6 and pH 10 for NaCl with dye

Upon addition of the dye-stuff to the solutions, the mean diameters of TiO_2 nanoparticles in NaCl, $CaCl_2$ and $MgCl_2$ became significantly reduced as observed in DI suspensions (see **Figures 15** and **16**). The main factors that influence dispersion are steric hindrance and electrostatic repulsions. The adsorption of the dye on the surfaces of TiO_2 nanoparticles induces steric hindrance and increases particle–particle repulsions (from electrostatic repulsions). The overall zeta potentials of the nanoparticles are negative across the entire pH range (see **Figure 11(b)**). This accounts for the reduction in mean diameters and rate of agglomeration, which was constant throughout the pH range. Mean diameters and rates of agglomeration of TiO_2 nanoparticles in NaCl suspensions were comparable to those carried out in water (see **Figure 15(a)**). The stability of suspensions in the presence of dye can be explained by the DLVO theory. The repulsive interaction forces were greatly enhanced by the presence of the dye-stuff (see **Figure 15(b)**), which accounts for the reduced mean diameter of the TiO_2 nanoparticles.

The ability of the Ca^{2+} cation to effectively reduce the EDL was observed, even in the presence of the dye. This is because the highest mean diameter of the Ca^{2+} cation is in the basic range, as observed for $CaCl_2$ suspension without addition of the dye-stuff. The rate of agglomeration increased from pH 8, which accounts for the neutralising ability of Ca^{2+} that leads to a reduced EDL and subsequently results in reduced stability (see **Figure 16(a)**). The interaction energies were comparable to those observed for $CaCl_2$ in the absence of a dye-stuff; however, the overall forces were found to be repulsive, thus confirming lower mean diameters for TiO_2 nanoparticle suspensions in $CaCl_2$ with the dye-stuff (see **Figure 16(b)**). The suspensions of TiO_2 nanoparticles in $MgCl_2$ solution in the presence of a dye-stuff behaved in a similar manner as those in $CaCl_2$ in the presence of the dye-stuff. The overall attractive forces, together with repulsive and steric hindrance forces, can be summarised by the scheme in **Figure 17**.

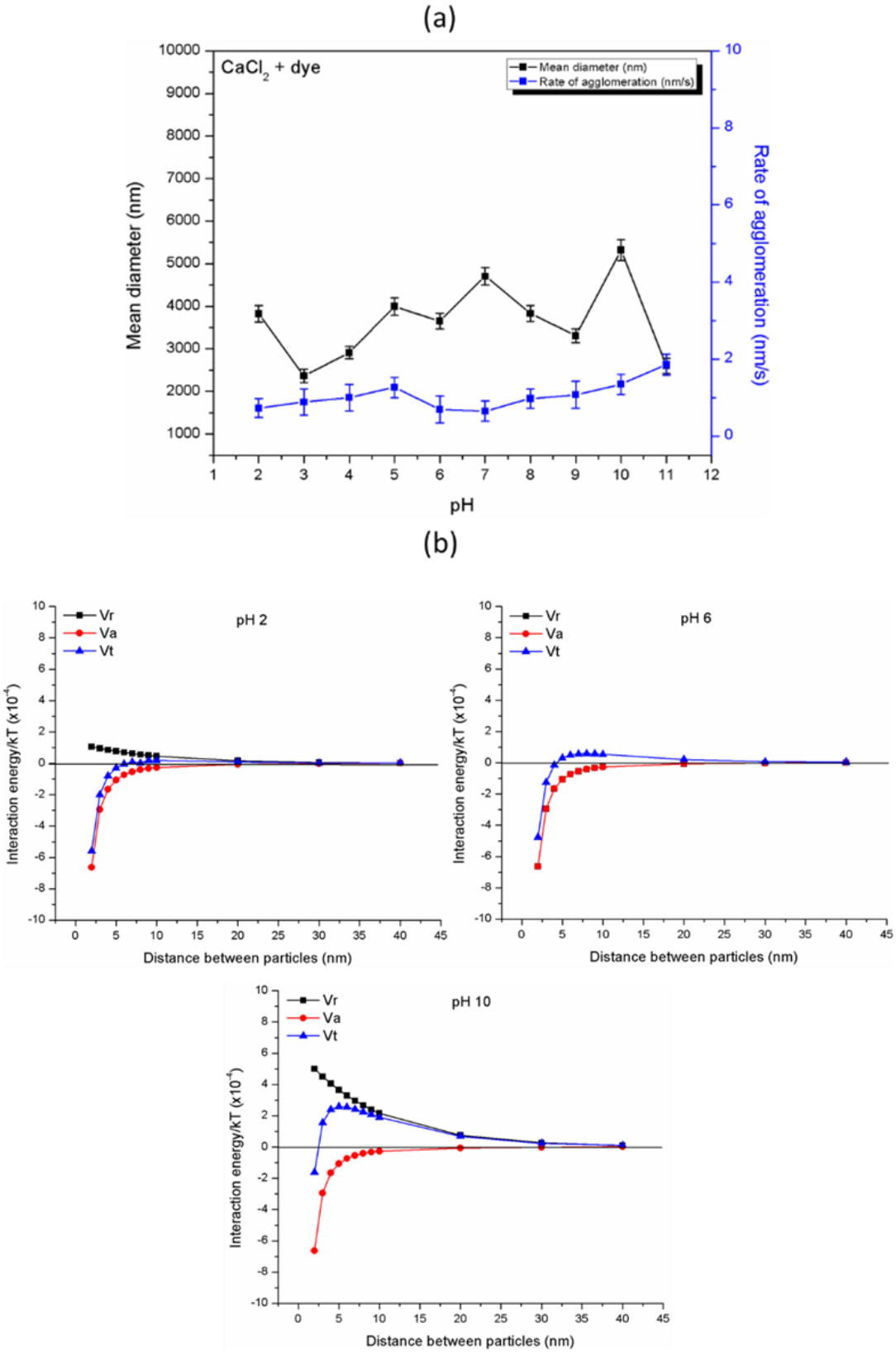

Figure 16 (a) Mean diameter and rate of agglomeration and (b) interaction energy plots at pH 2, pH 6 and pH 10 for $CaCl_2$ with dye

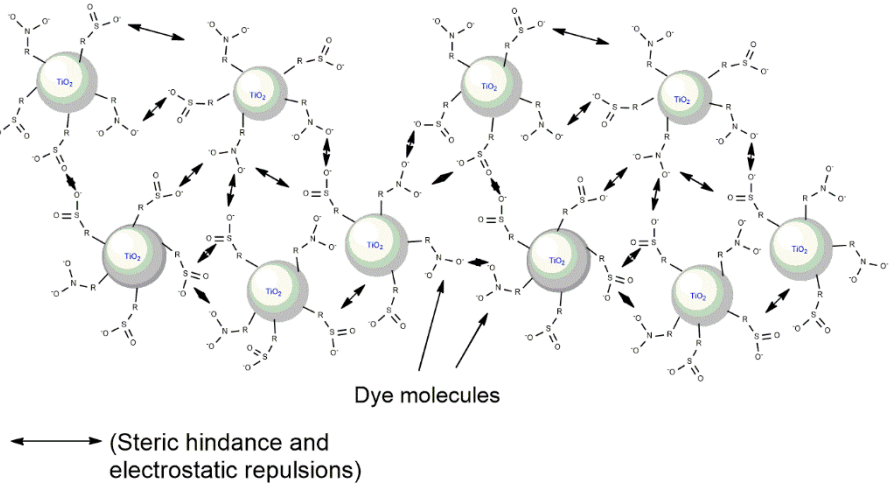

Figure 17 Graphical representation of phenomena that govern repulsions in the presence of dye-stuff

5.4 Fate and behaviour studies of TiO_2 nanoparticles

5.4.1 Acclimatisation and steady state

Acclimatisation of activated sludge to the synthetic industrial dye-stuff effluent was successfully conducted over 70 days (seven SRTs). At day 61, the SWWTP was already being fed with 100% synthetic industrial dye-stuff effluent. For the acclimatisation, COD and BOD_5 were analysed to monitor the survival of the microbes that constituted the activated sludge in the aeration chambers. **Figure 18** illustrates the efficiency of COD removal during the acclimatisation and steady state of the system, before exposure to the TiO_2 nanoparticles. According to the OECD 303A guideline, a test is considered valid when COD elimination in the reactor units is >80% (OECD, 2005). In this case, as illustrated by **Figure 18(a)**, the observed overall removal efficiency during the acclimatisation was >80%. However, at days 5-6 of the SRT a decrease in COD removal was observed after the system was fed with 30:70 of 2º influent to synthetic industrial dye-stuff effluent from a 50:50 composition. This might have caused an abrupt shock to the microbes in the aeration chambers, since decreases were observed in both the test and control units. Therefore, the influent was changed back to 40:60 of 2º influent/synthetic industrial dye-stuff effluent and again changed to 20:80 two days before the completion of SRT 6. Thereafter, COD removal improved to >80% before SRT 7 in both the units. Acclimatisation of activated sludge is a process for improving the ability of the biological treatment process to handle toxic contaminants; this process involves a step-wise introduction of the toxic influent and step-wise reduction of a non-toxic influent while monitoring the microbes' behaviour (El Bestawy et al., 2013; Fernández-Morales et al., 2010; Keskinkan & Göksu, 2007; Martinez et al., 2007). Therefore, the decrease in COD removal was attributed to the composition of the influent, which was composed largely of the synthetic industrial dye-

stuff effluent. This created an alien environment for the microbes thus resulting in a reduced COD removal.

During acclimatisation, BOD_5 removal efficiency was monitored at SRT 6–7 (day 51–70) and was found to be >50%, with the highest removal efficiency of 64% and 67% for the test and control units, respectively, being achieved (**Figure 19**). Adaptation of the microbes to the 100% synthetic industrial dye-stuff effluent was important before the addition of the nanoparticles in the test unit. This was to ensure that any decline in the removal of COD and BOD_5 is attributed solely to the TiO_2 nanoparticles added to the system. According to the OECD 303A, once the units are running efficiently, the system has to be allowed to run for one to six weeks, for the adaptation to reach a steady state (OECD, 2005). Thus, the system was allowed to run with 100% synthetic industrial dye-stuff effluent for a further two sludge retention times (SRT 8–9 (day 71–90)). A clear plateau phase is evident for COD removal (**Figure 18(b)**) from SRT 7–9 (day 71–90), which confirmed the adaptation of the microbes to the synthetic industrial dye-stuff effluent. This phase was characterised as an elimination curve in a continuous test where the maximum removal takes place (OECD, 2005). For the BOD_5, instead of a steady state occurring during SRT 7–9 (day 71–90), the removal improved to >70%; the highest removal percentage achieved was about 95% for the control unit and 94% for the test unit (**Figure 19**).

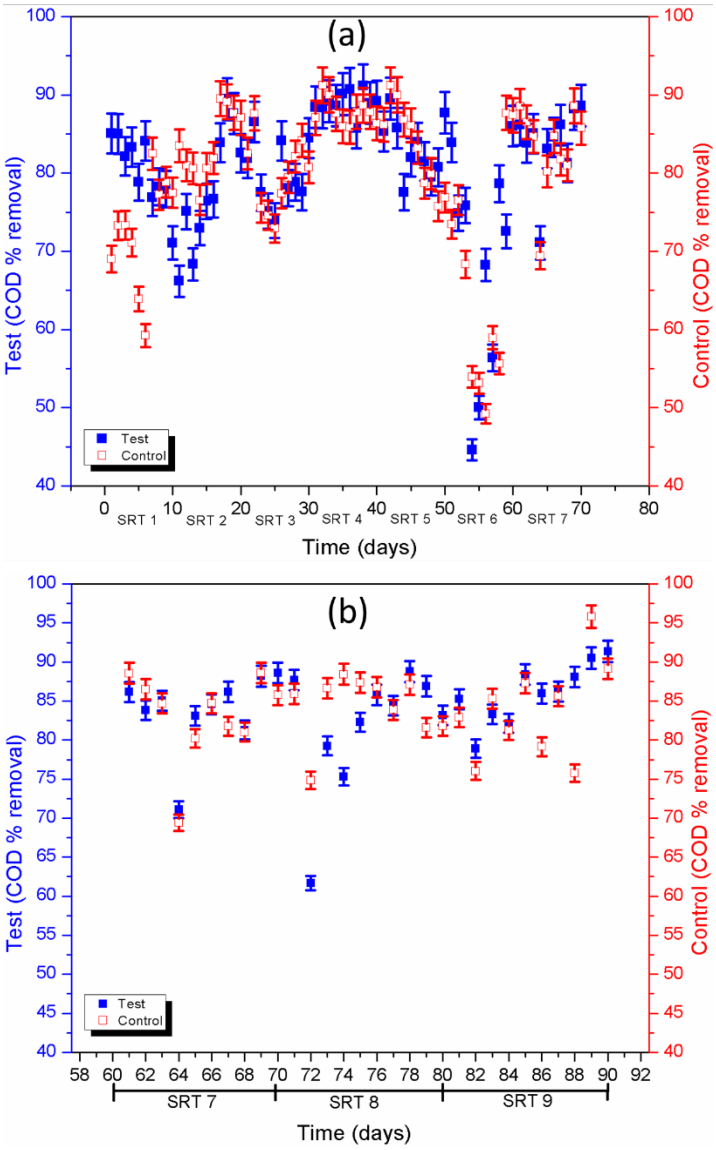

Figure 18 COD removal efficiency during (a) acclimatisation and (b) steady state of the treatment process (error bars indicate SD, n=3)

5.4.2 Treatment process functionality

The removal of the synthetic industrial dye-stuff effluent in the test unit was comparable with that in the control unit (see **Table 7**). As shown in **Figure 20**, a mean COD removal >80% was recorded at all concentrations (5 mg/L, 10 mg/L and 15 mg/L) of the TiO_2 nanoparticles. Therefore, no effect of the nanoparticles was observed on COD removal efficiency when the concentration of the nanoparticles was varied. At the beginning of SRT 10, the BOD_5 removal percentage decreased from 83% to 56% for the test unit and increased slightly from 71% to 73% for the control unit when 5 mg/L of TiO_2 was added. At day 95, the BOD_5 removal percentage increased to 78% and 82% for the test and control units respectively. The reduction in the BOD_5 removal percentage may be ascribed to the addition of a foreign component in the system in the form of nanoparticles. A comparative study of the removal

percentage of both BOD_5 and COD for all the SRTs in the presence of nanoparticles revealed that the nanoparticles had no observed effect on the overall efficiency of the treatment process. The COD concentrations of the SWWTP effluent were found to be below local and international wastewater discharge limits for COD (DWA, 2010; Grob et al., 2014).

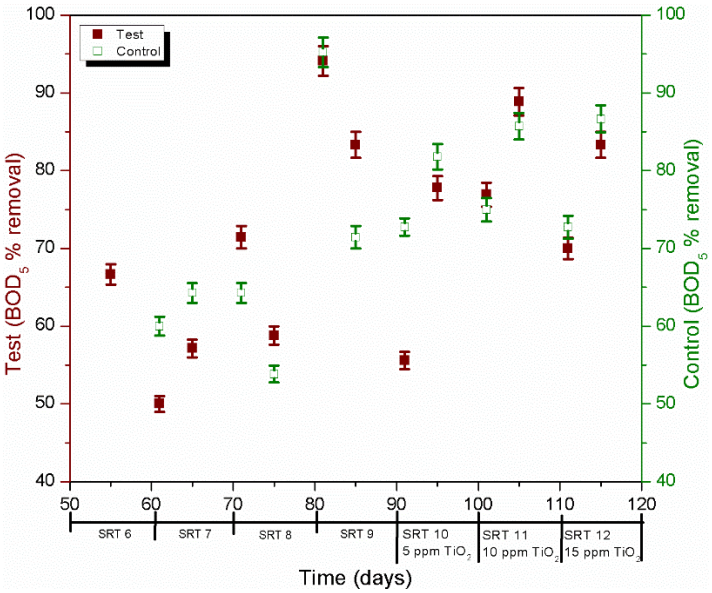

Figure 19 BOD_5 removal during the treatment process, before and after the addition of nanoparticles (error bars indicate SD, n=3)

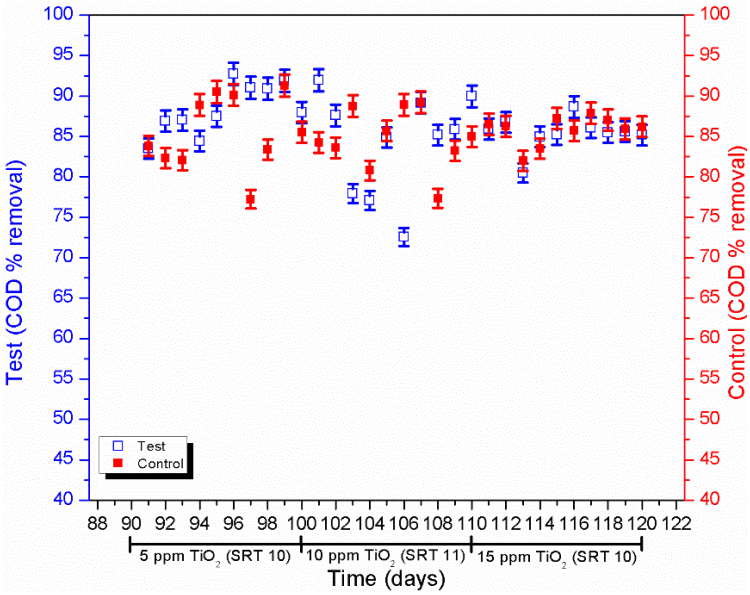

Figure 20 COD removal during exposure to TiO_2 nanoparticles in the treatment process (error bars indicate SD, n=3)

Table 7 Monitored parameters during treatment in the aerobic tanks and effluents

	5 mg/L TiO_2 (SRT 10: day 91–100)		10 mg/L TiO_2 (SRT 11:day 101–110)		15 mg/L TiO_2 (SRT 12: day 111–120)	
Parameters	*Mean*	*SD*	*Mean*	*SD*	*Mean*	*SD*
Test						
pH	Range: 6.0–7.4 Mode: 6.6	N/A	Range: 6.6–7.7 Mode: 7.3	N/A	Range: 6.2–7.7 Mode: 6.9	N/A
Dissolved oxygen (mg/L)	4.1	0.3	4.7	0.4	4.7	0.3
Temperature (˚C)	23.4	0.5	23.7	0.5	23.9	0.8
Conductivity (µS/cm)	821.5	38.2	872.1	53.9	892.7	57.2
MLSS (mg/L)	1248.3	272.8	1793.1	256.3	1616.9	175.3
MLVSS (mg/L)	1049.8	305.1	1603.1	283.7	1360.7	137.9
COD (mg/L)	40.8	13.6	48.8	17.7	51.3	8.0
BOD_5 (mg/L)	0.4	0.00	0.4	0.14	0.2	0.14
TN (mg/L)	48.0		53.0		70.0	
TSS (mg/L)	8.4	2.9	10.2	3.8	9.7	1.3
Control						
pH	Range: 6.3–7.3 Mode: 7.1	N/A	Range: 6.9–7.6 Mode:7.6	N/A	Range: 6.6–7.6 Mode: 7.0	N/A
Dissolved oxygen (mg/L)	3.8	0.6	4.7	0.4	4.3	0.5
Temperature (˚C)	23.9	0.6	21.8	0.8	23.9	0.9
Conductivity (µS/cm)	858.8	30.9	849.1	67.0	838.9	88.1
MLSS (mg/L)	1653.5	197.0	1959.9	118.3	1654.6	128.7
MLVSS (mg/L)	1475.9	187.1	1737.4	131.7	1431.7	151.0
COD (mg/L)	46.7	11.3	51.4	12.4	52.3	9.6
BOD_5 (mg/L)	0.3	0.14	0.15	0.07	0.25	0.07
TN (mg/L)	60.5		60.5		70.5	
TSS (mg/L)	7.3	2.5	8.7	2.4	11.4	1.6

SD: Standard Deviation

During the treatment, the removal of TN was not as efficient as the removal of COD and BOD_5 (see **Appendix 9** and **Table 7**). The removal percentage of TN in the test unit was found to be 44%, 40% and 30% when 5 mg/L, 10 mg/L and 15 mg/L of TiO_2 was added, respectively, (i.e. for SRT 10, SRT 11 and SRT 12, respectively). The percentage removal in the control unit was comparable to that in the test unit. The removal percentage of TN in the control unit was found to be 37%, 39% and 32% for SRT 10, SRT 11 and SRT 12, respectively. Efficient removal of TN in the SWWTP was not expected, given the aerobic nature of the treatment process. Nitrogen removal normally happens by consecutive alternations between oxic and anoxic operational conditions. Thus, in activated sludge systems where both oxic and anoxic microenvironments are present, TN removal can be realised, as this allows for efficient nitrification and denitrification (Nourmohammadi et al., 2013). The low removal percentage of TN cannot be attributed to the addition of nanoparticles as it was similar in both the test and control units.

The well-being of the microbes was further monitored by calculating the MLVSS/MLSS ratio (see **Appendix 9** and **Table 7**). In a conventional wastewater treatment system, the ratio of MLVSS/MLSS should be around 0.75 (Fan et al., 2015; Wentzel et al., 2002). In the case of the SWWTP test unit, the ratios were 0.84 (5 mg/L TiO_2 added), 0.89 (10 mg/L TiO_2 added) and 0.84 (15 mg/L TiO_2 added) for SRT 10, SRT 11 and SRT 12, respectively. The control unit showed comparable ratios (i.e. 0.89, 0.89 and 0.87 for SRT 10, SRT 11 and SRT 12, respectively. From these values, it can be concluded that the MLSS consisted largely of organic matter signifying the population of the microbes in the mixed liquor of the aeration tanks during the treatment process. These values are slightly more than the expected value for a conventional wastewater treatment system of 0.75. This is due to the fact that the synthetic sewage that was used for making the synthetic industrial dye-stuff effluent contained no suspended inorganic solids similar to ones found in the secondary influent of a conventional wastewater treatment system.

Total plate count (TPC) measurements seem to indicate that the bacteria in the sludge remained viable during the addition of TiO_2 nanoparticles. The TPC for the control unit at SRT 10 was comparable to the TPC for the test unit at SRT 10–12, which involved an addition of 5, then 10, and then 15 mg/L of nanoparticles, respectively (see **Figure 21**). Similarly, the correlation of these values appears to infer a comparable bacterial population in both the control and test units even during the addition of nanoparticles. From these results, it can be concluded that addition of the TiO_2 nanoparticles had no material effect on the treatment process.

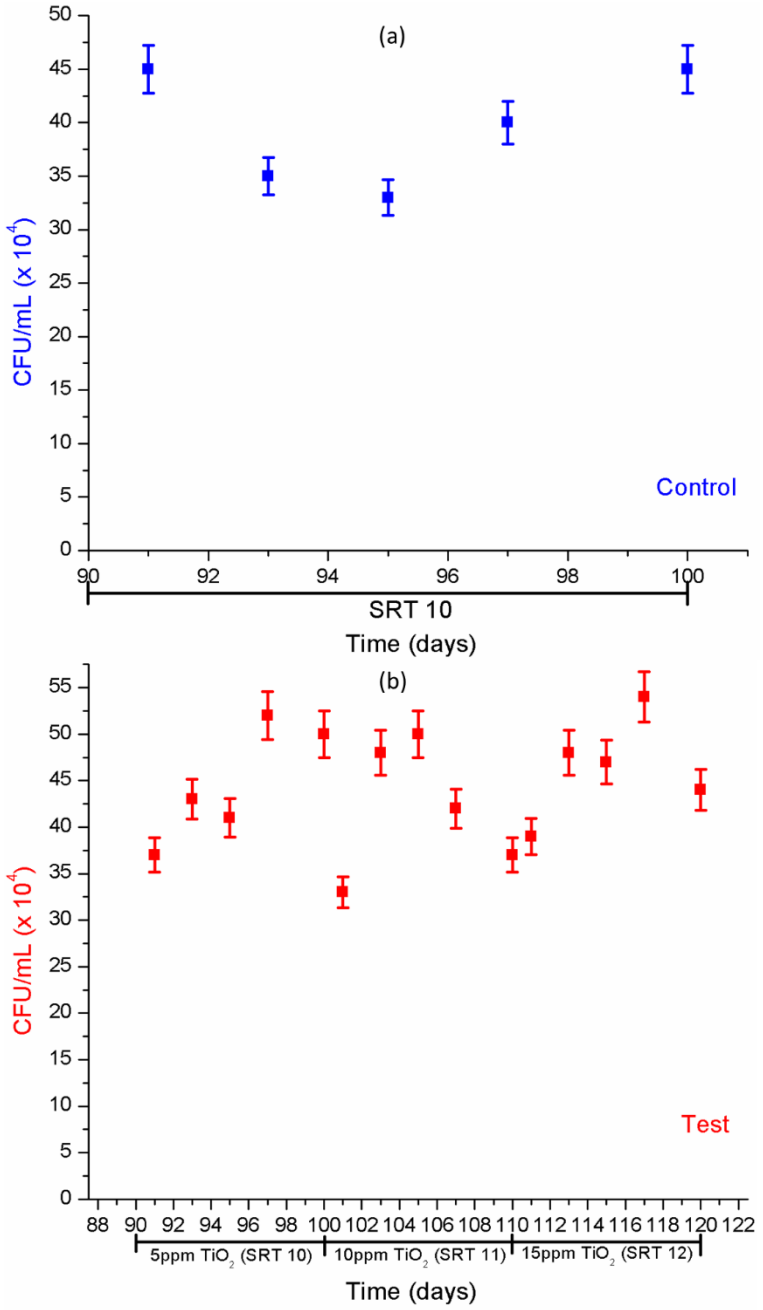

Figure 21 Total plate counts for (a) control unit and (b) test unit during the addition of TiO_2 nanoparticles (error bars indicated SD; n=3)

Efficient wastewater treatment also includes systematic removal of suspended solids. Removal of the TSS was poor, as the TSS in the influent was found to be approximately equal to that in the effluent (see **Appendix 9** and **Table 7**). Furthermore, the values of the MLSS were found to be below the expected value of 2500 mg/L(see **Table 7**). The use of disperse dyes influenced the settling ability of the flocs in the clarifier, thus contributing to the values of MLSS being lower than the expected value (2500 mg/L). This decrease in the sludge content can be attributed to the increase in the TSS values of the effluents. Mahlalela et al. (2017) reported that the addition of a similar dye-stuff in TiO_2 suspensions reduced the hydrodynamic

size of the nanoparticles in solution even in the presence of divalent cations that can effectively increase the hydrodynamic size. Thus, this further confirms the ability of the disperse dye to affect the settling ability of the sludge by dispersing it in solution. Another factor that might have affected the settling is the high amount of DO in the aeration tanks. During the treatment process, the sludge solids rose to the top of the clarifier with gas bubbles around them. This was caused by the degassing of the sludge solids in the clarifier due to the high amounts of DO, which led to the formation of the bubbles lifting the solids to the surface. Even though the settling ability was poor, the TSS values met both local and international wastewater discharge standards (DWA, 2010; Grob et al., 2014).

When the conductivity and pH of the SWWTP were measured, the conductivity measurement of the test unit effluent was found to be 821.5 µS/cm (5 mg/L TiO_2 added), 872.1 µS/cm (10 mg/L TiO_2 added) and 892.7 µS/cm (15 mg/L TiO_2 added) for SRT 10 (day 91–100), SRT 11 (day 101–110) and SRT 12 (day 111–120), respectively (see **Table 7**). The conductivity measurements of the test unit effluent were higher than those of the control. This can be attributed to the possible dissolution of the titanium dioxide nanoparticles during the treatment processes.

5.4.3 Behaviour of TiO_2 nanoparticles in the simulated wastewater treatment plant

An XRD scan of the dried sludge showed that the TiO_2 nanoparticles polymorph (anatase) of the initial TiO_2 nanoparticles (**Figure 22(a)**) before exposure to the treatment process did not change. Supporting evidence was provided by the XRD scan of the test dried activated sludge (see **Figure 22(b)**), which showed peaks corresponding to (101), (004), (200), (105), (211), (204), (116), (220) and (215) crystal planes. The ICDD: 04-013-5967 card confirmed the polymorph to be anatase as the peaks were in good agreement with the diffraction data. Therefore, it was concluded that the treatment process had no observable effect on the polymorph of the synthesised nanoparticles before exposure to the SWWTP.

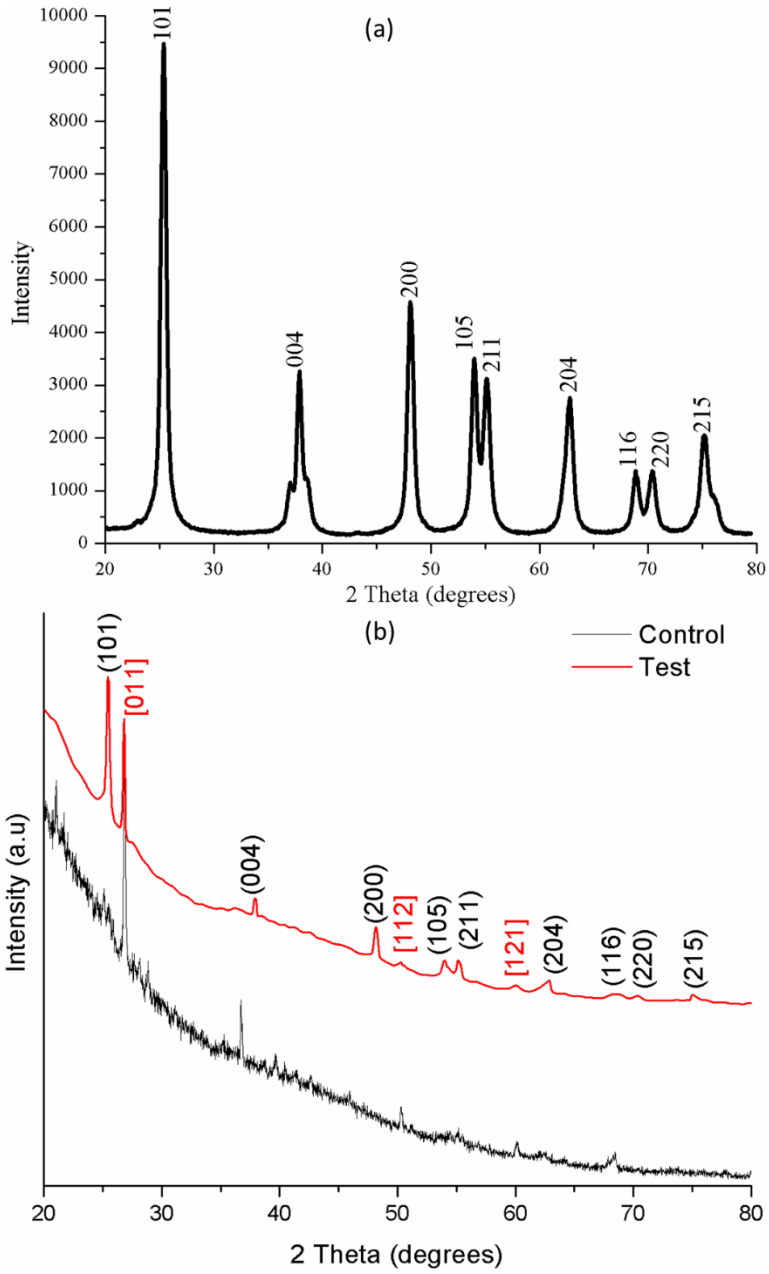

Figure 22 XRD patterns observed (a) Pristine TiO_2 and (b) after the analysis of dried activated sludge, for control and test units

Three peaks, ascribed to silicon dioxide (SiO_2) and corresponding to [011], [112] and [121] crystal planes (see **Figure 22(b)**), were also observed. The ICDD: 04-006-1757 card confirmed the crystal system to be hexagonal. Magdziarz et al. (2016) reported that SiO_2 was among the oxides found in sludge ashes in a study that examined the properties of ash generated during sewage sludge combustion. The main oxides in sewage sludge ash are reported as SiO_2, Al_2O_3, and CaO, while Fe_2O_3, Na_2O, MgO, P_2O_5, SO_3 and others are found in smaller amounts (Lynn et al., 2015). This was further confirmed by the XRD scan of the control dried activated sludge, which showed the presence of SiO_2 (see **Figure 22(b)**). Thus,

the SiO_2 was probably present in the activated sludge, which was used as inoculum for the SWWTP.

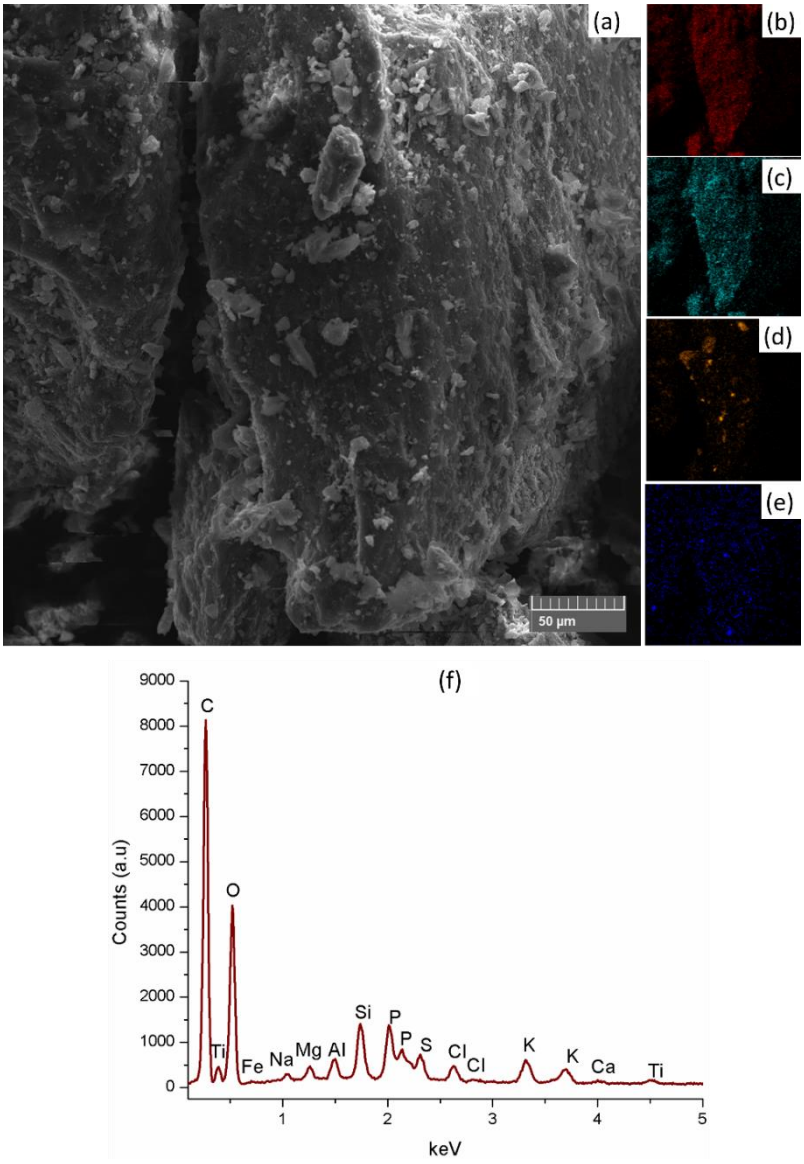

Figure 23(a) SE micrograph of dried activated sludge during the addition of 5 mg/L TiO_2 with the respective inserts of (b) carbon, (c) oxygen, (d) silicon, and (e) titanium after SEM mapping of the image. (f) EDS of the mapped image

SEM mapping further confirmed the presence of Ti in the sludge; this served to complement the XRD results and the residual elemental composition of the other elements in the sludge during the addition of 5 mg/L (SRT 10) (see **Figure 23**). Through the energy dispersive X-ray spectroscopy (EDS) spectrum of the sludge (see **Figure 23(f)**), it was possible to provide evidence for the presence of Ti peaks and all other elements present in the complex mixture of the sludge, as well as chemicals used during the treatment process. Therefore, the EDS spectrum suggests that some of the nanoparticles accumulate in the aeration tank by sorbing

on the sludge during treatment, or they agglomerate and settle in the clarifier during treatment and end up becoming part of the sludge. The SEM mapping micrographs also show the presence of C and O, which is expected for an entirely organic matter such as activated sludge; these peaks are the most intense peaks in the EDS spectrum. As shown in **Figure 23(d)**, the silicon (Si) mapping micrograph also supports the presence of SiO_2; XRD miller indices [011], [112] and [121], which are characteristic of SiO_2, are shown in **Figure 22**. Similar EDS results were observed for the addition of 10 mg/L (SRT 11) and 15 mg/L (SRT 12) TiO_2 nanoparticles (**Figure A11.1** and **Figure A11.2**, in **Appendix 11**, respectively).

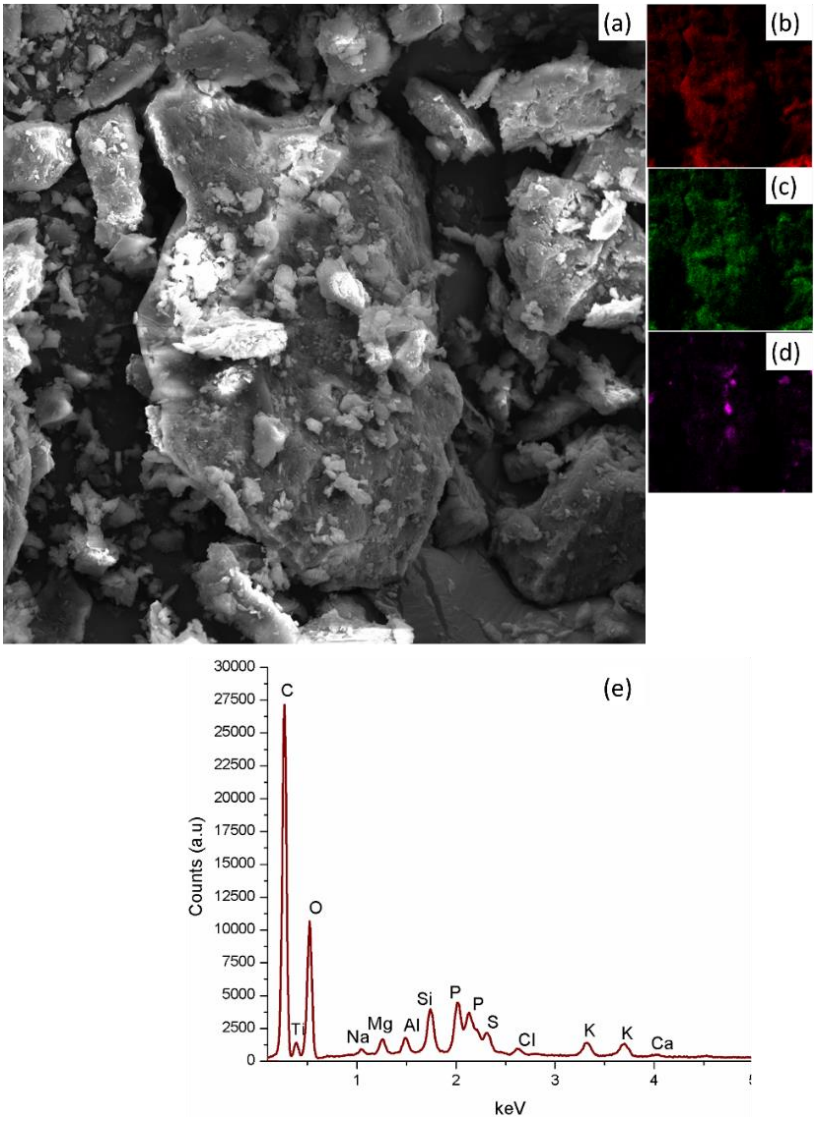

Figure 24 (a) SE micrograph of dried activated sludge from the control unit, at SRT 10, with the respective inserts of (b) carbon, (c) oxygen and (d) silicon. (e) EDS of the mapped image

Sludge from the control unit, at SRT 10, was also subjected to SEM mapping and EDS to validate the presence of Ti and compare the composition of this sludge with that of the test unit (**Figure 24**). Although SEM mapping results indicated no presence of Ti, the EDS

spectrum showed a Ti peak at around 0.4 keV (**Figure 24(e)**). The presence of Ti in sludge is expected, as TiO_2 nanoparticles often find their way into wastewater treatment systems due to their common use in consumer products such as food packaging materials, cosmetics, sunscreens and paints (Gartiser et al., 2014; Gottschalk & Nowack, 2011; Kiser et al., 2009). Another Ti peak, which was expected around 4.5 keV (see **Figure 24(e)**), only appeared in the EDS spectrum of the sludge from the test unit (see **Figure 23(f), Figure A11.1(f)** and **Figure A11.2(f)** (**Appendix 11**)).

5.4.4 Fate of TiO_2 nanoparticles in the simulated wastewater treatment plant

When the Ti concentration in the waste activated sludge was compared with that in the outflow of the SWWTP, a high correlation value of 0.88 was noted; the concentration of Ti in the sludge was higher by a factor of about 9 (see the slope of the graph illustrated in **Figure 25**) compared to the Ti concentration in the outflow (effluent) after the subtraction of background concentration analysed from the control unit waste activated sludge and outflow. This clearly shows that about 90% (1-1/8 = 0.88) of the TiO_2 nanoparticles reported to the activated sludge solids. The reporting mechanism may have been active or passive sorption to the solids, aggregation with the microorganisms, entrapment in the extracellular polysaccharides, or a combination of more than one mechanism. Furthermore, it may be that the majority of the effluent TiO_2 was associated with the effluent TSS rather than freely suspended. Similar results were reported in a study by Gartiser et al. (2014), in which more than 95% of TiO_2 nanoparticles were adsorbed onto the activated sludge in the outflow of a lab-scale sewage treatment plant. In summary, the results of this study show that the Ti in the treated effluents accounted for 10-12% of the total TiO_2 nanoparticles introduced to the SWWTP.

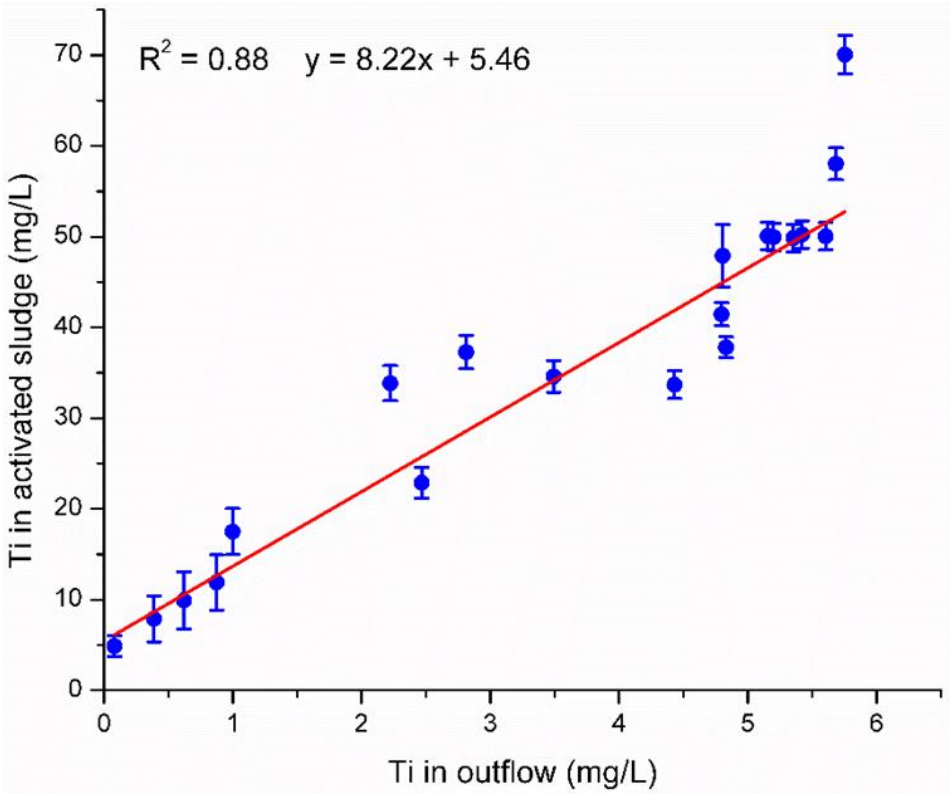

Figure 25 Ti in activated sludge compared to that in the outflow of the SWWTP

Several studies reported below, which involved simulation of treatment processes following the OECD 303A, seem to be in agreement with the results of this study. While no impact on the treatment process after addition of nanoparticles was experienced, the results show that the majority of the nanoparticles were retained on the sludge, while a very small fraction went out with the effluent. Chaüque et al. (2016) investigated the fate, behaviour and implications of ZnO nanoparticles in a SWWTP following the OECD guidelines, and a high efficiency of removal of ZnO ENPs (>96%) from effluent wastewater was reported.

Gomez-Rivera et al. (2012) studied the fate of CeO_2 nanoparticles in municipal wastewater during activated sludge treatment, and reported that around 97% of CeO_2 nanoparticles were removed over a period of 63 days during the treatment process. Furthermore, synthetic wastewater, simulated according to OECD 303A, resulted in more stable CeO_2 nanoparticles. This proves the applicability of OECD 303A in assessing the behaviour of nanoscale materials in SWWTPs.

Results obtained from the simulation of treatment processes in assessing the fate of nanoparticles in treatment systems are often comparable to those reported for full-scale wastewater treatment systems. For example, Westerhoff et al. (2011) monitored the occurrence and removal of titanium at ten full-scale wastewater treatment plants and concluded that these plants removed more than 96% of the influent titanium, with effluent

concentrations of less than 25 µg/L being reported. Therefore, most of these studies report a >90% removal of the nanoscale material from influent wastewater, which is in good agreement with results obtained from this study. Biosorption of activated sludge is generally regarded as the main mechanism for removing the nanoparticles (Gartiser et al., 2014; Kiser et al., 2009; Kiser et al., 2010; Westerhoff et al., 2011). Furthermore, this shows that nanoparticles received by wastewater treatment systems will reach the environment through the disposal of the waste sludge, which may be by landfill, ocean outfall, or incineration.

6 CONCLUSIONS

The objective of this work was to monitor the fate and behaviour of TiO_2 nanoparticles in a SWWTP that contains industrial dye-stuff effluent. The synthesised nanoparticles were characterised using SEM, TEM, Malvern zetasizer nanoZS, BET, EDS and XRD before introducing them into the SWWTP. The stability of the nanoparticles was determined prior to their exposure to the SWWTP. The preliminary stability studies were undertaken with a view to understanding the challenge the industrial dye-stuff might pose to the fate and behaviour of the nanoparticles. Thereafter, the nanoparticles were exposed to the SWWTP, after which their presence in the sludge and in the effluent was monitored using ICP-OES. SEM mapping was used to confirm the presence of the nanoparticles in the sludge. The effect of the TiO_2 nanoparticles on the functionality of the SWWTP was then monitored by taking measurements of COD, BOD_5, TN, TSS, MLSS, MLVSS, pH and conductivity. Based on these objectives, several conclusions can be made.

The TiO_2 nanoparticles were successfully synthesised. Characterisation of the nanoparticles with XRD and Raman confirmed an anatase crystal structure. The average particle size, according to TEM analysis, was 12.15 nm, which was found to be comparable to the 15 nm calculated from the XRD using the Debye-Scherrer equation. BET analysis of the TiO_2 nanoparticles indicated a mesoporous material ascribed to the type VI characteristic isotherm, which contains a type H1 hysteresis loop. This type of hysteresis loop is ascribed to porous materials that have agglomerates. The agglomerates were observed on the TEM and SEM images of the nanoparticle.

Characteristics of solution matrices such as ionic strength, the nature of the electrolytes, solution pH and dye-stuff were paramount in explaining the stability of TiO_2 nanoparticles in solution as they affect properties such as surface charge and electrical double layer.

It was observed that an increase in ionic strength increased the agglomeration of TiO_2 nanoparticles, while the dye-stuff decreased the hydrodynamic sizes. An increase in the hydrodynamic sizes of the TiO_2 nanoparticles in this experiment carried out under alkaline pH conditions in the presence of $CaCl_2$ was observed, and this was due to the Ca^{2+} effectively reducing the electrical double layer. An increase in the hydrodynamic sizes of the TiO_2 nanoparticles was observed even in the presence of the dye-stuff. Thus, factors such as steric hindrance were important in explaining the role of dye-stuff in the stability of the nanoparticles. However, the presence of Ca^{2+} effectively neutralised negatively charged TiO_2 surfaces, even in the presence of negatively charged dye-stuff molecules on the surfaces of nanoparticles.

Divalent cations were found to have a neutralising effect on the surfaces of nanoparticles as Mg^{2+} behaved in a similar manner.

The extent of stability and/or agglomeration of nanoparticles was explained using the DLVO theory. The TEM and SEM images also confirmed the agglomeration of TiO_2 nanoparticles to even larger hydrodynamic sizes in solution. Thus, the variation in the behaviour of the TiO_2 nanoparticles in different suspensions provided evidence that nanoparticles will undergo several environmental pathways, which are influenced by their size, surface charge and agglomeration states.

Prior to exposure to TiO_2 nanoparticles in the SWWTP, acclimatisation of the activated sludge to the synthetic industrial dye-stuff effluent was conducted and successfully achieved. Measurements of COD removal clearly affirmed the acclimatisation, after a steady state with an average removal of >80% was observed at SRT 7–9. The addition of nanoparticles was conducted at SRT 10–12 and the removal of COD remained at >80%, which implied that the nanoparticles had no effect on the treatment process.

Parameters such as pH, conductivity and TSS further confirmed the efficiency of the treatment process as these parameters met the limit values of both local and international standards. An XRD analysis was used to investigate the behaviour of the nanoparticles. The analysis showed that the TiO_2 that was present in the sludge had not changed, as it maintained the anatase crystal structure of the TiO_2 nanoparticles before exposure to the SWWTP.

With respect to the fate of the nanoparticles, the results showed that about 90% of the TiO_2 was retained in the activated sludge, and 10–11% escaped with the treatment effluents. The TiO_2 nanoparticles were removed effectively by the SWTP from the influent. Sorption of the nanoparticles on the activated sludge facilitated their removal. SEM mapping showed the presence of Ti on the sludge; this served as further confirmation for the sorption of the TiO_2 nanoparticles on the activated sludge.

7 RECOMMENDATIONS

Work still needs to be carried out on culturing the activated sludge microorganisms to determine the genera, and thus the structural properties of the cells. It is important to understand the interactions between the TiO_2 nanoparticles and the cell walls of the microorganisms; this will enable us to make proper conclusions on the type of sorption process that is involved (i.e. whether it is chemisorption, physisorption or biosorption). Furthermore, such a study will contribute towards a deeper understanding of the removal of the dye-stuff during treatment.

Apart from the removal of organics, utilisation of the small fraction of nanoparticles that escapes with the effluent can be investigated. This may be used in conjunction with UV light to assist in disinfection of the effluent, for the removal of any microorganisms present in the effluent before release into the environment.

Modifications to the simulated WWTP to include anaerobic and anoxic stages can be considered in future studies. This would provide a more realistic approach in the study of the fate of nanomaterials in WWTPs. Wastewater treatment plants in South Africa are not limited to aerobic treatment but include a combination of anaerobic, aerobic and anoxic.

Lastly, the system needs to be extended to include a photocatalytic component that uses photocatalysts, either in suspension or embedded on a support, to provide a more realistic approach to the photocatalytic removal of organics. The positioning of the photocatalytic component would be determined by the type of wastewater to be degraded, based on parameters such as toxicity.

8 LIST OF REFERENCES

ADAMS LK, LYON DY and ALVAREZ PJJ (2006) Comparative eco-toxicity of nanoscale TiO_2, SiO_2 and ZnO water suspensions. *Water Research* **40** (19) 3527–3532.

ASAHI R, MORIKAWA T, OHWAKI T, AOKI K and TAGA Y (2001) Visible-light photocatalysis in nitrogen-doped titanium oxides. *Science* **293** (5528) 269–271

AZELLA ZSN (2011) Synthesis and characterization of pure anatase TiO_2 aggregates. *Journal of Applied Sciences* **11** (8) 1326–1330.

BA-ABBAD MM, KADHUM AAH, MOHAMAD AB, TAKRIFF MS and SOPIAN K (2012) Synthesis and catalytic activity of TiO_2 nanoparticles for photochemical oxidation of concentrated chlorophenols under direct solar radiation. *International Journal of Electrochemical Science* **7** (6) 4871–4888.

BERMUDEZ E, MANGUM JB, ASGHARIAN B, WONG BA, REVERDY EE, JANSZEN DB, HEXT PM, WARHEIT DB and EVERITT JI (2002) Long-term pulmonary responses of three laboratory rodent species to subchronic inhalation of pigmentary titanium dioxide particles. *Toxicological Sciences* **70** (1) 86–97.

BERMUDEZ E, MANGUM JB, WONG BA, ASGHARIAN B, HEXT PM, WARHEIT DB and EVERITT JL (2004) Pulmonary responses of mice, rats, and hamsters to subchronic inhalation of ultrafine titanium dioxide particles. *Toxicological Sciences* **77** (2) 347–357.

BERSANI D, ANTONIOLI G, LOTTICI PP and LOPEZ T (1998) Raman study of nanosized titania prepared by sol-gel route. *Journal of Non-Crystalline Solids* **232-234** 175–181.

BRAR SK, VERMA M, TYAGI RD and SURAMPALLI RY (2010) Engineered nanoparticles in wastewater and wastewater sludge – evidence and impacts. *Waste Management* **30** (3) 504–520.

BYRANVAND MM, KHARAT AN, FATHOLAHI L and BEIRANVAND ZM (2013) A review on synthesis of nano-TiO_2 via different methods. *Journal of Nanostructures* **3** 1–9.

CAN OT, KOBYA M, DEMIRBAS E and BAYRAMOGLU M (2006) Treatment of textile wastewater by combined electrocoagulation. *Chemosphere* **62** (2) 181–187.

CHAKRABORTY L (2009). Effects of man-made nanoparticles on the aquatic biosphere. **5**

50. Retrieved from http://www.ibp.ethz.ch/research/aquaticchemistry/teaching/archive_past_lectures/Term_Paper_HS2009/BURGERCHAKRABORTY_termpaper_HS09.pdf Date: 20 March 2015.

CHAMPION JA and MITRAGOTRI S (2006) Role of target geometry in phagocytosis. *Proceedings of the National Academy of Science USA* **103** (13) 4930–4934.

CHAÜQUE EFC (2012) Monitoring of physicochemical parameters and the behavior of zinc oxide nanoparticles in a simulated wastewater treatment plant. MSc. Dissertation. Faculty of Science. University of Johannesburg. Retrieved: http://ujdigispace.uj.ac.za Date: 28 February 2015.

CHAÜQUE EFC, ZVIMBA JN, NGILA JC and MUSEE N (2016) Fate, behaviour, and implications of ZnO nanoparticles in a simulated wastewater treatment plant. *Water SA* **42** (1), 72–81.

CHERCHI C and GU AZ (2010) Impact of titanium dioxide nanomaterials on nitrogen fixation rate and intracellular nitrogen storage in *Anabaena varialbilis*. *Environmental Science and Technology* **44** (21) 8302–8307.

CHOI HS, ASHITATE Y, LEE JH, KIM SH, MATSUI A, INSIN N, BAWENDI MG, SEMMLER-BEHNKE M, FRANGIONI JV and TSUDA A (2010) Rapid translocation of nanoparticles from lung airspaces to the body. *Nature Biotechnology* **28** 1300–1303.

CHONG MN, JIN B, CHOW CWK and SAINT C (2010) Recent developments in photocatalytic water treatment technology: A review. *Water Research* **44** (10) 2997–3027.

CHONG MN, LEI S, JIN B, SAINT C and CHOW CWK (2009) Optimisation of an annular photoreactor process for degradation of Congo Red using a newly synthesized titania impregnated kaolinite nano-photocatalyst. *Separation and Purification Technology* **67** (3) 355–363.

CONG Y, ZHANG J, CHEN F and ANPO M (2007) Synthesis and characterization of nitrogen-doped TiO_2 nanophotocatalyst with high visible light activity. *The Journal of Physical Chemistry* A **111** (19) 6976–6982.

CROSERA M, BOVENZI M, MAINA G, ADAMI G, ZANETTER C, FLORIO C and LARESE FF (2009) Nanoparticle dermal adsorption and toxicity: a review of literature. *International Archives of Occupational and Environmental Health* **82** (9) 1043–1055.

DAVIES PS (2005) The Biology Basis of Wastewater Treatment. Strathkelvin Instruments. 1.05 Kelvin Campus. West of Scotland Science Park. Glasgow G20 OSP. UK. Retrieved: http://www.s-can.nl/media/1000154/thebiologicalbasisofwastewatertreatment.pdf Date: 28 February 2015.

DAVIS J, WANG A and SHTAKIN J (2010) Nanomaterial case studies: nanoscale titanium dioxide in water treatment and in topical sunscreen. US EPA: Research Triangle Park, NC, (November). Retrieved: https://doi.org/EPA/600/R-09/057F Date: 17 April 2015.

DLAMINI LN, KRAUSE RW, KULKARNI GU and DURBACH SH (2011) Photodegradation of bromophenol blue with fluorinated TiO_2 composite. *Applied Water Science* **1** (1-2) 19–24.

DUNPHY-GUZMAN KA, FINNEGAN MP and BANFIELD JF (2006) Influence of surface potential on aggregation and transport of itiania nanoparticles. *Environmental Science & Technology* **40** (24) 7688–7693.

DURENKAMP M, PAWLETT M, RITZ K, HARRIS JA, NEAL AL and MCGRATH, SP (2016) Nanoparticles within WWTP sludges have minimal impact on leachate quality and soil microbial community structure and function. Environmental Pollution **211** 399–405.

DWA (2010) National Water Act - Waste Discharge Standards DWA 2010 guidelines. *Water*. Department of Water Affairs, South Africa. Retrieved from http://wateronline.co.za/wastewater/downloads/dwa-general-standards-2010.pdf Date: 20 March 2015.

EL BESTAWY E, HELMY S, HUSSEIN H and FAHMY M (2013) Optimization and/or acclimatization of activated sludge process under heavy metals stress. *World Journal of Microbiology and Biotechnology*, **29** (4) 693–705.

FAISAL M, TARIQ MA and MUNEER M (2007) Photocatalysed degradation of two selected dyes in UV-irradiated aqueous suspensions of titania. *Dyes and Pigments* **72** (2) 233–239.

FAN J, JI F, XU X, WANG Y, YAN D, XU X and HE Q (2015) Prediction of the effect of fine grit on the MLVSS/MLSS ratio of activated sludge. *Bioresource Technology* **190** 51–56.

FERNÁNDEZ-MORALES FJ, VILLASEÑOR J and INFANTES D (2010) Modeling and monitoring of the acclimatization of conventional activated sludge to a biohydrogen producing culture by biokinetic control. *International Journal of Hydrogen Energy* **35** (20) 10927–10933.

FIELD RSJA (2012) Fate of Emerging Nanoparticle Contaminants during Aquifer Recharge

with Treated Wastewater (Project #2012AZ476B). Tucson. Retrieved: https://wrrc.arizona.edu/sites/wrrc.arizona.edu/files/pdfs/104b final-report-Sierra-12-END.pdf Date: 01 June 2015.

FRENCH RA, JACOBSON AR, KIM B, ISLEY SL, PENN LR and BAVEYE PC (2009) Influence of ionic strength, pH, and cation valence on aggregation kinetics of titanium dioxide nanoparticles. *Environmental Science and Technology* **43** (5) 1354-1359.

FU G, VARY PS and LIN C-T (2005) Anatase TiO_2 nanocomposites for antimicrobial coatings. *Journal of Physical Chemistry B* **109** (18) 8889–8898.

FUJISHIMA A, ZHANG X and TRYK DA (2008) TiO_2 photocatalysis and related surface phenomena. *Surface Science Reports* **63** (12) 515–582.

GARTISER S, FLACH F, NICKEL C, STINTZ M, DAMME S, SCHAEFFER A and KUHLBUSCH TAJ (2014) Behavior of nanoscale titanium dioxide in laboratory wastewater treatment plants according to OECD 303 A. *Chemosphere* **104** 197–204.

GHALY MY, FARAH JY and FATHY AM (2007) Enhancement of decolorization rate and COD removal from dyes containing wastewater by the addition of hydrogen peroxide under solar photocatalytic oxidation. *Desalination* **217** (1–3), 74–84.

GOMEZ-RIVERA F, FIELD JA, BROWN D and SIERRA-ALVAREZ R (2012) Fate of cerium dioxide (CeO_2) nanoparticles in municipal wastewater during activated sludge treatment. *Bioresource Technology* **108** 300–304.

GOTTSCHALK F and NOWACK B (2011) The release of engineered nanomaterials to the environment. *Journal of Environmental Monitoring* **13** 1145–1155.

GRADY CPL, DAIGGER GT, LOVE NG and FILIPE CDM (2011) *Biological Wastewater Treatment*. 3rd Edition. CRC Press Taylor & Francis Group.

GREENBERG AE, CLESCERI LS and EATON AD (1992) *Standard Methods for the Examination of Water and Wastewater.*18th Edition. Washington: American Public Health Association.

GROB M, KLIPPSTEIN C, MAURER P, SALAZAR Y, SCHWAB T, TREFFRY-GOATLEY K and VOORTMAN J (2014) Wastewater treatment. Retrieved: https://courses.edx.org/c4x/DelftX/CTB3365x/asset/Wastewater_Lecture_Note.pdf Date: 20 April 2016.

GRZECHULSKA J and MORAWSKI AW (2002) Photocatalytic decomposition of azo-dye acid black 1 in water over modified titanium dioxide. *Applied Catalysis B: Environmental* **36** (1) 45–51.

GUILLARD C, LACHHEB H, HOUAS A, KSIBI M, ELALOUI E, HERRMANN J-M (2003) Influence of chemical structure of dyes, of pH and of inorganic salts on their photocatalytic degradation by TiO_2 comparison of the efficiency of powder and supported TiO_2. *Journal of Photochemistry and Photobiology A: Chemistry* **158** (1) 27–36.

GÚMÚŞ D and AKBAL F (2011) Photocatalytic degradation of textile dye and wastewater. *Water Air and Soil Pollution* **216** (1-4) 117–124.

GURR J-R, WANG ASS, CHEN C-H and JAN K-J (2005) Ultrafine titanium dioxide particles in the absence of photoactivation can induce oxidative damage to human bronchial epithelial cells. *Toxicology* **213** (1-2) 66–73.

IAVICOLI I, LESO V, FONTANA L and BERGAMASCHI A (2011) Toxicology effects of titanium dioxide nanoparticles: a review of *in vitro* mammalian studies. *European Review for Medical and Pharmacological Sciences* **15** (5) 481–508.

JIANG J, OBERDÖRSTER G and BISWAS P (2009) Characterization of size, surface charge, and agglomeration state of nanoparticle dispersions for toxicological studies. *Journal of Nanoparticle Research* **11** (1) 77–89.

JONER E, HARTNIK T and AMUNDSEN C (2007) Environmental fate and ecotoxicity of engineered nanoparticles. Norwegian Pollution Control Authority Report no. TA 2304/2007. Retrieved: http://scholar.google.com/scholar?hl=en&btnG=Search&q=intitle:ENVIRONMENTAL+FATE+AND+ECOTOXICITY+OF+ENGINEERED+NANOPARTICLES#5 Date: 08 February 2015.

KAEGI R, ULRICH A, SINNET B, VONBANK R, WICHSER A, ZULEEG S, SIMMLER H, BRUNNER S, VONMONT H, BURKHARDT M and BOLLER M (2008) Synthetic TiO_2 nanoparticle emission from exterior facades into the aquatic environment. *Environmental Pollution* **156** (2) 233–239.

KAEGI R, VOEGELIN A, SINNET B, ZULEEG S, HAGENDORFER H, BURKHARDT M and SIEGRIST H (2011) Behavior of metallic silver nanoparticles in a pilot wastewater treatment plant. *Environmental Science and Technology* **45** (9) 3902–3908.

KAEWAMATAWONG T, KAWAMURA N, OKAJIMA N, SAWADA M, MORITA T and

SHIMADA A (2005) Acute pulmonary toxicity caused by exposure to colloidal silica: particle size dependent pathological changes in mice. *Toxicologic Pathology* **33** (7) 745–751.

KAKINOKI K, YAMANE K, TERAOKA R, OTSUKA M and MATSUDA Y (2004) Effect of relative humidity on the photocatalytic activity of titanium dioxide and photostability of famotidine. *Journal of Pharmaceutical Sciences* **93** (3) 582–589.

KELLER AA, WANG H, ZHOU D, LENIHAN HS, CHERR G, CARDINALE BJ, MILLER R and JI Z (2010) Stability and aggregation of metal oxide nanoparticles in natural aqueous matrices. *Environmental Science and Technology* **44** (6) 1962–1967.

KESKINKAN O and GÖKSU MZL (2007) Assessment of the dye removal capability of submersed aquatic plants in a laboratory-scale wetland system using ANOVA. *Brazilian Journal of Chemical Engineering* **24** (2) 193–202.

KIM H-C and YU M-J (2005) Characterization of natural organic matter in conventional water treatment processes for selection of treatment processes focused on DBPs control. *Water Research* **39** (19) 4779–4789.

KIM Y (2014) Nanowastes treatment in environmental media. *Environmental Health and Toxicology* 29 1–7.

KISER MA, RYU H, JANG H, HRISTOVSKI K and WESTERHOFF P (2010) Biosorption of nanoparticles to heterotrophic wastewater biomass. *Water Research* **44** (14) 4105–4114.

KISER MA, WESTERHOFF P, BENN T, WANG Y, PEREZ-RIERA J and HRISTOVSKI K (2009) Titanium nanomaterial removal and release from wastewater treatment plants. *Environmental Science and Technology* **43** (17) 6757–6763.

KLAINE SJ, ALVAREZ PJJ, BATLEY GE, FERNANDES TF, HANDY RD, LYON DY, MAHENDRA S, MCLAUGHLIN MJ and LEAD J R (2008) Nanomaterials in the environment: behaviour, fate, bioavailability, and effects. *Environmental Toxicology and Chemistry* **27** (9) 1825–1851.

KLESING J, WIEHE A, GITTER B, GRÄFE S and EPPLE M (2010) Positively charged calcium phosphate/polymer nanoparticles for photodynamic therapy. *Journal of Materials Science: Materials in Medicine* **21** (3) 887–892.

KÖHLER AR, SOM C, HELLAND A and GOTTSCHALK F (2008) Studying the potential release of carbon nanotubes throughout the application life cycle. *Journal of Cleaner*

Production **16** (8-9) 927–937.

LIMBACH LK, BEREITER R, MULLER E, KREBS R, GALLI R and STARK WJ (2008) Removal of oxide nanoparticles in a model wastewater treatment plant: Influence of agglomeration and surfactants on clearing efficiency. *Environmental Science and Technology* **42** (15) 5828–5833.

LIN J and HARICHUND C (2011) Industrial effluent treatments using heavy-metal removing bacterial bioflocculants. *Water SA* **37** (2) 265–270.

LIU Y, LI W, LAO F, LIU Y, WANG L, BAI R, ZHAO Y and CHEN C (2011) Intracellular dynamics of cationic and anionic polystyrene nanoparticles without direct interaction with mitotic spindle and chromosomes. *Biomaterials* **32** (32) 8291–8303.

LIU Z-H, KANJO Y and MIZUTANI S (2009) Removal mechanisms for endocrine disrupting compounds (EDCs) in wastewater treatment – physical means, biodegradation and chemical advanced oxidation: a review. *Science of the Total Environment* **407** (2) 731–748.

LUYTS K, NAPIERSKA D, NEMERY B and HOET PHM (2013) How physico-chemical characteristics of nanoparticles cause their toxicity: complex and unresolved interrelations. *Environmental Science: Process and Impacts* **15** (1) 23–38.

LYNN CJ, DHIR RK, GHATAORA GS and WEST RP (2015) Sewage sludge ash characteristics and potential for use in concrete. *Construction and Building Materials* **98** 767–779.

MAGDZIARZ A, WILK M, GAJEK M, NOWAK-WOŹNY D, KOPIA A, KALEMBA-REC I and KOZIŃSKI JA (2016) Properties of ash generated during sewage sludge combustion: A multifaceted analysis. *Energy* **113** 85–94.

MAHLALELA LC, NGILA JC and DLAMINI LN (2017) Characterization and Stability of TiO_2 Nanoparticles in Industrial Dye Stuff Effluent. *Journal of Dispersion Science and Technology* **38** (4) 584–593.

MANESS P-C, SMOLINSKI S, BLAKE DM, HUANG Z, WOLFRUM EJ and JACOBY WA (1999) Bactericidal activity of photocatalytic TiO_2 reaction: toward an understanding its killing mechanism. *Applied and Environmental Microbiology* **65** (9) 4094–4098.

MARTINEZ F, BETANCUR MJ, MORENO JA, BUITRON G and MORENO-ANDRADE I (2007) Acclimation model of an aerobic bioreactor for the treatment of toxic wastewater. IFAC

Proceedings Volumes (IFAC-PapersOnline) **10** (4) 67–72.

MAUTER MS and ELIMELECH M (2008) Environmental application of carbon-based nanomaterials. *Environmental Science and Technology* **42** (16) 5843–5859.

METCALF and EDDY (2003). *Wastewater Engineering: Treatment and Reuse.* 4th Edition. New York. McGraw-Hill Companies, Inc.

MIN S, WANG F and HAN Y (2007) An investigation on synthesis and photocatalytic activity of polyaniline sensitized nanocrystaline TiO_2 composites. *Journal of Materials Science* **42** (24) 9966–9972.

MORIMOTO Y, KOBAYASHI N, SHINOHARA N, MYOJO T, TANAKA I and NAKANISHI J (2010) Hazard assessments of manufactured nanomaterials. *Journal of Occupational Health* **52** (6) 325–334.

MUHD JULKAPLI N, BAGHERI S and BEE ABD HAMID S (2014) Recent advances in heterogeneous photocatalytic decolorization of synthetic dyes. *Scientific World Journal* **2014** 1–7.

MUSEE N (2011) Simulated environmental risk estimation of engineered nanomaterials: a case of cosmetics in Johannesburg City. *Human & Experimental Toxicology* **30** (9) 1181–1195.

MUSIĆ S, GOTIC M, IVANDA M, POPOVIC S, TURKOVIC A, TROJKO R, SEKULIC A and Furic K (1997) Chemical and microstructural properties of TiO_2 synthesized by sol-gel method. *Materials Science and Engineering: B* **47** 33–40.

NI MÃMKHL, LEUNG DYC and SUMATHY K (2007) A review and recent developments in photocatalytic water-splitting using TiO_2 for hydrogen production. *Renewable and Sustainable Energy Reviews* **11** 401–425.

NKAMBULE TI (2007). An analytical approach to the characterization and removal of natural organic matter from water using ozone and cyclodextrin polyurethanes. MSc. Dissertation. Faculty of Science. University of Johannesburg. Retrieved: http://ujdigispace.uj.ac.za Date: 28 April 2015.

NOURMOHAMMADI D, ESMAEELI MB, AKBARIAN H and GHASEMIAN M (2013) Nitrogen removal in a full-scale domestic wastewater treatment plant with activated sludge and trickling filter. *Journal of Environmental and Public Health* **2013**.

NOWACK B, RANVILLE JF, DIAMOND S, GALLEGO-URREA JA and METCALFE C (2012) Potential scenarios for nanomaterial release and subsequent alteration in the environment. *Environmental Toxicology and Chemistry* **31** (1) 50–59.

OBERDÖRSTER G, MAYNARD A, DONALDSON K, CASTRANOVA V, FITZPATRICK J, AUSMAN K, CARTER J, KARN B, KREYLING W, LAI D, OLIN S, MONTEIRO-RIVIERE N, WARHEIT D and YANG H (2005) Principles for characterizing the potential human health effects from exposure to nanomaterials: elements of a screening strategy. *Particle and Fibre Toxicology* **2** (8) DOI: 10.1186/1743-8977-2-8.

OECD (2005) OECD guideline for the testing of chemicals. OECD guideline for testing of chemicals 303A. Retrieved: http://www.oecd.org/chemicalsafety/testing/34898616.pdf Date: 10 January 2015.

OZAKI A (2013) Assessing the effects of titanium dioxide nanoparticles on microbial communities in stream sediment using artificial streams and high throughput screening. MSc dissertation. Loyola University Chicago. Paper 1823. Retrieved: http://ecommons.luc.edu/luc_theses/1823 Date: 01 April 2015.

PARRA R, GOES MS, CASTRO MS, LONGO E, BUENO PR and VARELA JA (2008) Reaction pathway to synthesis of anatase via the chemical modification of titanium isopropoxide with acetic acid. *Chemistry of Materials* **20** (1) 143–150.

PAULAUSKAS IE, MODESHIA DR, ALI TT, EL-MOSSALAMY EH, OBAID AY, BASAHEL SN and SARTAIN FK (2013) Photocatalytic activity of doped and undoped titanium dioxide nanoparticles synthesised by flame spray pyrolysis platinum-doped TiO_2 composites show improved activity compared to commercially available product. *Platinum Metals Review* **57** (1) 32–43.

PELAEZ M, NOLAN NT, PILLAI SC, SEERY MK, FALARAS P, KONTOS AG, DUNLOP PSM, HAMILTON JWJ, BYRNE JA, O'SHEA K, ENTEZARI MH and DIONYSIOU DD (2012) A review on the visible light active titanium dioxide photocatalysts for environmental applications. *Applied Catalysis B: Environmental* **125** 331–349.

PETTIBONE JM, CWIERTNY DM, SCHERER M and GRASSIAN VH (2008) Adsorption of organic acids on TiO_2 nanoparticles: effect of pH, nanoparticles size and nanoparticle aggregation. *Langmuir* **24** (13) 6659–6667.

PIRKARAMI A and OLYA ME (2014) Removal of dye from industrial wastewater with an emphasis on improving economic efficiency and degradation mechanism. *Journal of Saudi*

Chemical society. Retrieved: http://dx.doi.org/10/1016/j.jscs.2013.12.008 Date: 3 June 2015.

PORKODI K and AROKIAMARY AD (2007) Synthesis and spectroscopic characterization of nanostructured anatase titania: A photocatalyst. *Materials Characterization* **58** (6) 495–503.

PRACHI, GAUTAM P, MADATHIL D and NAIR ANB. (2013). Nanotechnology in waste water treatment: a review. *International Journal of ChemTech Research* **5** (5) 2303–2308.

PRIYANKA KP, SHEENA PA, ALOYSIUS SABU N, GEORGE T, BALAKRISHNA KM and VARGHESE T (2014) Characterization of nanophase TiO_2 synthesized by sol–gel method. *Indian Journal of Physics* **88** (7) 657–663.

QU X, ALVAREZ PJJ and LI Q (2013) Applications of nanotechnology in water and wastewater treatment. *Water Research* **47** (12) 3931–3946.

REIJNDERS L (2009) The release of TiO_2 and SiO_2 nanoparticles from nancomposites. *Polymer Degradation and Stability* **94** (5) 873–876.

ROCCARO P, SGROI M and VAGLIASINDI GA (2013) Removal of xenobiotic compounds from wastewater for environment protection: treatment processes and costs. *Chemical Engineering Transactions* **32** 505–510.

ROMANELLO MB and FIDALGO DE CORTALEZZI MM (2013) An experimental study on the aggregation of TiO_2 nanoparticles under environmentally relevant conditions. *Water Research* **47** (12) 3887–3898.

SACCO O, STOLLER M, VAIANO V, CIAMBELLI P, CHIANESE A and SANNINO D (2012) Photocatalytic degradation of organic dyes under visible light on N-doped TiO_2 photocatalysts. *International Journal of Photoenergy* **2012** 626759.

SAIEN J and SOLEYMANI AR (2007) Degradation and mineralization of direct blue 71 in a circulating upflow reactor by UV/TiO_2 process and employing a new method in kinetic study. *Journal of Hazardous Materials* **144** (1-2) 506–512.

SAYES CM, WAHI R, KURIAN PA, LIU Y, WEST JL, AUSMAN KD, WARHEIT DB and COLVIN VL (2006) Correlating nanoscale titania structure with toxicity: a cytotoxicity and inflammatory response study with human dermal fibroblasts and human lung epithelial cells. *Toxicological Sciences* **92** (1) 174–185.

SHARIF F, WESTERHOFF P and HERCKES P (2013) Sorption of trace organics and engineered nanomaterials onto wetland plant material. *Environmental Science: Processes &*

Impacts **15** (1) 267.

SHARMA VK (2009) Aggregation and toxicity of titanium dioxide nanoparticles in aquatic environment – a review. *Journal of Environmental Science and Health Part A* **44** (14) 1485–1495.

SILLANPÄÄ M, PAUNU TM and SAINIO P (2011) Aggregation and deposition of engineered TiO_2 nanoparticles in natural fresh and brackish waters. *Journal of Physics: Conference Series* **304** 12018.

SIMON-DECKERS A, LOO S, MAYNE-L'HERMITE M, HERLIN-BOIME N, MENGUY N, REYNAUD C, GOUGET B and CARRIERE M (2009) Size-, composition- and shape-dependent toxicological impact of metal oxide nanoparticles and carbon nanotubes toward bacteria. *Environmental Science and Technology* **43** (21) 8423–8429.

SING KSW (1985) Reporting physisorption data for gas/solid systems with special reference to the determination of surface area and porosity (Recommendations 1984). *Pure and Applied Chemistry* **57** (4) 603–619.

SINHA S, CHATTOPADHYAY P, PAN L, CHATTERJEE S, CHANDA P, BANDYOPADHAY D, DAS K and SEN SK (2009) Microbial transformation of xenobiotics for environmental bioremediation. *African Journal of Biotechnology* **8** (22) 6116–6027.

Sonune A and Ghate R (2004) Developments in wastewater treatment methods. *Desalination* **167** 55–63.

SPELLMAN FR (2014) *Water and Wastewater Treatment Plant Operations.* 3rd Edition. CRC Press Taylor & Francis Group.

SUN TY, BORNHÖFT NA, HUNGERBÜHLER K and NOWACK B (2016) Dynamic probabilistic modeling of environmental emissions of engineered nanomaterials. *Environmental Science and Technology* **50** (9) 4701–4711.

SUDANA K, WATANABE T and HASHIMOTO K (2003) Studies on photokilling of bacteria on TiO_2 film. *Journal of Photochemistry and Photobiology A: Chemistry* **156** (7) 227–233.

SVENSON A, ALLARD A-S and EK M (2003) Removal of estrogenicity in Swedish municipal sewage treatment plants. *Water Research* **37** (18) 4433–4443.

TAN YN, WONG CL and MOHAMED AR (2011) An overview on the photocatalytic activity of nano-doped-TiO_2 in the degradation of organic pollutants. ISRN *Materials Science* **2011**

261219.

TIEDE K, BOXALL ABA, TEAR SP, LEWIS J, DAVID H and HASSALLÖV M (2008) Detection and characterization of engineered nanoparticles in food and the environment. *Food Additives and Contaminants: Part A* **25** (7) 795–821.

VIJAYALAKSHMI R and RAJENDRAN V (2012) Synthesis and characterization of nano-TiO_2 via different methods. *Scholar Research Library* **4** (2) 1183–1190.

WAGNER M, LOY A, NOGUEIRA R, PURKHOLD U, LEE N and DAIMS H (2002) Microbial community composition and function in wastewater treatment plants. *Antonie van Leeuwenhoek* **81** (1–4) 665–680.

WARHEIT DB, WEBB TR, REED KL, FRERICHS S and SAYES CM (2007) Pulmonary toxicity study in rats with three forms of ultrafine-TiO_2 particles: differential responses related to surface properties. *Toxicology* **230** (1) 90–104.

Water Research Australia (2013) Fact sheet: engineered nanomaterials in wastewater. Retrieved: http://www.waterra.com.au Date: 26 March 2015

WEI X, ZHU G, FANG J and CHEN J (2013) Synthesis, characterization, and photocatalysis of well-dispersible phase-pure anatase TiO_2 nanoparticles. *International Journal of Photoenergy* **2013** 1–6.

WENTZEL MC, UBISI MF, LAKAY MT and EKAMA GA (2002) Incorporation of inorganic material in anoxic/aerobic-activated sludge system mixed liquor. *Water Research* **36** (20) 5074–5082.

WESTERHOFF P, SONG G, HRISTOVSKI K and KISER MA (2011) Occurence and removal of titanium at full scale wastewater treatment plants: implications for TiO_2 nanomaterials. *Journal of Environmental Monitoring* **13** (5) 1195–1203.

WHITE C, SAYER JA and GADD GM (1997) Microbial solubilisation and immobilization of toxic metals: key biogeochemical process for treatment of contamination. *FEMS Microbiology Reviews* **20** (3-4) 503–516.

World Health Organization/United Nations Environment Programme (WHO/UNEP) (2012) WHO | State of the science of endocrine disrupting chemicals 2012: summary for decision-makers. Retrieved: www.who.int/ceh/risks/cehemerging2/en/ Date: 2 June 2015.

XUAN L. (2011) Fate of Silver Nanoparticles in Surface Water Environments. The Ohio State

University. Date: 20 May 2015.

YANG K, LIN D and XING B (2009) Interactions of humic acid with nanosized inorganic oxides. *Langmuir* **25** (6) 3571–3576.

ZHANG Y, CHEN Y, WESTERHOFF P and CRITTENDEN J (2009) Impact of natural organic matter and divalent cations on the stability of aqueous nanoparticles. *Water Research* **43** (17) 4249-4257.

APPENDICES

Appendix 1 Mean diameter (nm) versus Time (s) plots for water (DI) with no dye added

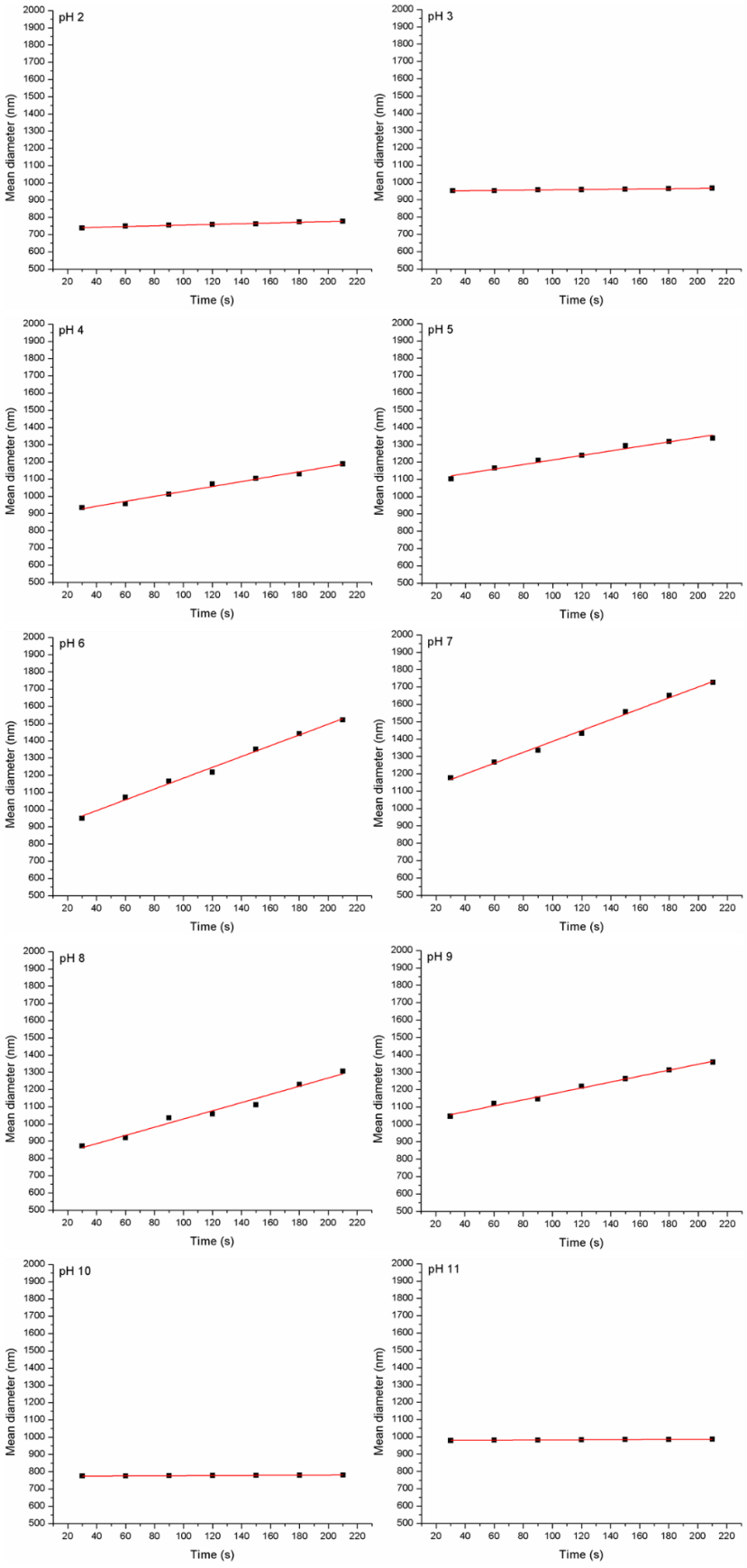

Appendix 2 Mean diameter (nm) versus Time (s) plots for NaCl with no dye added

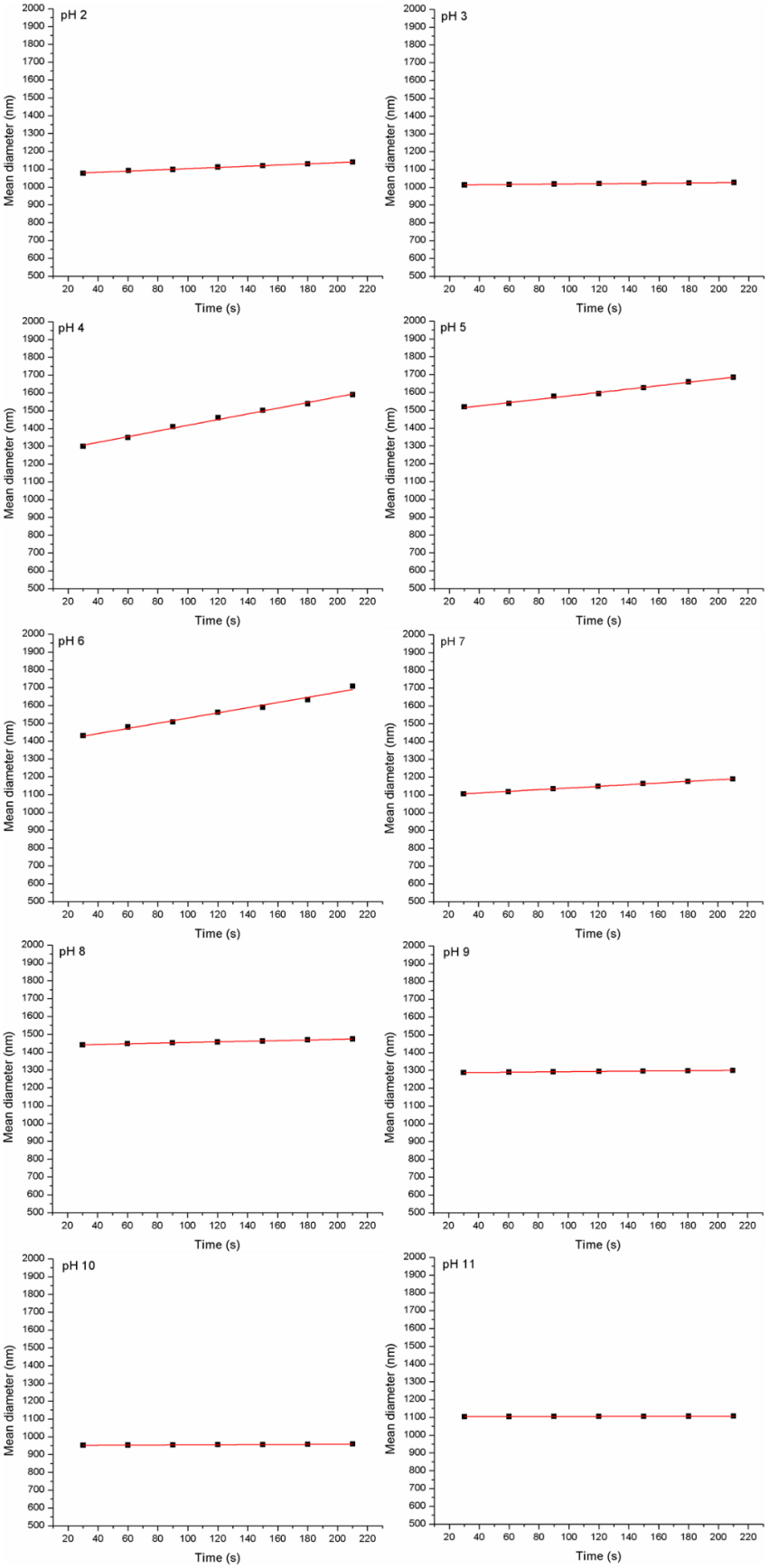

Appendix 3 Mean diameter (nm) versus Time (s) plots for $CaCl_2$ with no dye added

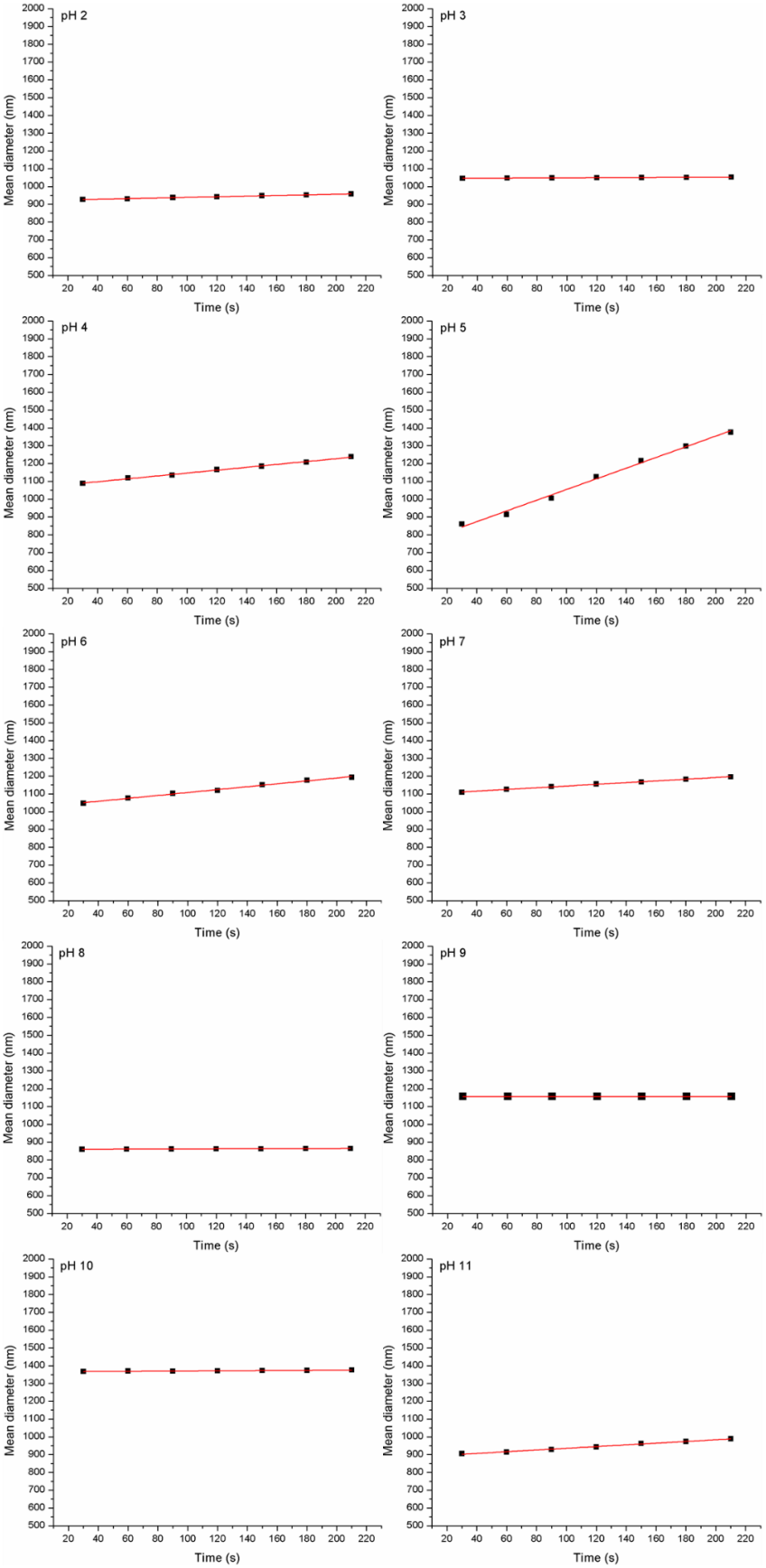

Appendix 4 Mean diameter (nm) versus Time (s) plots for $MgCl_2$ with no dye added

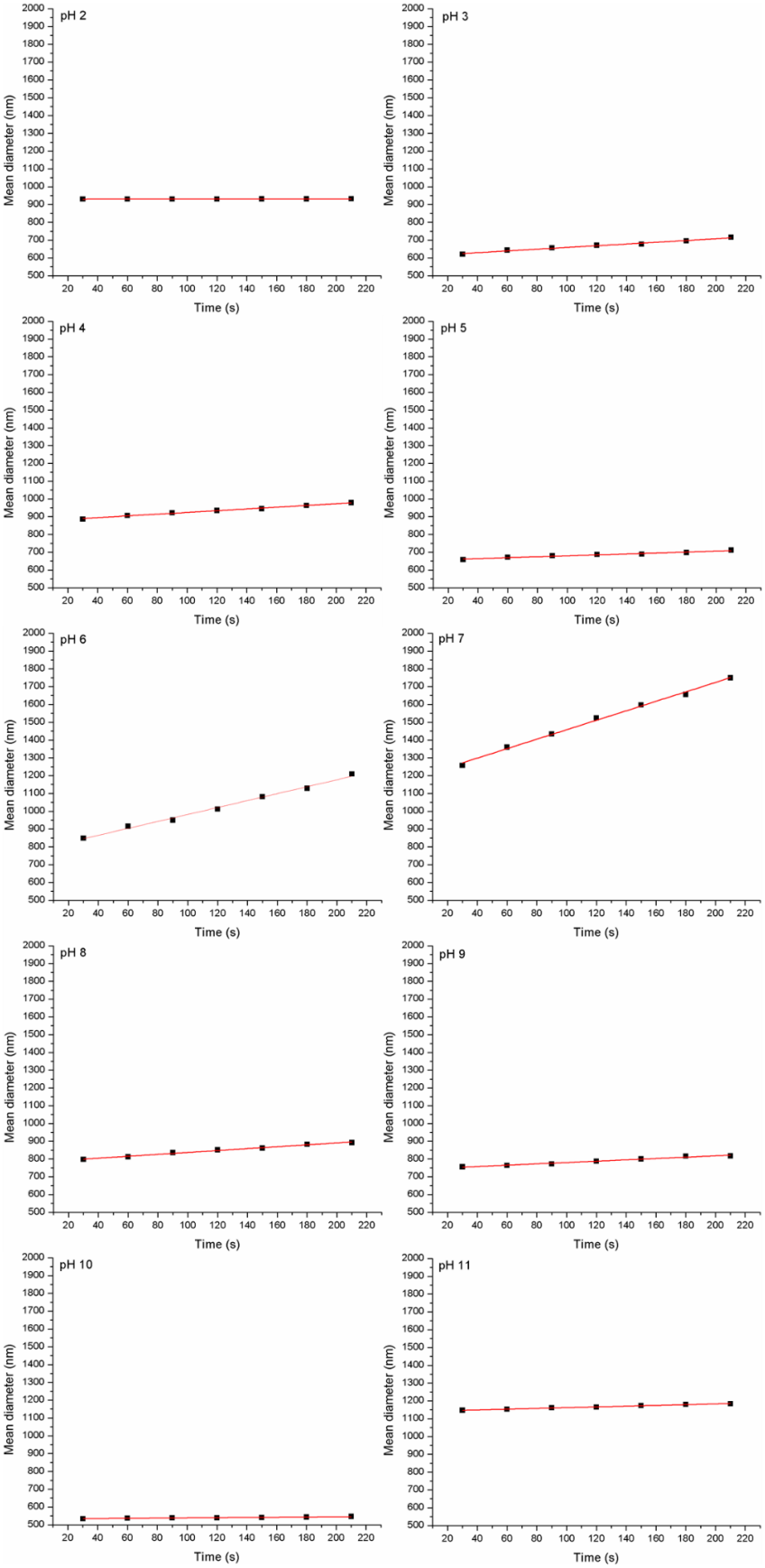

Appendix 5 Mean diameter (nm) versus Time (s) plots for water (DI) with dye added

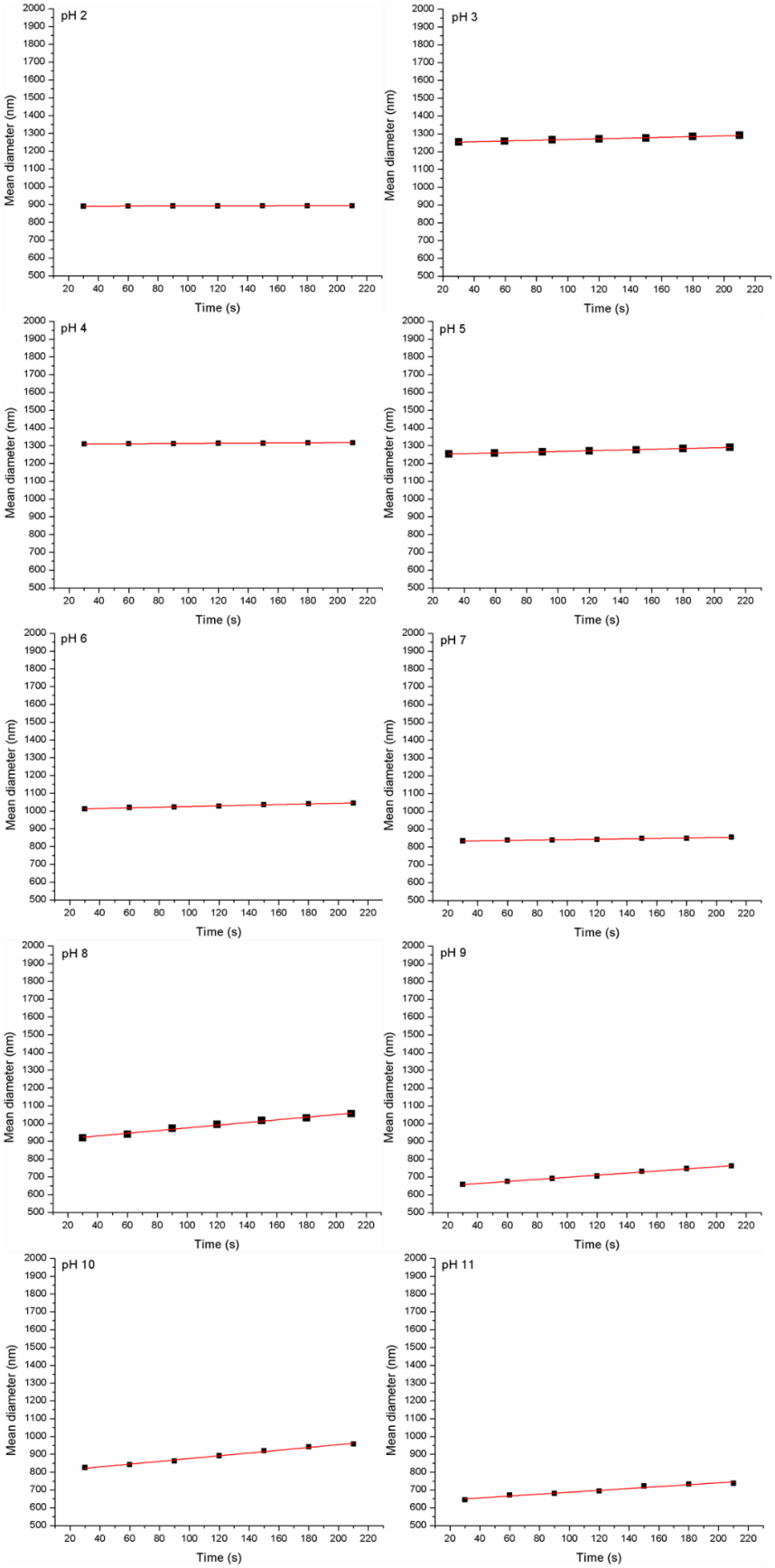

Appendix 6 Mean diameter (nm) versus Time (s) plots for NaCl with dye added

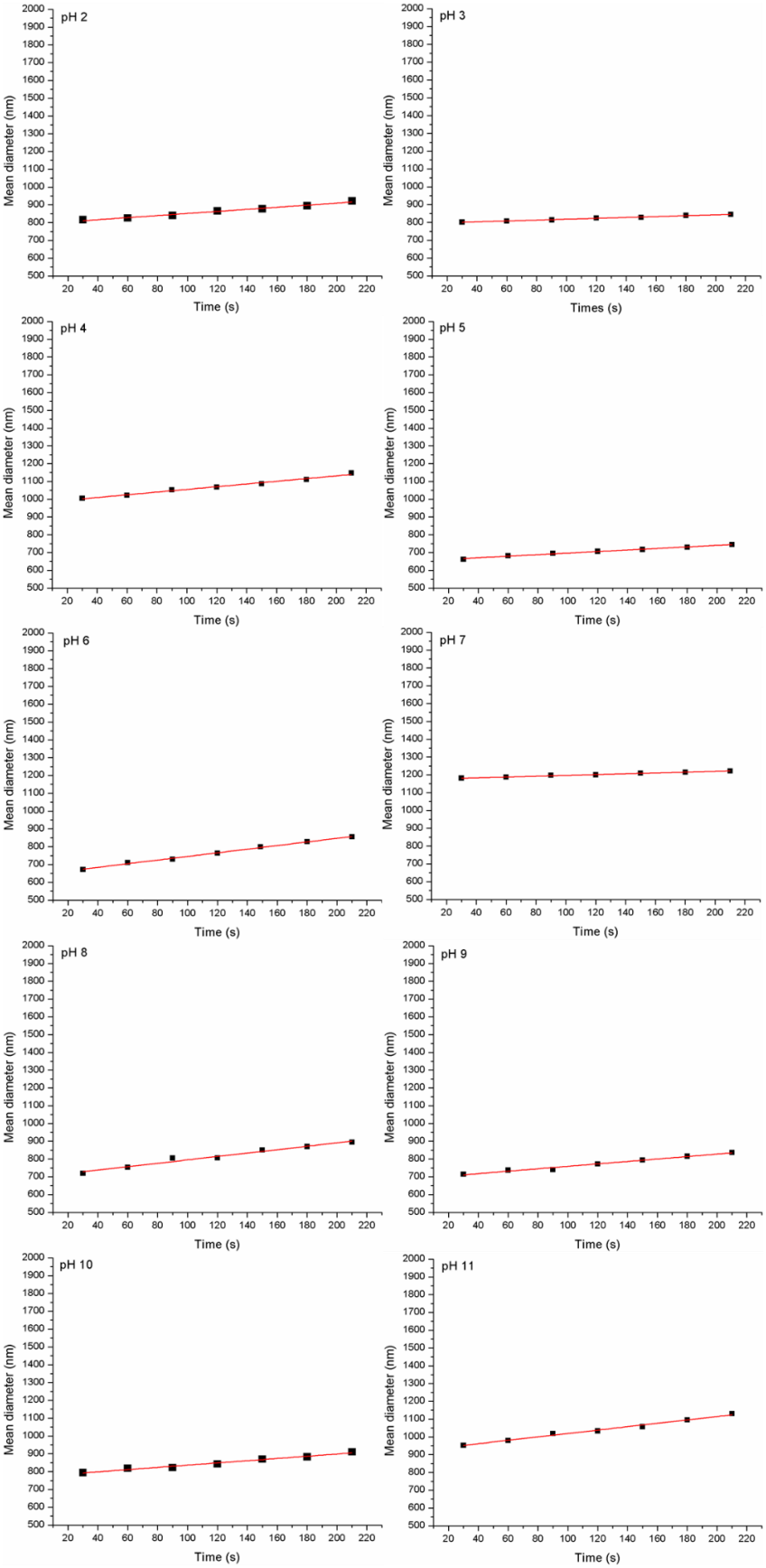

Appendix 7 Mean diameter (nm) versus Time (s) plots for $CaCl_2$ with dye added

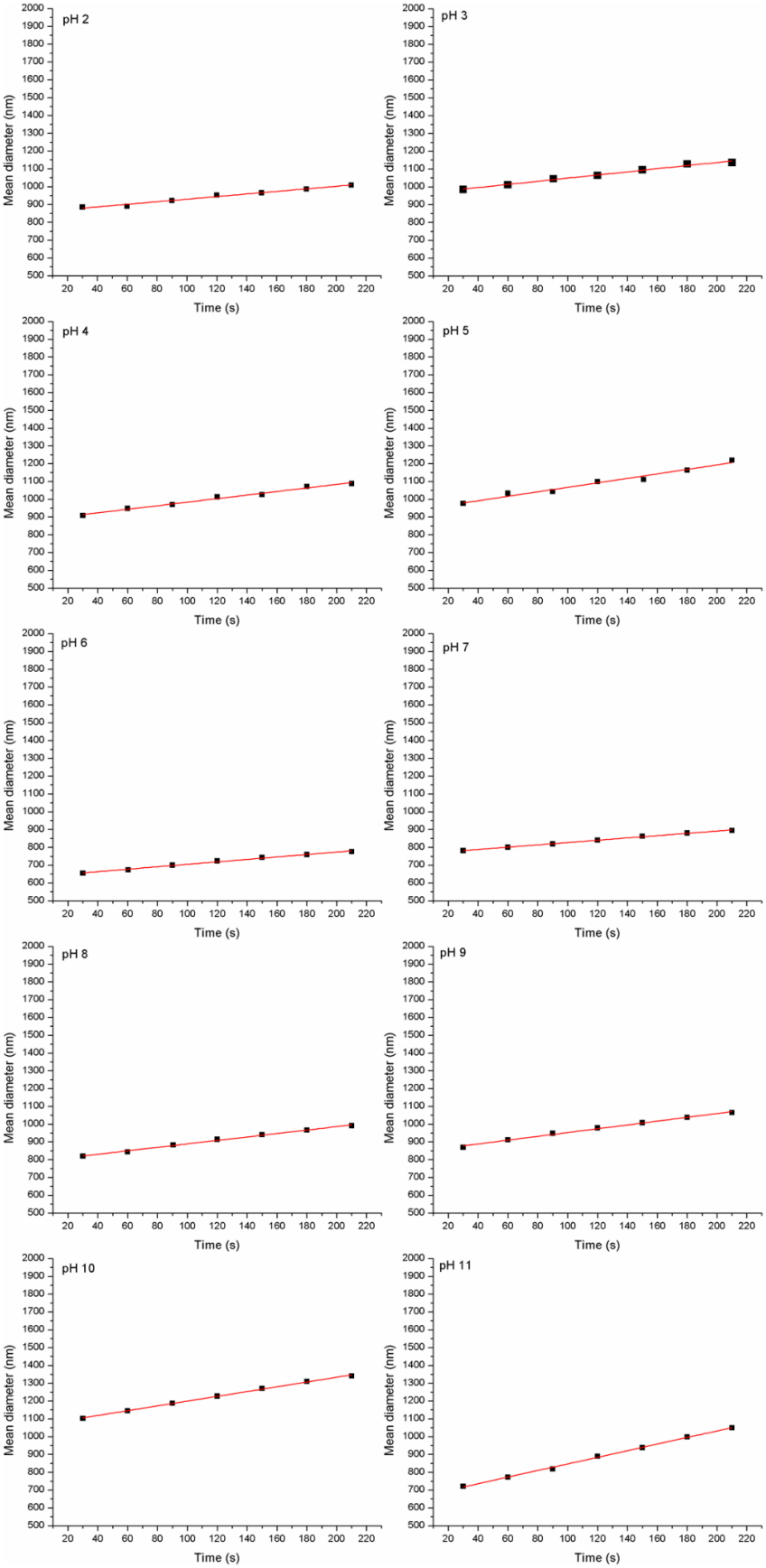

Appendix 8 Mean diameter (nm) versus Time (s) plots for $MgCl_2$ with dye added

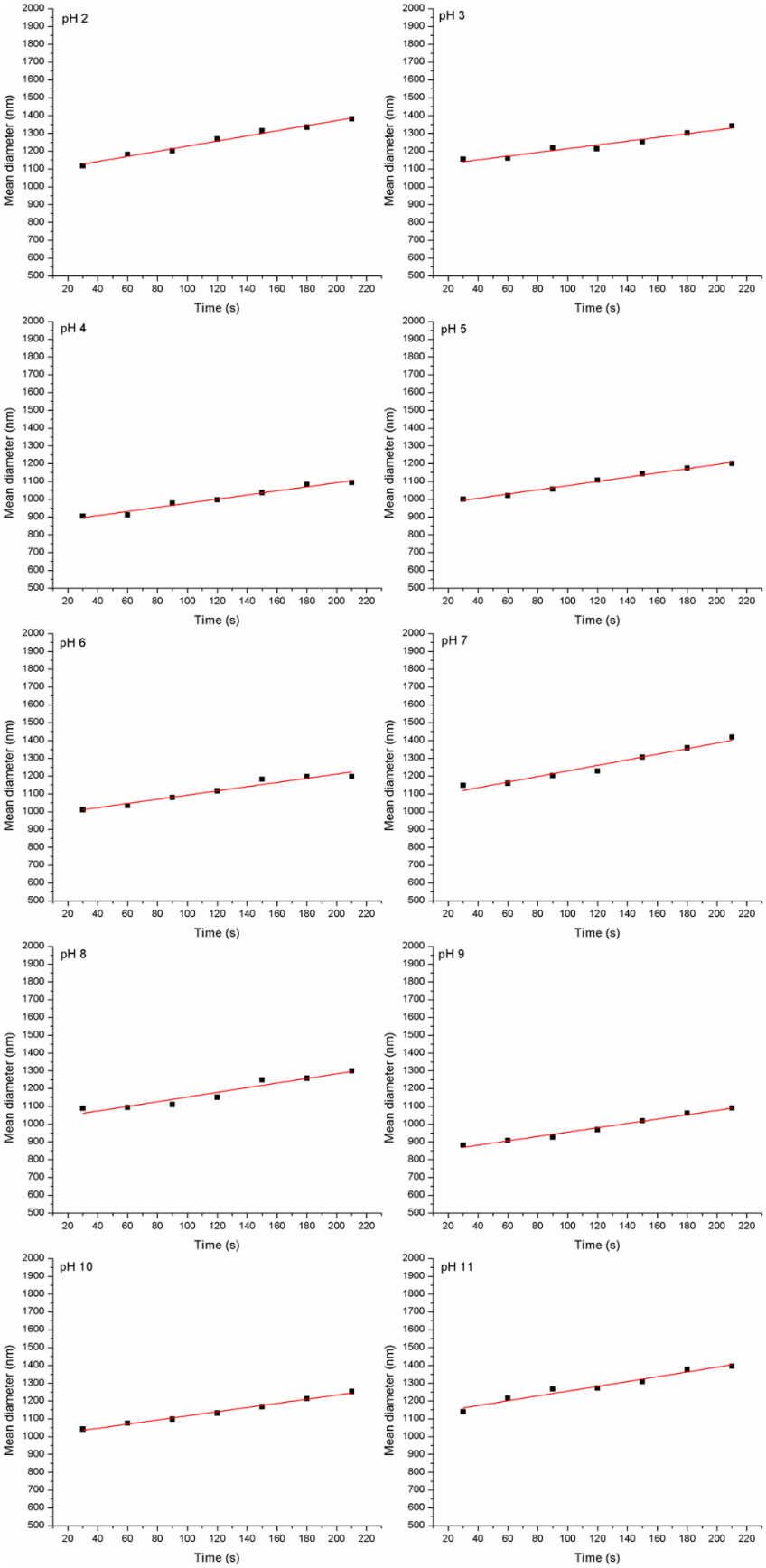

Appendix 9 Measured parameters of the prepared influents during the treatment process

SRT	1 (day 1-10)		2 (day 11-20)		3 (day 21-30)		4 (day 31-40)		5 (day 41-50)	
Parameters	Mean	SD	Mean	SD	Mean	SD	Mean	SD	Mean	SD
Test										
COD (mg/L)	402.6	67.2	249.7	33.2	182.2	7.3	313.8	8.4	251.3	14.0
Control										
COD (mg/L)	288.7	35.4	382.4	14.9	182.8	5.2	260.4	12.5	249.1	12.1
SD: Standard Deviation										-

SRT	6 (day 51-60)		7 (day 61-70)		8 (day 71-80)		9 (day 81-90)	
Parameters	Mean	SD	Mean	SD	Mean	SD	Mean	SD
Test								
pH			Range: 7.5-8.4 Mode: 7.5	N/A	Range: 7.5-7.9 Mode: 7.8	N/A	Range: 7.6-8.6 Mode: 7.7	N/A
Conductivity (µS/cm)			435.5	14.9	377.0	79.3	417.3	98.7
COD (mg/L)	282.4	181.3	421.5	169.8	325.1	31.7	384.2	102.2
BOD_5 (mg/L)	0.6		0.5	0.4	1.6	0.2	1.2	0.8
TSS (mg/L)	14.7	4.6	10.7	4.7	11.1	4.4	16.3	9.5
Control								
pH			Range: 7.4-8.4 Mode: 7.6	N/A	Range: 7.6-7.8 Mode: 7.7	N/A	Range: 6.4-8.7 Mode: 7.7	N/A
Conductivity (µS/cm)			450.5	20.5	392.0	89.0	430.3	116.4
COD (mg/L)	261.9	180.6	412.3	173.8	344.1	25.1	393.6	95.2
BOD_5 (mg/L)	0.8		1.0	0.6	1.4	0.1	1.4	1.0
TSS (mg/L)	12.2	8.6	15.3	6.9	11.4	6.5	8.7	3.2
SD: Standard Deviation	-	-	-	-	-	-	-	-

SRT	10 (day 91-100)		11 (day 101-110)		12 (day 111-120)	
Parameters	Mean	SD	Mean	SD	Mean	SD
Test						
pH	Range: 7.1-7.9 Mode: 7.7	N/A	Range: 7.0-7.8 Mode: 7.5	N/A	Range: 7.0-7.8 Mode: 7.0	N/A
Conductivity (µS/cm)	548.2	31.6	612.5	84.4	578.3	22.0
COD (mg/L)	347.2	35.7	318.9	55.6	352	39.6
BOD_5 (mg/L)	2.5	1.1	4.1	0.6	2.2	0.4
TN (mg/L)	85.0		89.0		104.0	
TSS (mg/L)	9.0	3.7	10.1	4.0	11.6	4.0
Control						
pH	Range: 7.0-8.0 Mode: 7.8	N/A	Range: 7.0-7.8 Mode: 7.8	N/A	Range: 7.0-8.0 Mode: 7.8	N/A
Conductivity (µS/cm)	542.6	65.6	565.3	102.5	552.7	36.1
COD (mg/L)	330.0	36.7	340.2	46.1	370.5	63.6
BOD_5 (mg/L)	2.1	0.2	2.0	0.6	2.7	0.7
TN (mg/L)	96.0		99.0		100.0	
TSS (mg/L)	10.5	2.3	9.1	3.2	12.0	1.3

SD: Standard Deviation

Appendix 10 Measured parameters of the aerobic tanks and effluents during treatment process

SRT	1 (day 1-10)		2 (day 11-20)		3 (day 21-30)		4 (day 31-40)		5 (day 41-50)	
Parameters	Mean	SD	Mean	SD	Mean	SD	Mean	SD	Mean	SD
Test										
COD (mg/L)	77.6	11.9	55.3	20.1	36.7	7.6	34.3	4.7	41.5	8.0
Control										
COD (mg/L)	77.8	17.4	62.1	17.3	37.2	9.1	31.5	4.0	41.1	13.8

SD: Standard Deviation

SRT	6 (day 51-60)		7 (day 61-70)		8 (day 71-80)		9 (day 81-90)	
Parameters	Mean	SD	Mean	SD	Mean	SD	Mean	SD
Test								
pH			Range: 6.2-7.3 Mode: 6.7	N/A	Range: 5.8-7.4 Mode: 7.4	N/A	Range: 5.2-7.1 Mode: 6.6	N/A
Dissolved oxygen (mg/L)			4.1	0.4	4.3	0.5	3.8	0.8
Temperature (˚C)			21.4	1.5	22.8	1.3	23.5	0.9
Conductivity (µS/cm)			833.8	77.4	770.1	69.3	816.6	61.3
MLSS (mg/L)	1691.0	28.4	1161.4	175.8	1216.7	524.8	1843.1	569.8
MLVSS (mg/L)	1539.0	86.3	1061.0	126.2	1083.4	463.3	1683.4	562.8
COD (mg/L)	72.6	34.9	66.4	27.1	58.8	21.4	52.2	12.73
BOD_5 (mg/L)	0.2		0.2	0.1	0.6	0.2	0.1	0
TSS (mg/L)	53.2	16.8	51.9	16.6	6.5	2.2	8.8	2.9
Control								
pH			Range: 6.0-7.6 Mode: 6.0	N/A	Range: 5.7-7.4 Mode: 6.5	N/A	Range: 5.5-7.6 Mode: 7.2	N/A
Dissolved oxygen (mg/L)			3.7	0.6	3.9	0.8	3.8	0.4
Temperature (˚C)			21.8	1.6	23.2	1.3	23.7	0.6
Conductivity (µS/cm)			819.8	72.5	864.6	67.6	820.7	57.7
MLSS (mg/L)	1330.0	70.7	1178.4	175.0	1409.0	399.6	1821.3	597.7
MLVSS (mg/L)	1117.0	4.2	1067.1	122.9	1314.0	399.6	1688.9	535.3

COD (mg/L)	69.9	19.0	64.6	20.0	53.4	13.3	60.3	20.8
BOD_5 (mg/L)	0.5		0.4	0.2	0.6	0.1	0.2	0.1
TSS (mg/L)	43.2	18.6	50.9	9.9	8.3	11.6	9.6	9.0

SD: Standard Deviation

Appendix 11 Scanning electron micrograph and EDS of sludge during addition of 10 mg/L and 15 mg/L of TiO_2 respectively

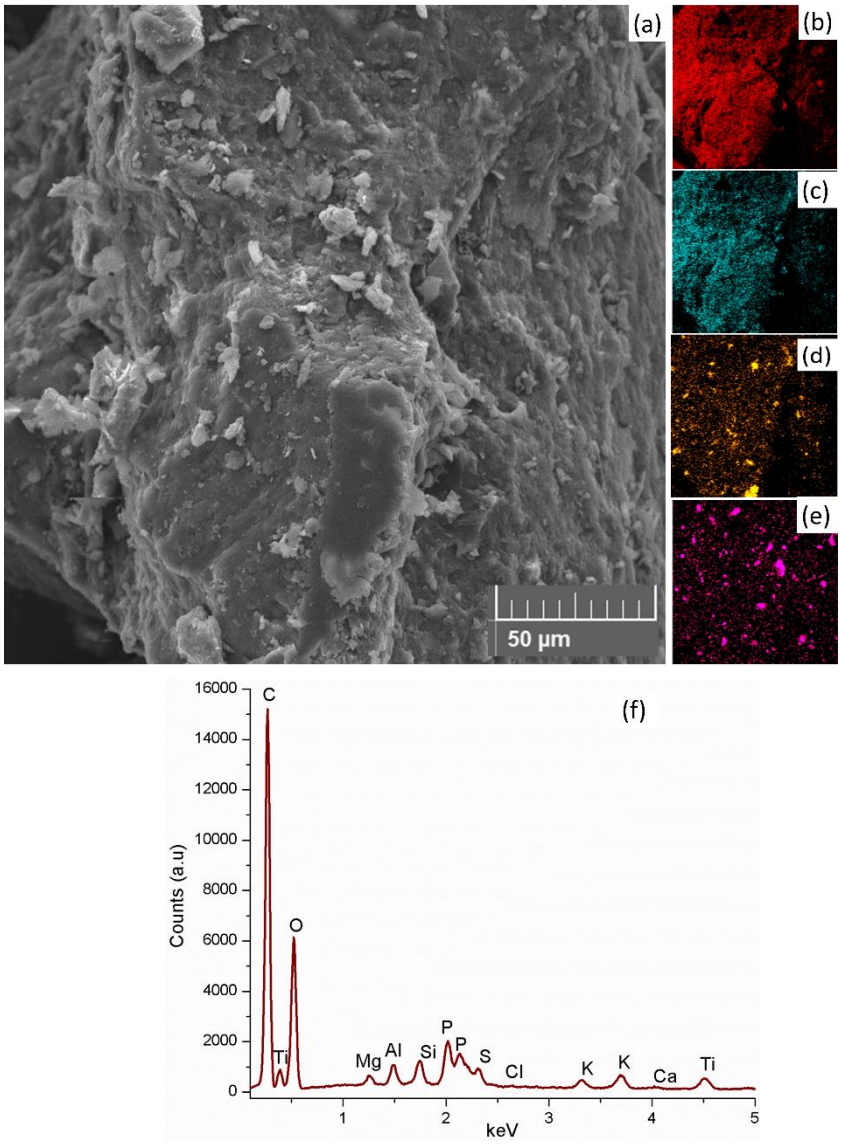

Figure A11.1 (a) SEM image of dried activated sludge during the addition of 10 mg/L TiO_2 with the respective inserts of (b) carbon, (c) oxygen, (d) silicon and (e) titanium after SEM mapping of the image. (f) EDS of the mapped image

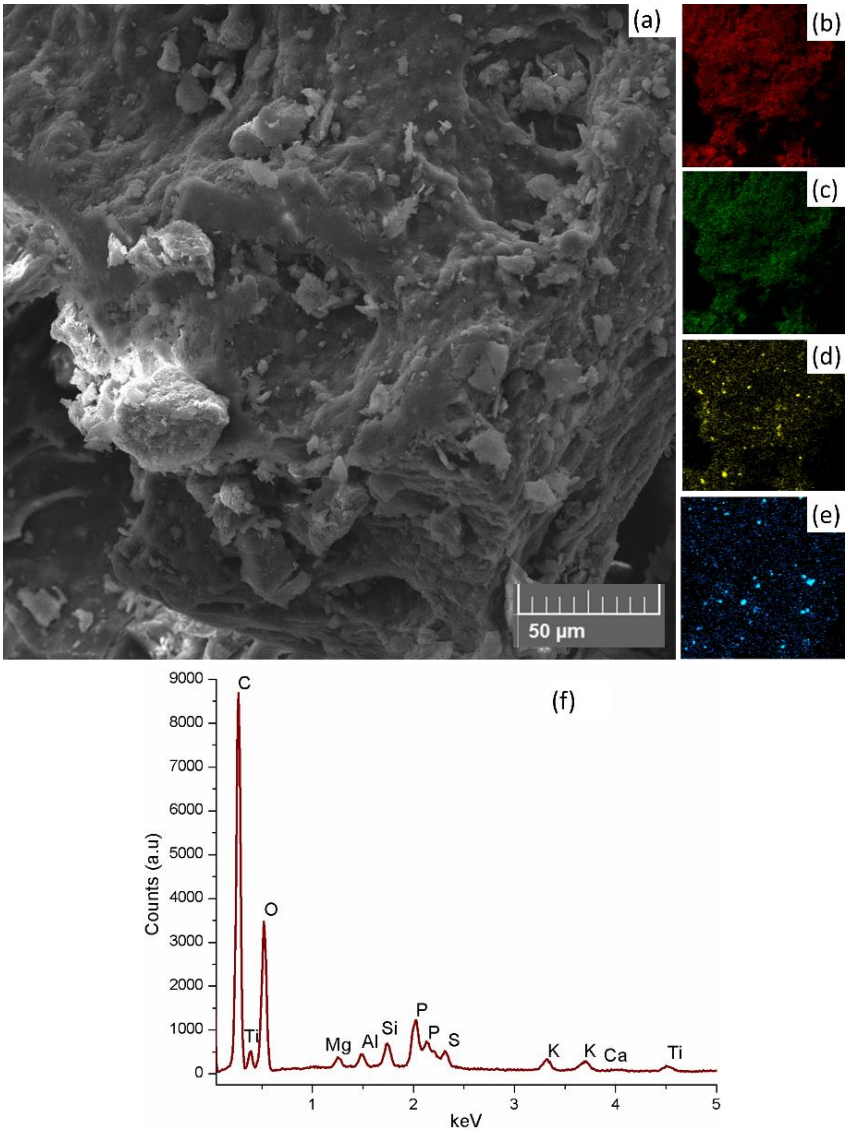

Figure A11.2 (a) SEM image of dried activated sludge during the addition of 15 mg/L TiO_2 with the respective inserts of (b) carbon, (c) oxygen, (d) silicon and (e) titanium after SEM mapping of the image. (f) EDS of the mapped image

Appendix 12 Plate examples